UNIVERSITY OF CALIFORNIA, IRVINE

A Multivariate Perspective on the Impacts of Anthropogenic Climate Change on Hydroclimatic Extremes

DISSERTATION

submitted in partial satisfaction of the requirements
for the degree of

DOCTOR OF PHILOSOPHY

in Civil and Environmental Engineering

by

Felicia Chiang

Dissertation Committee:
Professor Amir AghaKouchak, Chair
Distinguished Professor Efi Foufoula-Georgiou
Associate Professor Steven J. Davis

2020

DEDICATION

To

my dear parents and sister,

Thank you for all the love and support you have given to me over the years.
I could not have come this far without the three of you.

my treasured friends, near and far,

and

our pale blue dot.

"Non est ad astra mollis e terris via."
"The trip from the earth to the stars is not an easy one."
-Seneca

TABLE OF CONTENTS

LIST OF FIGURES

LIST OF TABLES

ACKNOWLEDGEMENTS

I would like to express my deepest appreciation to my committee chair and advisor, Professor Amir AghaKouchak, who has been a mentor, a teacher, and a friend throughout my time at University of California, Irvine. Without his mentorship and support, this dissertation would not have been possible.

I would like to thank my committee members, Professor Efi Foufoula-Georgiou and Professor Steven Davis, for their valuable feedback and support on my research and dissertation writing and presentation.

In addition, I would like to thank my supervisors at the International Institute of Applied Systems Analysis (IIASA), Drs. Peter Greve, Yoshihide Wada, and Ted Veldkamp. My time at IIASA helped me grow as a researcher and a person, and I'm so grateful for their guidance during my time there.

I would also like to thank my co-authors, Drs. Omid Mazdiyasni, Laurie Huning, Charlotte Love, Iman Mallakpour, Hamed Moftakhari, Simon Papalexiou, Elisa Ragno, and Mojtaba Sadegh, for their feedback and support on the publications mentioned in the dissertation.

Part of the research was developed in the Young Scientists Summer Program at the International Institute for Applied Systems Analysis, Laxenburg (Austria) with financial support from the U.S. National Academy of Sciences through their contributions as a National Member Organization. I also acknowledge the World Climate Research Programme's Working Group on Coupled Modeling, responsible for CMIP5, and thank the modeling groups for producing and making their model output available to the public. For CMIP, the U.S. Department of Energy's Program for Climate Model Diagnosis and Intercomparison provides coordinating support and led development of software infrastructure in partnership with the Global Organization for Earth System Science Portals.

VITA

Felicia Chiang

Ph.D. in Civil and Environmental Engineering, University of California, Irvine	2020
M.S. in Civil Engineering, University of California, Irvine	2017
B.S. in Environmental Sciences, University of California, Berkeley	2013

FIELD OF STUDY

Hydrology and Water Resources Systems

PUBLICATIONS

Chiang, F., Greve, P., Mazdiyasni, O., Veldkamp, T., Wada, Y., AghaKouchak, A., "Impacts of Anthropogenic Forcing on Concurrent Temperature and Precipitation Extremes." *In prep.*

Chiang, F., Mazdiyasni, O., AghaKouchak, A., "Evidence of anthropogenic impacts on global drought frequency, duration, and intensity." *Under review.*

AghaKouchak, A., **Chiang, F.**, Huning, L. S., Love, C. A., Mallakpour, I., Mazdiyasni, O., Moftakhari, H., Papalexiou, S. M., Ragno, E., Sadegh, M., 2020, "Climate Extremes and Compound Hazards in a Warming World." *Annual Review of Earth and Planetary Sciences,* 48.

Mazdiyasni, O., Sadegh, M., **Chiang, F.**, AghaKouchak, A., 2019, "Heat wave Intensity Duration Frequency Curve: A Multivariate Approach for Risk and Attribution Analysis." *Scientific Reports,* 9, 1-8.

Tarroja, B., Forrest, K., **Chiang, F.**, AghaKouchak, A., Samuelsen, S., 2019, "Implications of Hydropower Variability from Climate Change for a Future, Highly-Renewable Electric Grid in California." *Applied Energy*, 237, 353-366.

Forrest, K., Tarroja, B., **Chiang, F.**, AghaKouchak, A., Samuelsen, S., 2018, "Assessing Climate Change Impacts on California Hydropower Generation and Ancillary Services Provision." *Climatic Change,* 151, 395-412.

Tarroja, B., **Chiang, F.**, AghaKouchak, A., Samuelsen, S., 2018, "Assessing future water resource constraints on thermally based renewable energy resources in California." *Applied Energy,* 226, 49-60.

AghaKouchak, A., Huning, L. S., **Chiang, F.**, Sadegh, M., Vahedifard, F., Mazdiyasni, O., Moftakhari, H., Mallakpour, I., 2018. "How do natural hazards cascade to cause disasters?" *Nature,* 561, 458-460.

Tarroja, B., **Chiang**, **F.,** AghaKouchak, A., Samuelsen, S., Raghavan, S. V., Wei, M., Sun, K., Hong, T., 2018. "Translating Climate Change and Heating System Electrification Impacts on

Building Energy Use to Future Greenhouse Gas Emissions and Electric Grid Capacity Requirements in California." *Applied Energy,* 225, 522-534.

Chiang, F., Mazdiyasni, O., and AghaKouchak, A., 2018. "Amplified Warming of Droughts in Southern United States in Observations and Model Simulations." *Science Advances,* 4(8), eaat2380.

ABSTRACT OF THE DISSERTATION

A Multivariate Perspective on the
Impacts of Anthropogenic Climate Change on Hydroclimatic Extremes

by

Felicia Chiang

Doctor of Philosophy in Civil and Environmental Engineering

University of California, Irvine, 2020

Professor Amir AghaKouchak, Chair

Hydroclimatic extreme events such as droughts and heatwaves can produce significant impacts on environmental, socioeconomic, and public health sectors. Evidence shows that extreme events are becoming more common, severe, and costly as a result of anthropogenic climate change; therefore, the study of hydroclimatic extremes is necessary to combat the rising costs associated with these extremes. In general, previous studies of climate extremes have focused on one variable or feature at a time. In this dissertation, we provide novel investigations of the interactions between different climatic extremes and different features of extremes. Here, we present observational and model-based evidence that climate change has influenced 1) temperature shifts conditioned on drought conditions, 2) changes in the likelihood and magnitude of drought duration, frequency, and severity, and 3) changes in the likelihood of concurrent warm and dry events in response to anthropogenic warming.

Chapter 1 first provides a broad overview of the literature framing this dissertation and identifies key research opportunities that following chapters pursue. Chapter 2 presents a conditional perspective of how droughts have been warming in the 20th century and how they are projected to change in a warming climate. This chapter concluded that temperatures during dry

meteorological conditions are warming faster than average climate conditions, which have strong implications for future risks of concurrent warm and dry extremes under changes in background climate. This chapter also investigates the physical mechanisms causing substantial warming of droughts. Chapter 3 examines the influence of anthropogenic forcing on general drought characteristics, including drought frequency, duration, and intensity, to illustrate the contribution of human activities to our current hydroclimatic state. Using model simulations with and without anthropogenic forcing, this study found substantial regional shifts in drought frequency, maximum drought duration, and maximum drought intensity, especially in the wetter regions of the globe. Chapter 4 presents a study of the impacts of anthropogenic climate change on compound warm and dry extremes. Previous attribution studies have ignored dependencies between climate variables. Thus, in this chapter, we focus on attribution of changes in compound water and dry extremes in response to anthropogenic emissions. This study showed that most of the global land area has experienced significant increases in meteorological warm and dry months that can be attributed to human activities. We also introduce a new conditional indicator that demonstrates the impact of climate change on high temperature exceedances under dry conditions (conditional warm spells).

The research presented in this dissertation provides insight into the drivers and feedback mechanisms that influence warm and dry conditions and quantify how climate change has impacted the nature of hydroclimatic extremes. From the results of these studies, we have provided a novel perspective on temperature change conditioned on droughts and created a foundation for understanding the impacts of climate change on droughts and concurrent warm and dry events. By better understanding these hydroclimatic extremes, local and national decision-makers can better prepare for future extreme events in the near and distant future.

Chapter 1

Climate Extremes and Compound Events

Part of this Chapter has been published in Annual Review of Earth and Planetary Sciences.

Citation: AghaKouchak, A., Chiang, F., Huning, L. S., Love, C. A., Mallakpour, I., Mazdiyasni, O., Moftakhari, H., Papalexiou, S. M., Ragno, E., Sadegh, M., 2020, "Climate Extremes and Compound Hazards in a Warming World." *Annual Review of Earth and Planetary Sciences,* 48.

1.1 Introduction

In the literature, the term "climate extreme" is generally defined as the occurrence of a climate variable at the upper or lower tails of the observed distribution (Karl et al., 2008; Seneviratne et al., 2012). Due to the vast number of climate variables that describe the physical conditions here on Earth, climate extremes can manifest in many ways. Climate extremes range from the fast-paced oppression of a heatwave to the slow onset and, sometimes ambiguous, departure of a drought event. In addition, some climate events may not be statistically rare, such as the occurrence of a tropical storm or cyclone, but can still cause extreme impacts (Seneviratne et al., 2012). Due to the strong, significant impacts that climate extremes can have on existing environmental and ecological conditions, the built infrastructure of human settlements, and socioeconomic and public health, climate extremes are a critical field of study (Karl et al., 2008). The study of climate extremes is crucial to gain a better understanding of their drivers, probability of occurrence, and corresponding impacts.

In general, climate extremes occur due to natural interannual and interdecadal climate variability (Seneviratne et al., 2012). Therefore, for any given climate variable, we can generate distributions that represent the probability of occurrence of observable values driven by natural climate variability. However, under the influence of anthropogenic climate change, many atmospheric variables have undergone significant changes that cannot be attributed to natural variability (Bindoff et al., 2013; IPCC, 2013). For example, if we examine the distribution of daily air temperature values, we can see historically observed changes in the mean and variance of the distribution (IPCC, 2013). The lower and upper ends or "tails" of the temperature distribution can be sensitive to small changes in the mean and variance, which can translate into large, significant increases/decreases in hot and cold extremes (IPCC, 2013). Rising average

global temperatures have already been shown to translate to more frequent and severe heatwaves in many regions across the globe (Fischer & Knutti, 2015; IPCC, 2013; Mazdiyasni & AghaKouchak, 2015). In addition, rising temperatures have also been linked to changes in the global water cycle, increasing heavy precipitation events and even the nature of tropical storms (Easterling et al., 2000; Fischer & Knutti, 2015; IPCC, 2013).

Although the field of climate extremes has advanced substantially in recent decades, there are still many challenges that researchers face when studying climate extremes in detail (Karl et al., 2008). Recent papers are still improving on the definition of climate extremes and the identification and understanding of the drivers behind these extreme events (for example, the recognition of anthropogenic drought (AghaKouchak et al., 2015). The consideration of human activities (outside of anthropogenic emissions) in contributing to extremes has just begun to emerge as a field, and there are still many research gaps and opportunities when considering human influences on hydroclimatic conditions. In addition, since extreme events are, by definition, rare events, many datasets are still not long enough to adequately understand the risk and likelihood of these rare events (Smolka, 2006).

In this chapter, we review the existing literature related to climate extremes, with special attention to droughts and concurrent warm and dry events. We also review literature related to concurrent climate hazards, which is an emerging subfield of interest, especially in the context of climate change. In addition, we review the existing literature related to the detection and attribution of anthropogenic climate change and highlight the research opportunities that are present in the detection and attribution field. Overall, this chapter provides the general background of the literature framing this dissertation and identifies key research gaps that the following chapters address.

1.2 Progress in Climate Extremes Literature

Across the globe, climate extremes have been significantly impacting human civilization since the beginning of recorded history (Heim, 2015). Due to anthropogenic climate change, the likelihood of many climate extremes has increased as average global temperatures have risen (AghaKouchak et al., 2013; Easterling et al., 2000). In the past four decades, the occurrence of climate extreme events have cost the United States over 1.7 trillion US dollars and nearly ten thousand lives, with more and more costs incurred in recent years (Smith & NOAA National Centers For Environmental Information, 2020). Due to the projected impacts that climate extremes are anticipated to incur in the near and distant future, it is critical that the field of climate science moves toward a better understanding of the drivers and triggers of extreme events and improves our capacity to predict and project climate extremes and their associated impacts.

1.2.1 Droughts

The phenomenon of drought has been defined many times over, with many different drought indices currently serving to represent different aspects of water availability and many indices still being introduced to better encompass the extreme event (Dracup et al., 1980; Gumbel, 1963; IPCC, 2013; Palmer W, 1965; Van Loon et al., 2016). The most traditional drought classification schemes include: meteorological, agricultural, and hydrological drought, which correspond to precipitation, soil moisture, and surface runoff/groundwater deficits (Wehner et al., 2017; Wilhite, 2000). In recent years, new terms, such as “socioeconomic drought” have been introduced into the literature to acknowledge the significant role that human

factors and actions play in determining water availability (Van Loon et al., 2016; Wilhite et al., 2007).

As the effects of anthropogenic climate change grow more apparent, research efforts in recent decades have shifted towards characterizing and understanding droughts in a warming world (IPCC, 2013). Many studies show observed changes in regional precipitation rates and predict a redistribution of global precipitation, which may have serious implications for transitional regions sensitive to changes in soil moisture (IPCC, 2013; Seneviratne et al., 2006; K. Trenberth, 2011). Due to changes in global climate patterns, there is evidence that these transitional zones will be shifting, resulting in changes in the influence of land surface moisture on local drought events (Seneviratne et al., 2006). As new transitional zones emerge, regional studies will be crucial for understanding how localized feedbacks and processes respond to changes in surface moisture.

Due to differences in observational datasets and methods accounting for natural climate patterns such as the El Niño-Southern Oscillation, global studies have not reached a consensus regarding how droughts have changed in response to climate change. For instance, Dai (2013) concluded that droughts have experienced an 8% increase in global land area between the 1980s and the 2000s, while Sheffield et al. (2012) could not find an observable global drought trend in recent history. This uncertainty highlights the need for more consistency among drought indices and observational data for independent studies to arrive at similar conclusions (Dai, 2013; IPCC, 2013; Sheffield et al., 2012; K. E. Trenberth et al., 2014).

Furthermore, the relative contributions of natural variability and anthropogenic warming are still not well defined. Therefore, studies improving our understanding of natural variations in drought would increase our understanding of historical and projected drought trends (IPCC,

2013). We must also broaden our efforts to characterize the effects of human activities (such as agriculture, deforestation, and increasing human water use) on the occurrence and severity of drought events (Mehran et al., 2015). AghaKouchak et al. highlighted the lack of studies researching the impacts of human activities (beyond anthropogenic emissions) on water stress and emphasized the importance of understanding the roles that human activities play in determining water availability (AghaKouchak et al., 2015). Van Loon et al. also called attention to the need to incorporate the role of humans in exacerbating (as well as alleviating) drought conditions (Van Loon et al., 2016). To improve regional and global drought management, we must improve our understanding of the relative contributions of human activities, natural variability, and anthropogenic climate change on droughts.

Using a global multi-model ensemble, Sheffield and Wood predicted that soil moisture drought events will become more common and more severe and will cover twice as much land area under moderate and high emissions scenarios at the end of the twenty-first century relative to the twentieth century (Sheffield & Wood, 2008). Global aridity (i.e., precipitation minus potential evapotranspiration) is expected to increase by 3.4% per degree Celsius increase in temperature over land, which will have negative ramifications on water availability as we move to a drier land state (Fu & Feng, 2014). Under a warming climate, we also anticipate a 10-23% expansion of global drylands between 1961-1990 and 2071-2100, increasing total dryland coverage to 50-56% of the global land surface (Huang et al., 2016). Increasing aridity and expanding drylands are projected to significantly increase the number of communities living in prolonged water stress (Huang et al., 2016). Projected increases in aridity and drought-prone regions will likely increase the occurrence of dust events (Prospero & Lamb, 2003), which can exacerbate human health issues and modify the hydrology of nearby and remote regions.

The projected increase in global aridity and dryland coverage is influenced by land-atmosphere and biosphere-atmosphere feedbacks. Berg et al. highlighted the projected contribution of land-atmosphere interactions to the expected doubling of aridity by isolating the influence of long-term soil moisture trends on precipitation, relative humidity, and temperature under a warming climate (Berg et al., 2016). In addition, increased dryland coverage and drought occurrences will degrade the ability of soils and vegetation to store carbon, feeding back to increase atmospheric concentrations of CO_2 and leading to further desertification (Huang et al., 2016). Large-scale deforestation, especially in tropical regions, may also influence the occurrence and severity of remote droughts (Spracklen et al., 2012).

While global models offer information regarding possible future climate scenarios, comparisons of historical and historical natural-only climate scenarios (historical simulations with and without the influence of anthropogenic emissions, respectively) have also improved our understanding of how anthropogenic climate change has contributed to changes in the water cycle (Fischer & Knutti, 2015). However, we lack attribution studies focused on drought events and stand to benefit from studying the impact of anthropogenic climate change on drought to reframe how we interpret historical observations and improve future modeling efforts.

Projected changes in droughts will also translate to changes in the vulnerability of human communities to droughts. Future drought events may challenge sectors that are dependent on water availability, such as the energy sector (for example, impacting hydropower energy portfolios and powerplant operations) (Tarroja et al., 2018). We need more studies on the range and magnitude of impacts that drought events will have in the future (for example, on the agricultural industry and food security), as well as the feedbacks that will occur on local and global scales to better prepare vulnerable populations for future events.

1.2.2 Multivariate Extremes

Although univariate climate hazards can cause severe impacts on an individual basis, the interconnected nature of our climate system suggests that the occurrence of one climate hazard can influence and even trigger the occurrence of one or more associated climate hazards. The concurrence of two or more interdependent climate hazards occurring simultaneously can be classified as an "extreme" or rare event with significant impacts on environmental, socioeconomic, and public health sectors, even if the climate hazards do not produce significant impacts independently (Seneviratne et al., 2012).

Traditionally, when studying the risk of climate extremes, we evaluate the occurrence of extreme events from a univariate perspective (AghaKouchak et al., 2014). Since traditional risk assessment frameworks fail to acknowledge additional risks that may arise from the joint occurrence of multiple climate hazards (AghaKouchak et al., 2014; Gräler et al., 2013), recent research efforts have introduced new multivariate risk assessments to more accurately represent the likelihood and associated impacts of concurrent climate events. In the past decade, formal frameworks for identifying and studying concurrent and compound events have rapidly developed, from the first discussion in the IPCC Report on Managing the Risks of Climate Extremes (Field et al., 2012), to Leonard et al.'s more detailed compound event framework (Leonard et al., 2014), to the more recent perspective put forth by Zscheischler et al. (Zscheischler et al., 2018). Zscheischler et al. highlighted that since many drivers and hazards are interdependent, the study of compound events is valuable for accurately assessing the risk of these extremes (Zscheischler et al., 2018).

Compound events may become more common in a warming climate, which makes the study of compound events even more vital for preparing for future climate extremes (AghaKouchak et al., 2014). Recent studies documented that concurrent droughts and heatwaves have become more frequent in the twentieth century (Diffenbaugh et al., 2015; Mazdiyasni & AghaKouchak, 2015). In California, Diffenbaugh et al. attributed an increased risk of concurrent warm and dry events to anthropogenic warming and projected that the increased risk of extreme warm and dry concurrences will continue throughout the twenty-first century (Diffenbaugh et al., 2015). One key mechanism responsible for compound drought and heat waves is land-atmosphere interactions. Moisture deficit during droughts limits land evaporation, which in turn increases the sensible heat to latent heat ratio, leading to a warming of the local area (Fischer et al., 2007; Hirschi et al., 2011; Mueller & Seneviratne, 2012).

Although progress has been made in the study and understanding of concurrent and compound extreme events, there are still many knowledge gaps in the present literature. The physical interactions between co-occurring climate hazards is still not well defined for many compound events, and gaining a better understanding of the key physical drivers of concurrent and compounding climate events is crucial to improve estimations of risks and impacts. In addition, the impact of anthropogenic forcing (i.e. anthropogenic emissions of greenhouse gases and aerosols) on the occurrence of concurrent and compound extreme events has not been examined in detail. The simple increase of global temperatures will redefine many distributions of univariate climate variables, and we expect to see significant changes in distributions of concurrent and compound events as well.

A cascading hazard is a special type of compound event where events occur in direct sequence and result in major socioeconomic and environmental impacts. Due to evidence that

suggests that climate hazards can promote or even trigger one or more related climate hazards, the study and understanding of cascading hazards is a major research gap in climate extremes literature. We provide a recent example of a cascading hazard that occurred in Southern California, where dry conditions, subsequent rain and fuel growth, followed by hot and dry fire weather conditions and fires, culminated in a deadly debris flow triggered by rainfall (Fig. 1.1).

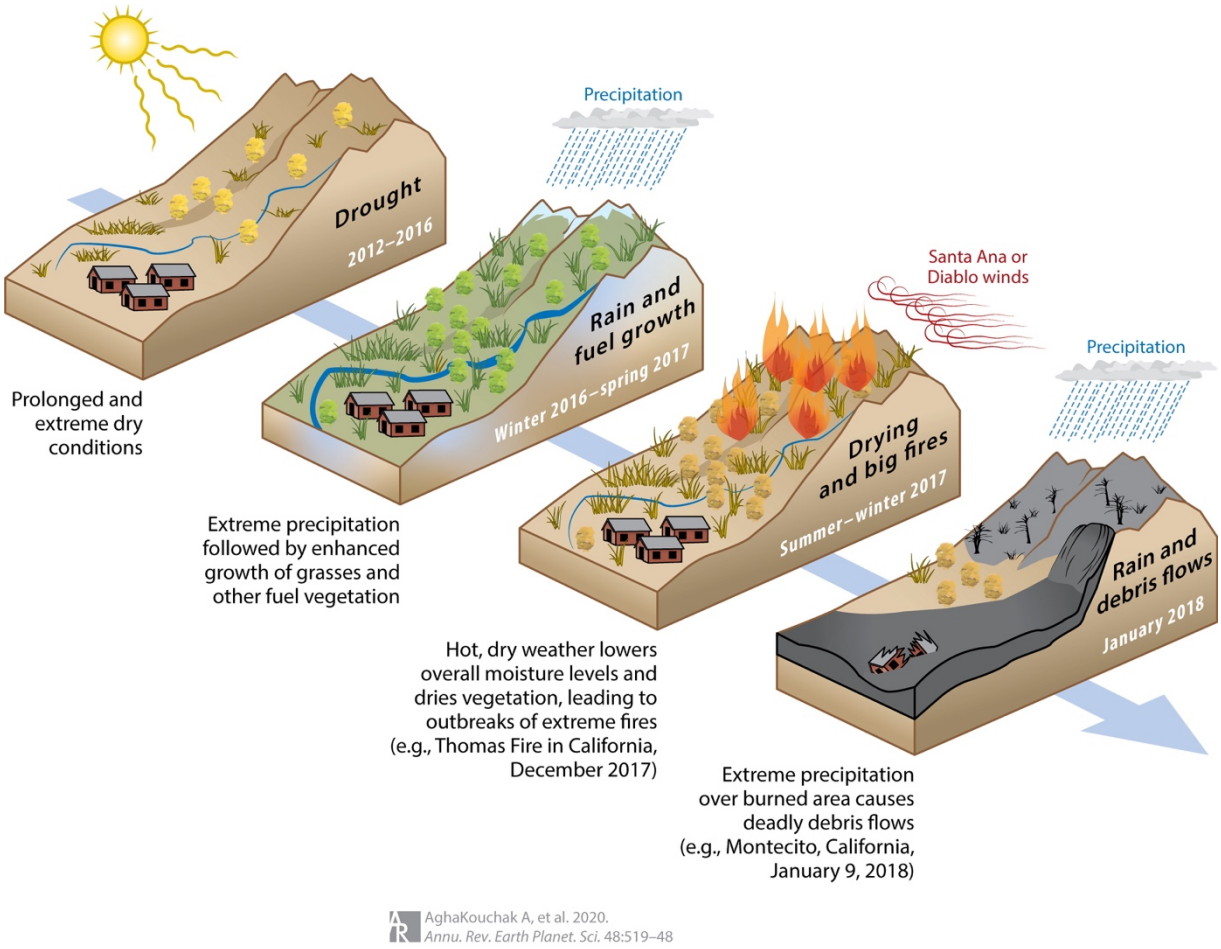

Fig. 1.1. Cascading hazard in Southern California. The consecutive events shown above resulted in significant human health and economic impacts in Southern California: a prolonged extreme drought from 2012 to 2016; heavy rainfall during the winter of 2017, which promoted the growth of fire fuels; a very dry, warm spring and summer, which aided in drying existing vegetation; followed by extreme fires and rainfall over the burned area in January 2018, leading to a deadly debris flow event.

1.3 Progress in Detection and Attribution Literature

With regards to anthropogenic climate change, the *detection* of change is currently defined as the study of determining that the climate system (represented by one or more climate variables) or associated systems that interact with the climate system have experienced a quantifiable change (Easterling et al., 2016; Hegerl et al., 2010; Stott et al., 2010). The *attribution* of the *detected* change is defined as the study of the identification and relative importance of the drivers behind this change (Hegerl et al., 2010; Stott et al., 2010). The detection of change and subsequent attribution of change to anthropogenic activities (such as the emission of greenhouse gas since the start of the Industrial Revolution) serves to deepen our understanding of how humans have externally forced changes in our climate (IPCC, 2013).

Detection and attribution studies present evidence of the physical consequences of anthropogenic forcings which allow us to characterize and quantify the many impacts of climate change. Many detection and attribution studies examine modeled realizations of our historical climate with and without anthropogenic forcings, which allow us to identify whether our observed climate states are due to natural variability, anthropogenic activities, or a combination of the two (Easterling et al., 2016; Stott et al., 2010). These studies also allow us to better interpret climate conditions (ranging from *little to no change* to *significant* changes in climate variables) that have occurred since the Industrial Revolution (Stone et al., 2009). Detection and attribution studies can lead to improvements of short-term predictions of climate states and long-term model projections of future climate scenarios (Easterling et al., 2016). Ideally, detection and attribution studies contribute to regional and global climate change mitigation and adaptation efforts (Stott et al., 2010).

In the early stages of the field, detection and attribution studies mainly examined mean changes in climate variables (Bindoff et al., 2013; Hegerl et al., 2006; Houghton, 1996). The earliest detection and attribution studies focused on attributing global temperature change to anthropogenic emissions (Allen et al., 1994; Barnett & Schlesinger, 1987; Hegerl et al., 1996, 2006; Santer et al., 1994, 1995; Stone et al., 2009; Stott, 2003; Tett et al., 1999; X. Zhang et al., 2006). Changes in mean precipitation and streamflow have also been detected and attributed to anthropogenic activities (Hidalgo et al., 2009; Lambert et al., 2004; Sarojini et al., 2012). Many of these attribution studies used traditional optimal fingerprinting (linear filter) to detect a climate change driven signal amidst the noise of natural climate variability (Hasselmann, 1993).

In recent years, the detection and attribution field has begun to seriously investigate changes in climate extremes (Christidis et al., 2005; Easterling et al., 2016; Fischer & Knutti, 2014, 2015; Meehl et al., 2007; Min et al., 2011, 2013). With respect to climate extremes, detection and attribution studies generally take one of two approaches: 1) statistically examining how anthropogenic activities have caused changes in the likelihood of an extreme event exceeding a specified threshold or 2) mechanistically examining how human changes in climate factors have impacted the severity of an extreme event (Easterling et al., 2016). In 2003, Allen first introduced the statistical approach of climate change attribution and Stott et al. subsequently applied this approach to the 2003 heatwave in Europe (Allen, 2003; Stott et al., 2004). The alternative, mechanistic approach disentangles mesoscale, synoptic, and planetary-scale meteorological phenomena contributing to the magnitude of extreme events (Easterling et al., 2016). Hoerling et al. more recently conducted a mechanistic examination of the physical drivers behind the 2011 Midwestern drought and heatwave extreme event (Hoerling et al., 2012).

Although significant progress has been made in the field of climate change-centric detection and attribution, there are still many research gaps and opportunities in the literature. Extreme event attribution is becoming a hot topic in the field, but many types of extreme events have thus far been ignored in detection and attribution literature. For example, although extreme precipitation has been examined on regional and global scales, there are few studies focusing on drought events (Fischer & Knutti, 2014, 2015; Marvel et al., 2019; Min et al., 2011). Drought events are complicated to examine due to the various ways that drought is defined and characterized in current literature. Traditional drought studies use observations to calculate parametrically based indices such as the Standardized Precipitation Index (SPI), the Standardized Precipitation-Evapotranspiration Index (SPEI), and the Palmer Drought Severity Index (PDSI) (Easterling et al., 2016). With different climate scenarios (e.g. historical climate with or without anthropogenic emissions), calculating equivalent numerical values of drought indices through traditional probability distribution fitting poses a computational challenge. Thus, the formal detection and attribution of changes in drought events is an existing research gap and should be filled to better prepare for future changes in drought events due to climate change. In addition, to our knowledge, compound events have not been formally studied in detection and attribution literature. Since compound events have already been associated with many substantial impacts and are already showing significant changes in present-day observations (Mazdiyasni & AghaKouchak, 2015; Zscheischler et al., 2018), we argue this is also a critical research gap that deserves attention in the literature.

1.4 Research Gaps and Opportunities

The definition, identification, and analysis of extreme events is difficult due to the rare nature of these events; however, much progress has been made in the past couple of decades, especially with regards to the developing field of compound climate extremes. Since the study of climate extremes is still a developing field, there are many research gaps and opportunities. In the following chapters, we present three studies that address critical research gaps in climate extremes literature:

1. In the 20th century, average annual temperatures in the United States have risen 0.7^{o}C (Wuebbles et al., 2017). In chapter 2, we studied long-term shifts in temperatures occurring during dry months to explore the effect of climate change on interactions between surface moisture and temperature conditions. Since there are established land surface-atmosphere feedbacks that connect drying and warming conditions, we explored whether observations and model simulations showed shifts in temperatures under droughts and whether conditional temperature shifts are also projected for the future.

2. Although current detection and attribution literature has examined the impacts of anthropogenic forcing on mean and extreme precipitation, to our knowledge, the long-term impacts of anthropogenic forcing on drought characteristics have not been explored. In chapter 3, we used historical (including anthropogenic forcing) and historical natural-only Coupled Model Intercomparison Project Phase 5 (CMIP5) model simulations to quantify the impact of anthropogenic forcing on meteorological drought characteristics.

3. Current detection and attribution studies generally evaluate the impacts of anthropogenic forcing on mean or extreme changes in individual climate variables and ignore dependencies between variables. Due to evidence that climate change has significantly impacted observed compound events, we used historical and historical natural-only CMIP5 model simulations to characterize the impact of anthropogenic forcing on concurrent warm and dry events. Chapter 4 presents the results and discussion of this study.

Chapter 2

Amplified Warming of Droughts in the United States in Observations and Model Simulations

This Chapter has been published in Science Advances.

Citation: Chiang, F., Mazdiyasni, O., and AghaKouchak A., 2018. "Amplified Warming of Droughts in Southern United States in Observations and Model Simulations." *Science Advances,* 4(8), eaat2380.

2.1 Introduction

The concurrence of drought and heatwave events have caused severe ecosystem and societal stresses as witnessed during 2014 in California and 2003 in Europe (AghaKouchak et al., 2014; Asner et al., 2015). Land surface and atmosphere interactions have been identified as a major driver in the occurrence of these concurrent extremes. During dry soil moisture conditions, we expect to see associated surface warming as the available energy will be expressed as sensible heat instead of being evaporated as latent heat, causing the concurrence of these conditions (Fischer et al., 2007; Seneviratne et al., 2006; Su et al., 2014). For example, in the European heatwave event, precipitation deficits in the Mediterranean region were noted to precede major heatwaves in neighboring regions (Vautard et al., 2007).

These short-term temperature changes are dependent on the negative and positive feedbacks between the local land surface condition and the atmosphere above (Chang & Wallace, 1987; Dirmeyer et al., 2013; Jin Huang & van den Dool, 1993; Livneh & Hoerling, 2016; Walsh et al., 1985). In addition to temperature changes, low soil moisture in mid-continental areas can alter planetary boundary layer dynamics which influence precipitation (Stéfanon et al., 2014). In contrast, coastal areas experience a thermal contrast between the land and the sea, which is magnified during periods of dry soil, resulting in increased transport of moist air from oceans (Stéfanon et al., 2014). Through many studies, land surface and atmosphere interactions have been established as major climate drivers, especially in transitional climate zones (Fischer et al., 2007; Seneviratne et al., 2006; Su et al., 2014). However, we still do not understand the feedbacks and interactions between all the existing components of the land

surface and the atmosphere. Moreover, we still do not completely understand the full spectrum of changes that will accompany the simple increase in greenhouse gases.

In this chapter, we examined long-term shifts in temperatures occurring during dry months to further explore the effect of climate change on feedbacks between surface moisture and temperature conditions. Drawing from established interactions between drying and warming conditions, we examined whether temperatures during droughts have experienced changes in the 20th century and whether shifts in dry temperatures are projected to occur in the 21st century. Due to projections showing droughts and high temperatures intensifying over the next century, the main objective of the chapter was to understand whether temperatures are projected to experience different rates of intensification when coupled with dry conditions. This chapter evaluated whether conditional temperature shifts under droughts are occurring while acknowledging the possible drivers of land surface-atmosphere interactions and feedbacks under climate change. In this chapter, we also examined changes in atmospheric moisture to evaluate concurrent shifts in the climate system.

For this study, we evaluated temperatures during different drought severities in two observed periods [1902-1951 and 1965-2014] and two modeled periods [1951-2000 and 2050-2099] in the contiguous United States. With the observations, we compared the late and early 20th century to quantify temperature changes that have already occurred. With the multi-model ensemble, we compared the late 21th and late 20th century periods to investigate future conditions relative to the recent historical past. To evaluate coincident changes in atmospheric moisture conditions, we used relative humidity and vapor pressure deficit (VPD) as quantitative measures of available moisture in the atmosphere.

2.2 Methodology

For observations, we used monthly temperature, precipitation, and vapor pressure data available from the Climatic Research Unit, CRU TS3.23, which is a gridded time-series climate dataset (30). The data coverage included all areas of the contiguous United States at a 0.5 degree resolution. Estimates for saturated vapor pressure (e_s) were derived using the 2008 WMO CIMO Guide conversion equation:

$$e_s = 6.112 \times \exp\left(\frac{22.46t}{272.62+t}\right) \quad (2.1)$$

where t is the temperature at a given grid point at a given time.

Relative humidity was derived with the standard equation from saturated and actual vapor pressure (e_a):

$$RH = \frac{e_a}{e_s} \times 100\% \quad (2.2)$$

For the model ensembles, we used the bias-corrected spatially disaggregated (BCSD) downscaled CMIP5 multi-model ensembles under representative concentration pathway (RCP) 8.5 at a 0.125 degree resolution available from the U.S. Bureau of Reclamation website (Edwin P. Maurer et al., 2007). The BCSD method is a statistical downscaling method that uses the probability density functions of model output mapped onto observations and then spatially aggregates the results to the desired scale (E. P. Maurer & Hidalgo, 2008). We took an average of the models listed in the Table 2.1 to form the model ensemble.

We used the standardized precipitation index (SPI) as a measure of the relative meteorological dryness of each pixel in the spatial area of interest. For our study, we employed a

non-parametric implementation of SPI to retain the spatial and temporal consistency of the original data, while describing precipitation in the context of the local climatology (Farahmand & AghaKouchak, 2015). We used the empirical Gringorten plotting position:

$$p(x_i) = \frac{i-0.44}{n+0.12} \tag{2.3}$$

where n is the sample size, i is the rank of non-zero precipitation data from smallest to largest, and $p(x_i)$ is the empirical probability for each data point (Farahmand & AghaKouchak, 2015). We standardized the probabilities, p, from Eq. (2.1) using the standard normal distribution function, ϕ :

$$SI = \phi^{-1}(p) \tag{2.4}$$

(18). Although drought can be characterized by many timescales, we chose to use a 6-month timescale to capture intra-annual seasons without including overly brief wet or dry periods.

We first calculated the average temperature shift associated with each dryness threshold for each pixel. To find the temperature shift between periods, we calculated the difference between the temperature average associated with each period. We used the United States Drought Monitor (USDM) classification scheme (D0, D1, D2, etc.) to define the drought severity thresholds. D0 begins with an SPI of -0.5, D1 begins with an SPI of -0.8, and D2 begins with an SPI of -1.3. For instance, for the D0 threshold, we isolated months that had an SPI value of -0.5 or lower and found the corresponding temperature average. We then summarized the temperature shifts within seven climatically consistent regions in the contiguous U.S. For average shifts of relative humidity and VPD between time periods, we used the same dryness thresholds for all pixels.

We used the two-sample Kolmogorov-Smirnov non-parametric test:

$$D^* = \max_x \left(\left|\hat{F}_1(x) - \hat{F}_2(x)\right|\right) \tag{2.5}$$

where $\hat{F}_1(x)$ is the proportion of values in the first distribution less than or equal to x and $\hat{F}_2(x)$ is the proportion of values in the second distribution less than or equal to x (Massey, 1951),

and Student's two-sample *t*-test:

$$t = \frac{\bar{x} - \bar{y}}{\sqrt{\frac{s_x^2}{n} + \frac{s_y^2}{m}}} \tag{2.6}$$

where $\bar{x}$ and $\bar{y}$ are the sample means, s_x and s_y are the sample standard deviations, and n and m are the sample sizes for the two data samples (McDonald, 2009), to determine whether regional shifts under the drier conditions were significant in comparison to the average temperature change experienced in the area ($\alpha = 0.05$).

Table 2.1 CMIP5 climate models used for chapter 2.

Modeling Center	Institute ID	Model Name
Commonwealth Scientific and Industrial Research Organization (CSIRO) and Bureau of Meteorology (BOM), Australia	CSIRO-BOM	ACCESS1.0 ACCESS1.3
Beijing Climate Center, China Meteorological Administration	BCC	BCC-CSM1.1 BCC-CSM1.1(m)
Canadian Centre for Climate Modeling and Analysis	CCCMA	CanESM2
National Center for Atmospheric Research	NCAR	CCSM4
Community Earth System Model Contributors	NSF-DOE-NCAR	CESM1(BGC) CESM1(CAM5)
Centro Euro-Mediterraneo per I Cambiamenti Climatici	CMCC	CMCC-CM
Centre National de Recherches Météorologiques / Centre Européen de Recherche et Formation Avancée en Calcul Scientifique	CNRM-CERFACS	CNRM-CM5
Commonwealth Scientific and Industrial Research Organization in collaboration with Queensland Climate Change Centre of Excellence	CSIRO-QCCCE	CSIRO-Mk3.6.0
LASG, Institute of Atmospheric Physics, Chinese Academy of Sciences and CESS, Tsinghua University	LASG-CESS	FGOALS-g2
The First Institute of Oceanography, SOA, China	FIO	FIO-ESM
NOAA Geophysical Fluid Dynamics Laboratory	NOAA GFDL	GFDL-CM3 GFDL-ESM2G GFDL-ESM2M
NASA Goddard Institute for Space Studies	NASA GISS	GISS-E2-R
National Institute of Meteorological Research/Korea Meteorological Administration	NIMR/KMA	HadGEM2-AO
Met Office Hadley Centre (additional HadGEM2-ES realizations contributed by Instituto Nacional de Pesquisas Espacials)	MOHC (additional realizations by INPE)	HadGEM2-CC HadGEM2-ES
Institute for Numerical Mathematics	INM	INM-CM4
Institut Pierre-Simon Laplace	IPSL	IPSL-CM5A-LR IPSL-CM5A-MR IPSL-CM5B-LR
Japan Agency for Marine-Earth Science and Technology, Atmosphere and Ocean Research Institute (The University of Tokyo), and National Institute for Environmental Studies	MIROC	MIROC-ESM MIROC-ESM-CHEM
Atmosphere and Ocean Research Institute (The University of Tokyo), National Institute for Environmental Studies, and Japan Agency for Marine-Earth Science and Technology	MIROC	MIROC5
Max-Planck Institut für Meteorologie (Max Planck Institute for Meteorology)	MPI-M	MPI-ESM-LR MPI-ESM-MR
Meteorological Research Institute	MRI	MRI-CGCM3
Norwegian Climate Centre	NCC	NorESM1-M NorESM1-ME

2.3 Results

Between the early and late 20th century observations from the Climatic Research Unit (CRU), the southern and northeastern U.S. experienced higher temperature shifts under dry conditions than the average climate (Fig. 2.1a).

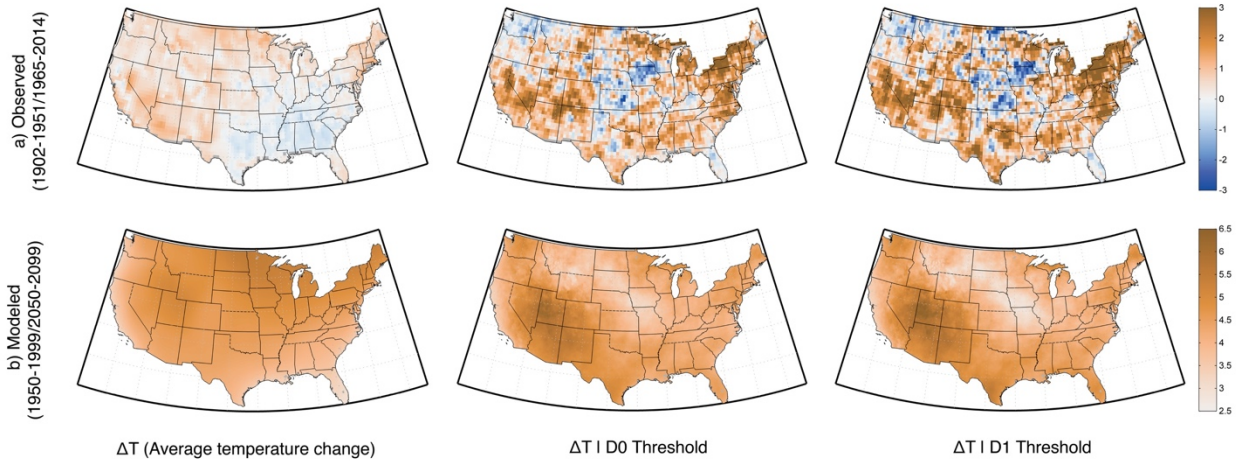

Fig. 2.1. Temperature shift associated with each dryness condition. Average temperature shift relating to each condition (including all wet and dry conditions, at or under the D0 threshold, at or under the D1 threshold). **(A)** We compare the period 1965-2014 relative to a baseline period of 1902-1951 with the observed CRU data. **(B)** We compare the future period 2050-2099 relative to the historical baseline of 1950-1999 with the CMIP5 model average ensemble.

The southern states experienced a similar pattern of change in the downscaled Coupled Model Intercomparison Project Phase 5 (CMIP5) multi-model ensemble (Fig. 2.1b). In the observations, the regions associated with amplified temperature change under the D0 and D1 thresholds contrasted with the warming regions highlighted in the average temperature change panel, indicating that the observed pattern was not purely an amplification of the temperature change observed under average climate conditions. The accelerated warming under dry conditions also does not correspond with regions commonly identified as semi-arid or arid. For example, the southern United States experiences a dry climate in the west and a humid climate in the east; however, all southern states experience similar accelerations in warming under dry conditions.

Around the globe, increasing aridity has been attributed to a more rapid increase in evaporative demand relative to precipitation supply (Berg et al., 2016; Fasullo, 2010; Ficklin & Novick, 2017). This increase in aridity has been expressed in the decreasing relative humidity and increasing vapor pressure deficit that is observable in Fig. 2.2a and 2.2b (Berg et al., 2016; Byrne & O'Gorman, 2016; Ficklin & Novick, 2017). Under the D0 and D1 thresholds, we observed concurrent increases and decreases in temperature, relative humidity, and VPD (Fig. 2.1a, 2.2a, 2.2b). In regions where temperature shifts under droughts have outpaced temperature changes in the average climate, relative humidity has decreased and VPD has increased. For example, the Northeastern region in Fig. 2.1a, 2.2a, and 2.2b shows positive temperature shifts corresponding with decreases in relative humidity and increases in VPD.

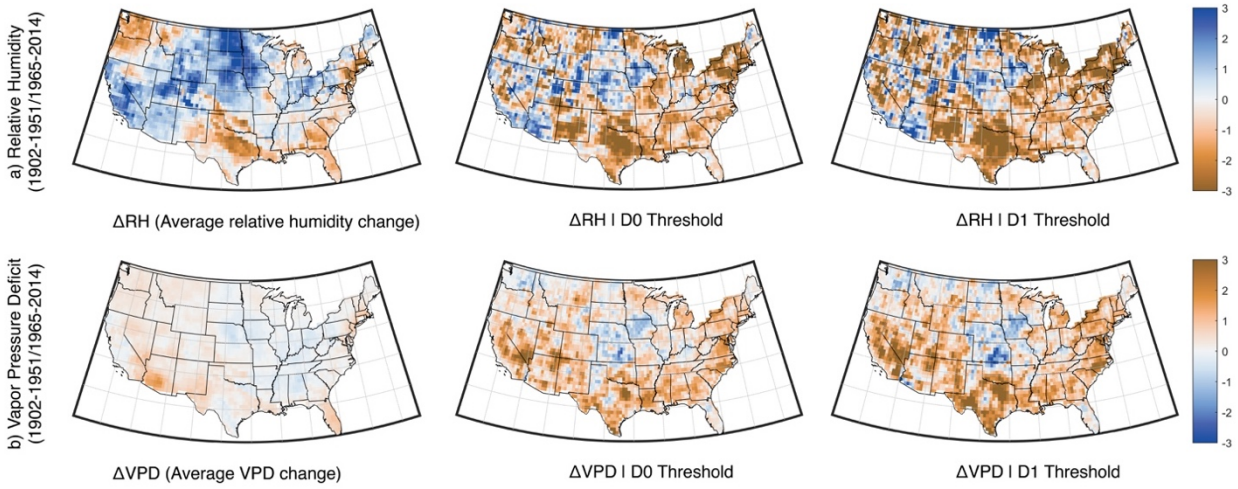

Fig. 2.2. Moisture shift associated with each dryness condition. Average shift between 1965-2014 relative to 1902-1951 associated with each dryness condition used in Fig. 1. **(A)** Observed average shift in relative humidity associated with each condition. **(B)** Observed average shift in VPD associated with each condition.

We also observed corresponding increases in moisture in regions where temperature shifts under the average climate have outpaced shifts under drought. For instance, in the upper Midwestern region, negative temperature shifts relate to increases in relative humidity and decreases in VPD (Fig. 1a, 2a, 2b). McHugh et al. recently established that non-rainfall water

sources – such as atmospheric moisture – can act as a significant source of moisture in drylands during periods when the relative humidity in the soil is lower than the relative humidity of the air above (McHugh et al., 2015). This finding explains the mechanism behind stagnant or cooling temperature shifts under drought conditions with respect to average temperatures. The effect of water vapor on soil moisture (and by proxy, land surface warming) highlights the importance of the general dryness or wetness of the area, which cannot be attributed to a single variable. In all regions, we hypothesize that during periods of drought, the concurrent shift in atmospheric moisture is contributing to the amplification of temperature changes relative to the average climate. It is important to note that when considering all months – wet or dry, this concurrence does not occur between the variables (see first column for Fig. 2.1a, 2.2a, 2.2b). This highlights the importance of meteorological drought in strengthening the correlation between changes in atmospheric moisture and temperature (Farahmand & AghaKouchak, 2015).

With regards to the spatial pattern of temperature, relative humidity, and VPD changes, we attach the decreasing availability of regional moisture relative to evaporative demand. Changes in relative humidity and VPD are the physical manifestations of the limits on land evaporation (Ficklin & Novick, 2017). The limit on land evaporation will increase the amount of local sensible heat, subsequently leading to a relative warming of the land surface. As shown in the results of this chapter, this is amplified during periods of drought. Although increases in temperature due to climate change have increased the upper limit of saturation vapor pressure, actual vapor pressure is limited by the relative lack of available moisture, especially during droughts (Byrne & O'Gorman, 2016; Ficklin & Novick, 2017).

We hypothesize that increases in drought frequencies due to the behavior of the Pacific Decadal Oscillation and the Southern Oscillation Index may have shaped the southern and

eastern patterns in the observed shift (Kam et al., 2014). Changes in atmospheric circulation patterns and vertical transport of moisture due to climate change may have contributed to the spatial patterns in the shift (IPCC, 2013). In addition, regional changes in human activities may have resulted in changes in soil moisture and temperature (Feng & Liu, 2015). Dampened summer temperature highs have been associated with intensifying irrigation in the upper Midwestern region (N. D. Mueller et al., 2016). These agriculturally-influenced climate trends relate directly to the Midwestern cooling signal shown in Fig. 2.1a. In contrast, since the 1960s, annual snow-cover extent has shrunken ten percent (Dore, 2005). The occurrence of snow cover significantly influences local temperatures due to albedo and emissivity properties of snow (T. Zhang, 2005). Snowmelt also acts as a latent heat sink, increasing soil moisture levels and regulating local temperatures (T. Zhang, 2005). Thus, a decrease in snow-cover extent could be associated with an increase in surface temperature, corresponding with the amplified temperature shifts along the East Coast in Fig. 2.1a.

As shown in Fig. 2.1b, the spatial pattern of temperature change does not coincide with the north to south gradient of latitudinal heating predicted under the RCP 8.5 scenario. Instead of the north experiencing greater shifts in comparison to the south, our results display the opposite pattern. The spatial patterns where amplified shifts in temperature are projected to occur can also be seen in the patterns in relative humidity and VPD. CMIP5 ensembles have predicted changes in water vapor concentrations and changes throughout the hydrologic cycle due to projected climate change, causing shifts in the distributions of precipitation and evaporation around the globe (Zhou et al., 2014). Significant decreases in the difference between precipitation and surface evaporation are projected to occur in the southern regions across all seasons (Sheffield et al., 2014), corresponding to the temperature conditions displayed in Fig. 2.1b.

Regional delineations in Fig. 2.3a and 2.3b highlight the differences between the historical observations and model projections. Historically, the northeastern region of the U.S. shows the amplified drought-associated temperature shift, while CMIP5 models predict a smaller, more muted future shift in temperature with respect to the average climate in the entire upper half of the U.S., including the Northeast. CRU observations show that the median dry temperature shifts 0.81 degrees higher than the average climate when we isolate regions with amplified temperature shifts. In the CMIP5 projections, the median dry temperature shifts 0.30 degrees higher than the average climate in the regions with amplified temperature change. The shifts quantified in the observations and models shows the influence of dry periods on the increasing intensity of climate conditions in the southern U.S. These changes occurred for VPD and relative humidity as well.

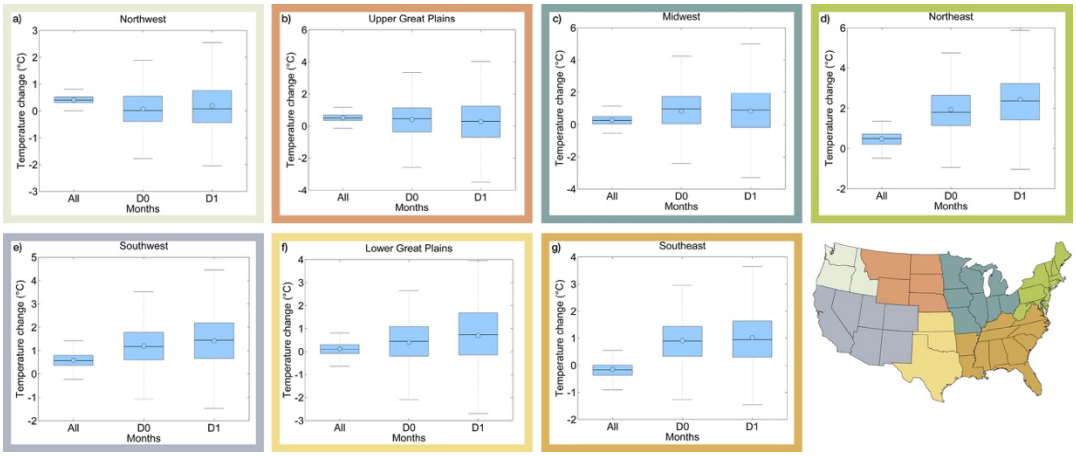

Fig. 2.3a. Regional temperature shift boxplots for observations. Regional boxplots displaying the temperature shifts corresponding to each dryness condition for the CRU observations [1965-2014 relative to 1902-1951].

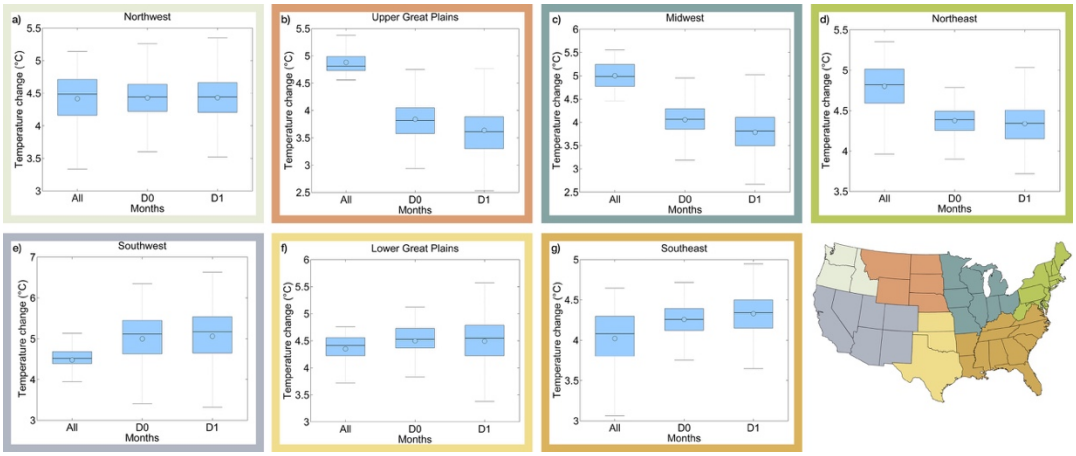

Fig. 2.3b. Regional temperature shift boxplots for model ensemble. Regional boxplots displaying the temperature shifts corresponding to each dryness condition for the CMIP5 model ensemble [2050-2099 relative to 1950-1999].

We also plotted cumulative distribution functions of the temperature shifts under different dryness conditions to illustrate distributional changes between the periods. Fig. 2.4a shows that observed temperatures in the southeastern U.S. shift to the right under D0 drought conditions. A shift to the right represents more severe temperature conditions. Fig. 2.4b also shows the modeled temperature distribution under the D0 condition increasing the emphasis on warmer months in comparison to the average climate. Distributional plots for the remaining regions reflect the results from the box plot figures (Fig. 2.5a, 2.5b).

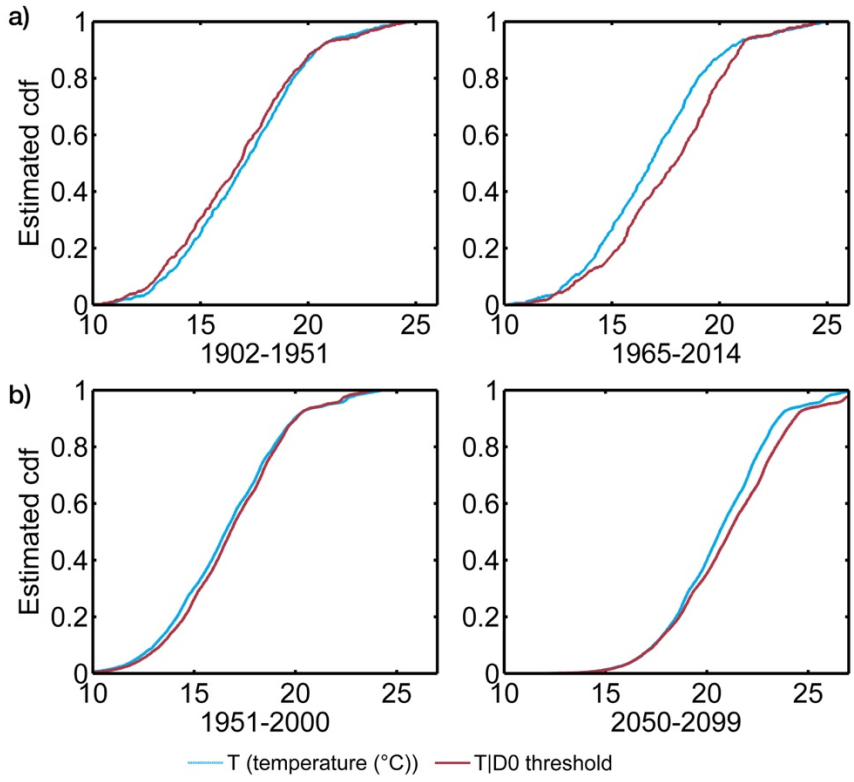

Fig. 2.4. Distributional shift associated with the southeastern U.S. Distributional plots comparing the shifts between the D0 condition and the average climate for the southeastern region of the U.S. **(A)** We compare the period 1965-2014 relative to a baseline period of 1902-1951 with the observed CRU data. **(B)** We compare the future period 2050-2099 relative to the historical baseline of 1950-1999 with the CMIP5 model average ensemble.

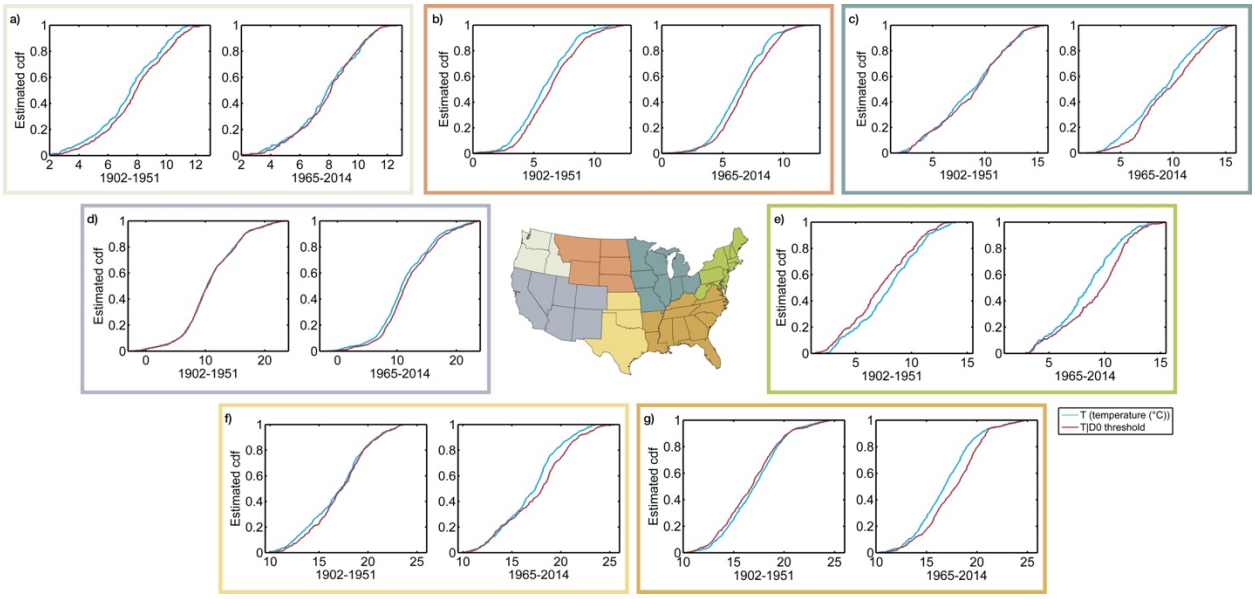

Fig. 2.5a. Distributional shifts for observed U.S. Distributional plots comparing the observed shifts between the D0 condition and the average climate for all regions using the CRU observations [1965-2014 relative to 1902-1951].

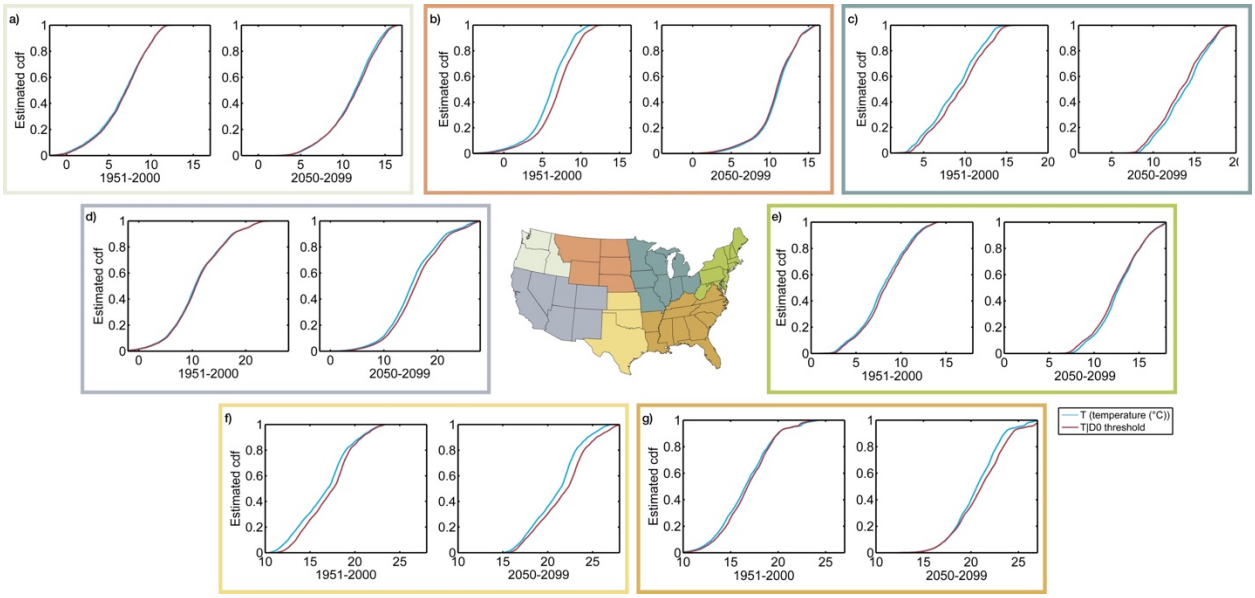

Fig. 2.5b. Distributional shifts for projected U.S. Distributional plots comparing the projected shifts between the D0 condition and the average climate for all regions using the CMIP5 ensemble [2050-2099 relative to 1950-1999].

The Kolmogorov-Smirnov and Student's t tests revealed statistically significant differences between the shifts seen from average temperatures and the shifts seen under the D0 threshold in the two observational periods in all regions. The K-S test also showed statistically significant differences between the average temperature and D0 threshold shifts in comparing the future projections relative to the modeled past. T-testing showed that all regions except the Northwest show statistical differences between the dry and average temperature shifts. The statistical tests highlight that the differences between the amplified temperature shifts recorded in the observations and models are statistically significant.

2.4 Discussion and Conclusion

The observed and projected amplifications in temperature change in the southern U.S. will have severe ramifications in environmental and social sectors. Droughts alone have had severe urban, agricultural, and ecological impacts in recent years, directly and indirectly reducing water availability (Rosenzweig & Urban Climate Change Research Network, 2011). Warm periods have also impacted many of the same sectors by stressing vulnerable populations, food resources, energy, and transportation systems (Mazdiyasni & AghaKouchak, 2015; Rosenzweig & Urban Climate Change Research Network, 2011). Under our future projections of amplified drought-conditioned temperature shifts in the southern U.S., the occurrence of concurrent extremes will likely increase and exacerbate the impacts anticipated from individual extremes. This is exceedingly important as dry lands are becoming more widespread under climate change, which will widen the documented temperature impact (Fu & Feng, 2014). Future studies should focus on the ramifications of these temperature shifts to quantify projected risks on population health, food supply, and infrastructure.

Our interpretations of the findings are limited by the accuracy of our observations and model projections. In some areas, the CMIP5 models may have inconsistent physical interpretations since representations of land-surface and atmospheric interactions vary across models. Although the models capture large-scale temperature patterns, extreme precipitation events are still not adequately represented (IPCC, 2013; Sheffield et al., 2014). The capture of extreme precipitation events has the potential to affect the timing of dry and wet periods in the models. Projections of ENSO timing and variability also suffer from model biases (IPCC, 2013). In addition, the CMIP5 projections have trouble with warm and cool sea surface temperature

biases in the Pacific and Atlantic oceans (Fu & Feng, 2014), which influence teleconnected climate variables such as precipitation. The known errors in the CMIP5 output prevent us from drawing concrete conclusions from the differences between the observations and the projections.

Our results show that droughts have been experiencing amplified temperature shifts relative to the average climate in the southern and northeastern regions of the United States. The spatial pattern of the drought conditioned temperature shift can largely be associated with observed shifts in atmospheric moisture content such as relative humidity and VPD. Although we cannot define which variable is the driver at this temporal scale, both temperature and moisture shifts are interacting and amplifying under drought conditions. Projections show that droughts will be significantly warmer than average conditions across the southern region of the U.S., and are also associated with modeled shifts in relative humidity and VPD. This study highlights the importance of atmospheric moisture in the absence of precipitation in driving changes in the energy and hydrologic cycles.

Chapter 3

The Impact of Anthropogenic Forcing on Drought Characteristics

This Chapter is currently under review.

Chiang, F., Mazdiyasni, O., and AghaKouchak A. "Evidence of anthropogenic impacts on global drought frequency, duration, and intensity."

3.1 Introduction

As we have previously expressed, droughts have severe direct and indirect impacts on ecological, agricultural, and economic sectors, such as damaging natural ecosystems and crippling crop yields (Vicente-Serrano et al., 2013; Wilhite et al., 2007). Relatively low water availability (i.e. droughts) can also have strong ramifications on solar thermal, geothermal, and hydropower generation (Forrest et al., 2018; Tarroja et al., 2018). In addition, drought events can influence the occurrence of dependent hazards, such as heatwaves, which we will explore in greater detail in the following chapter (Fischer et al., 2007). In recent historical observations, changes in meteorological drought frequency, duration, and intensity have been noted across the globe with Global Precipitation Climatology Center observations (Spinoni et al., 2014). In addition, Climatic Research Unit observations have also shown a significant positive trend in the percentage of land areas under meteorological drought (Nasrollahi et al., 2015). Since future climate projections suggest increases in drought frequency and severity will occur in the Americas, Europe, Asia, and Africa, the characterization of drought features is an important and relevant area of study in the field of hydrology (Herrera-Estrada et al., 2017; Hirabayashi et al., 2008; Martin, 2018; Spinoni et al., 2018).

Previous detection and attribution studies have used observations and model simulations to attribute increasing trends of mean and extreme temperature and precipitation occurrences to climate change (Easterling et al., 2016; Fischer & Knutti, 2014, 2015; Peter A. Stott et al., 2004; Williams et al., 2015; X. Zhang et al., 2007a). Using a fractional risk measure (referred to as 'fraction of attributable risk'), Fischer and Knutti (2015) found that 18% of moderate daily precipitation extremes can be attributed to the present-day 0.85 ^{o}C temperature increase. In addition, Fischer and Knutti attributed 75% of the moderate daily hot extremes to the present-day

temperature increase (Fischer & Knutti, 2015). Zhang et al. also detected an observable change in the latitudinal distribution of precipitation, which they argued could not be explained by natural variability (X. Zhang et al., 2007a).

Although there have been many detection and attribution studies on hydroclimatic variables in the literature (T. P. Barnett et al., 2008; Fischer & Knutti, 2015; Hidalgo et al., 2009; Peter A. Stott et al., 2010; X. Zhang et al., 2007b), the global influence of anthropogenic climate change on different drought characteristics (e.g., duration, frequency, severity) has not been explicitly quantified. Previously, Wehner et al. reviewed the changes that have occurred in different drought types in the United States (Wehner et al., 2017). So far, historical changes in meteorological drought conditions in the United States have not been formally attributed to anthropogenic forcing (Wehner et al., 2017). On the other hand, hydrological drought conditions in the Western U.S. have been attributed to anthropogenic forcing, since they are dependent on snowfall accumulation and eventual snowmelt, which are strongly influenced by temperature conditions (Hidalgo et al., 2009).

In 2019, Marvel et al. used tree ring records to present evidence of the influence of human activity on global agricultural (soil moisture) drought trends since the start of the 20th century (Marvel et al., 2019). With the Palmer Drought Severity Index (PDSI), Marvel et al. (2019) detected an overall increasing signal of human activity in the global drought atlas region, with a decreasing trend during 1950-1975 that may have resulted from anthropogenic aerosol emissions during the time period. On the whole, previous studies have shown that the influence of anthropogenic forcing on drought events is complicated, due to the variety of ways that drought can be characterized (meteorological, agricultural, hydrological).

The objective of this chapter is to present a global examination of the influence of anthropogenic forcing on meteorological drought characteristics. We focus our attention on meteorological droughts to isolate the impact of emissions on the lower tail of the precipitation distribution without the direct influence of temperature. We used historical and historical natural-only CMIP5 climate model simulations to attribute differences in meteorological drought characteristics to anthropogenic forcing. We quantified the drought frequency, maximum drought duration, and maximum drought intensity of both historical and natural-only climate scenarios to examine the impact of anthropogenic emissions on drought features (see Methods Section for more detail). Traditionally, drought indices are parametrically calculated, however, creating comparable drought indices from different model simulations with this approach can be complicated and computationally costly. In this chapter, we introduce the use of a generalized framework to compare droughts under different modeled climate scenarios in a consistent manner.

To directly quantify the impact of anthropogenic forcing on drought events, we estimated the probability of drought occurrences that can be attributed to anthropogenic climate change. We employed the probability ratio concept used in Fischer and Knutti (2015) to quantify the likelihood of drought months occurring in the historical model world relative to the historical natural-only model world in the late 20th century. By examining the global distribution of drought risk, we could identify regions of greater sensitivity to anthropogenic climate change from a meteorological drought perspective.

Separately, we examined the historical and historical natural-only zonal distributions of the three characteristics (frequency, maximum duration, maximum intensity) in the late 20th century and the spatial distributions of how the characteristics were modeled to change between

the late 19th and late 20th centuries. We also investigated if differences between anthropogenic and natural-only scenarios could be associated with specific climate regimes. To address this question, we aggregated shifts in drought features from dry, average, and wet land area pixels defined by annual precipitation data from the historical natural-only climate scenario. We also investigated the differences between drought features in the historical and the historical natural-only scenarios by aggregating all 'agricultural' pixels (see Methods for more detail) and aggregating all land pixels from both historical and historical natural-only conditions. By examining specific regional and global aggregations of drought features, we could better assess the influence of anthropogenic forcing on dry extremes. Understanding the contribution of anthropogenic climate change to present-day drought features (i.e. frequency, duration, and intensity) are important in our interpretation of historically observed drought shifts, and can also improve future climate projections. By exploring these drought features separately, we can better understand the sensitivities of the individual features to anthropogenic climate change.

3.2 Methodology

For our study, we used monthly precipitation data from the Coupled Model Intercomparison Project Phase 5 (CMIP5) historical and historical natural-only model simulations (see Table 3.1 for the list of models used for this study) (Taylor et al., 2011). To create a multi-model ensemble, we regridded the model output to a common 1 degree grid using nearest-neighbor interpolation and then calculated the multi-model median of each pixel. We included all land area within 60^{o}S and 60^{o}N in our analysis.

We used the non-parametric standardized precipitation index (SPI) to represent the relative meteorological dryness of each pixel in our study area (Farahmand & AghaKouchak, 2015). To quantify the features in the late 20th century (1956-2005) and feature shifts between the late 19th and 20th centuries (1851-1900 and 1956-2005), we generated 6-month SPI values for each month in each time period. The value corresponding to the month of June would include precipitation information from the 6-month period from January to June by first summing all monthly precipitation values. To create comparable SPI values in the historical and historical natural-only scenarios, we then ranked each month's precipitation sum by using the historical natural-only climatology of the corresponding pixel and month. We included a zero in our historical natural-only climatology to account for the minimum possible 6-month precipitation sum that could occur in either climate scenario. By basing the reference climatology on the historical natural-only data, we could ensure equivalent drought definitions even under differing climate forcings. More details on calculating SPI non-parametrically can be found in Farahmand and AghaKouchak (2015).

We defined drought frequency as the number of non-consecutive events below the drought threshold of SPI = -1.5, drought duration as the number of consecutive months

associated with each drought event, and drought intensity as the cumulative sum of SPI values associated with the months under drought for each event. Maximum duration and maximum intensity refer to the maximum value for each pixel in each period.

To evaluate how anthropogenic warming has impacted drought features in different climate regimes, we classified percentiles of annual precipitation into 3 classes, ranging from the driest (0-33th percentile) to wettest (67-100th percentile) land areas. We extracted the corresponding pixel values to compare the spatial distributions of drought feature change in each class. To assess anthropogenic impacts on the agricultural sector, we also explicitly examined drought features in pixels where more than 50 percent of the land area could be classified as cropland, using global agricultural data from Ramankutty et al. 2008 (Ramankutty et al., 2008). We estimated spatial distributions by fitting kernel density estimates to our extracted data points (Michael Waskom et al., 2016). We also conducted two-tailed two-sample t-tests on each historical and historical natural-only pair for pixels falling under each climate regime category (dry, average, wet land areas) as well as for cropland and global land area pixels.

Using the most recent 50 years of our model ensemble dataset (1956-2005), we also calculated the probability ratio (PR) concept to demonstrate the impact of anthropogenic climate change on drought occurrences. The PR of each pixel can be represented by a simple ratio:

$$PR = P_1/P_0 \tag{3.1}$$

where P_0 represents the probability of a drought occurring in historical natural-only conditions and P_1 represents the probability of a drought occurring in historical conditions (Fischer & Knutti, 2015).

Table 3.1. CMIP5 climate models used in chapter 3

Modeling Center	Institute ID	Model Name
Commonwealth Scientific and Industrial Research Organization (CSIRO) and Bureau of Meteorology (BOM), Australia	CSIRO-BOM	ACCESS1.3
Beijing Normal University (BNU)	BNU	BNU-ESM
Canadian Centre for Climate Modeling and Analysis	CCCMA	CanESM2
National Center for Atmospheric Research	NCAR	CCSM4
Centre National de Recherches Météorologiques / Centre Européen de Recherche et Formation Avancée en Calcul Scientifique	CNRM-CERFACS	CNRM-CM5
Commonwealth Scientific and Industrial Research Organization in collaboration with Queensland Climate Change Centre of Excellence	CSIRO-QCCCE	CSIRO-Mk3-6-0
LASG, Institute of Atmospheric Physics, Chinese Academy of Sciences and CESS, Tsinghua University	LASG-CESS	FGOALS-g2
NASA Goddard Institute for Space Studies	NASA GISS	GISS-E2-H GISS-E2-R
Institut Pierre-Simon Laplace	IPSL	IPSL-CM5A-LR IPSL-CM5A-MR
Japan Agency for Marine-Earth Science and Technology, Atmosphere and Ocean Research Institute (The University of Tokyo), and National Institute for Environmental Studies	MIROC	MIROC-ESM MIROC-ESM-CHEM
Meteorological Research Institute	MRI	MRI-CGCM3
Norwegian Climate Centre	NCC	NorESM1-M

3.3 Results

First, we can examine global patterns of historical natural-only and historical drought frequency, maximum drought duration, and maximum drought intensity from 1956-2005 (Figure 3.1). Figures 3.1a, b, and c, which represent a) drought frequency, b) maximum drought duration, and c) maximum drought intensity under historical natural-only conditions, show relatively uniform values across the global land area. As our definition of the drought threshold is based on the historical natural-only climatology from 1850-2005, our results correspond well with our expectation that only relatively small differences would occur from natural variations in meteorological conditions (between 1956-2005 and 1850-2005). In contrast, Figure 3.1d, which shows the number of drought events occurring under historical conditions, show substantial hotspots of drought occurrences in tropical regions as well as extratropical regions of Southern Europe, South America, and Africa. Figures 3.1e and 3.1f depict the presence of similar hotspots of e) maximum drought duration and f) maximum drought intensity. From our comparison of the historical spatial patterns of drought features to their historical natural-only analogs, we can highlight the recent impact of anthropogenic forcing on meteorological droughts.

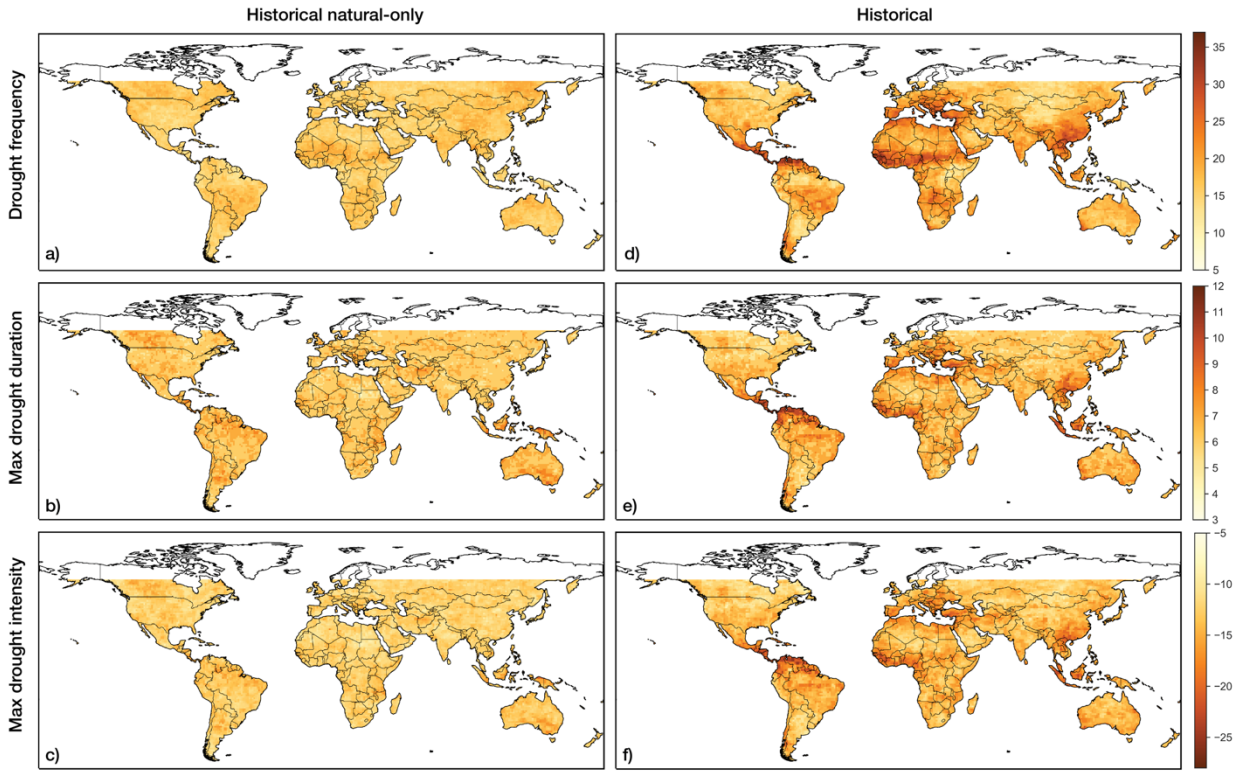

Figure 3.1. Global distribution of drought features. ***a)*** Drought frequency from the CMIP5 historical natural-only multi-model ensemble median. The value expressed in each pixel represents the number of droughts that occurred between 1956-2005. ***b)*** Maximum drought duration (number of months associated with the longest drought from 1956-2005) from the historical natural-only models. ***c)*** Maximum drought intensity (the cumulative SPI value from the most intense drought from 1956-2005) from the historical natural-only models. ***d)*** Drought frequency from the historical model median. ***e)*** Maximum drought duration from historical models. ***f)*** Maximum drought intensity from historical models.

We can also examine how drought frequency, duration, and intensity have evolved over our study period. Figures 3.2a, b, and c show that historical natural-only drought frequency, maximum drought duration, and maximum drought intensity have experienced minimal increases and decreases from the late 19th to the late 20th centuries. From a global perspective, the three features have shifted towards a slightly wetter profile. Figure 3.2d, e, and f allow us to examine historical shifts in our drought characteristics. Figure 3.2 shows a strong resemblance to Figure 3.1, with increases in drought frequency, maximum drought duration, and maximum drought intensity in the same hotspot regions shown in the previous figure. In general, the modeled changes in drought characteristics between the two time periods reflect trends in

observed drought frequency, duration, and severity that have been documented in Spinoni et al. 2014 (Spinoni et al., 2014). From our global analysis, we observe that the aforementioned 'hotspot' regions have also experienced increases in drought frequency, maximum drought duration, and maximum drought intensity under historical conditions that were not experienced under historical natural-only conditions.

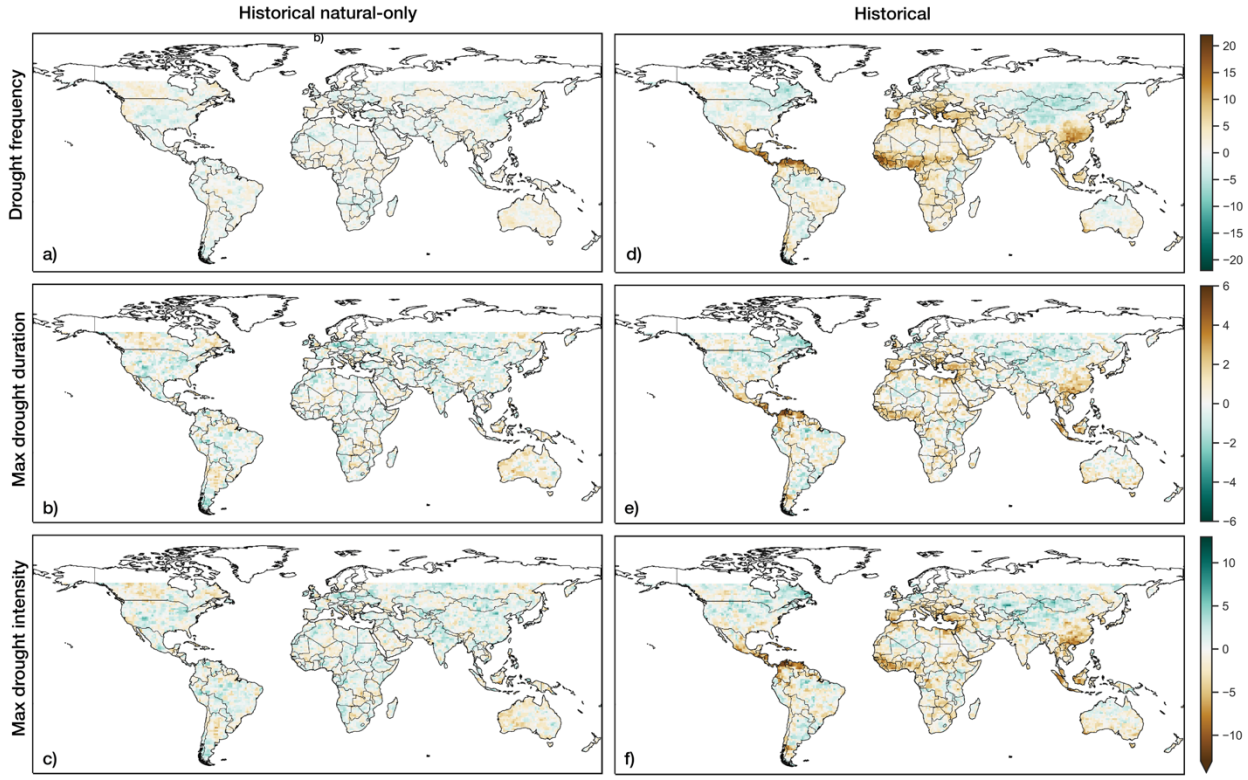

Figure 3.2. Global shifts in drought features. ***a)*** Difference in drought frequency between 1956-2005 and 1851-1900 from the CMIP5 historical natural-only multi-model ensemble median. ***b)*** Difference in maximum drought duration in historical natural-only models. ***c)*** Difference in maximum drought intensity in historical natural-only models. ***d)*** Difference in drought frequency under historical conditions. ***e)*** Difference in maximum drought duration under historical conditions. ***f)*** Difference in maximum drought intensity under historical conditions.

Regions such as the Eastern United States show very similar conditions in the historical and historical natural-only simulations. The Eastern U.S. is an example of a region where natural variability may still be dominating over human contributions to changes in climate. However, many of the regions where drought features have developed a stronger presence in historical

conditions are regions that experienced a slight weakening of drought features in historical natural-only conditions. This highlights the importance of accurately capturing natural variability in the models to understand the contribution of present-day and future anthropogenic climate change to drought features. When only examining observational data, we cannot fully understand how anthropogenic forcing have impacted shifts or trends in our historical climate.

When we take the latitudinal median of the global information from Figure 3.1, we can clearly see distinct distributions of drought frequency, maximum drought duration, and maximum drought intensity for historical natural-only (blue) and historical (red) simulations (Figures 3.3a, b, and c). In 1956-2005, drought frequency, maximum drought duration, and maximum drought intensity all exhibit strong differences in historical simulations relative to historical natural-only simulations, emphasizing the impact that anthropogenic emissions have had on drought features, especially between 0-40^{o}N. Historical conditions also clearly experience greater variability across many of the latitudinal bands in comparison to natural-only conditions. Figures 3.3d, e, and f summarize the global information from Figure 3.2, depicting how drought frequency, duration, and intensity have shifted from the late 19th century to the late 20th century. In addition to strongly resembling the distributions of drought features from the late 20th century, the patterns in Figure 3.3d, e, and f correspond well with the latitudinal pattern of precipitation change shown in 20th century observations (X. Zhang et al., 2007a). Within 10^{o} latitude bands, Zhang et al. (2007) highlighted detectable decreasing trends in mean annual precipitation between 0-30^{o}N as well as increasing trends between 0-30^{o}S and 50-70^{o}N. From our results, we show that latitudes with decreasing precipitation trends relate to stronger drought frequency, duration, and intensity values in historical relative to historical natural-only conditions, while

latitudes with increasing precipitation trends exhibit relatively smaller differences between historical and natural-only drought conditions.

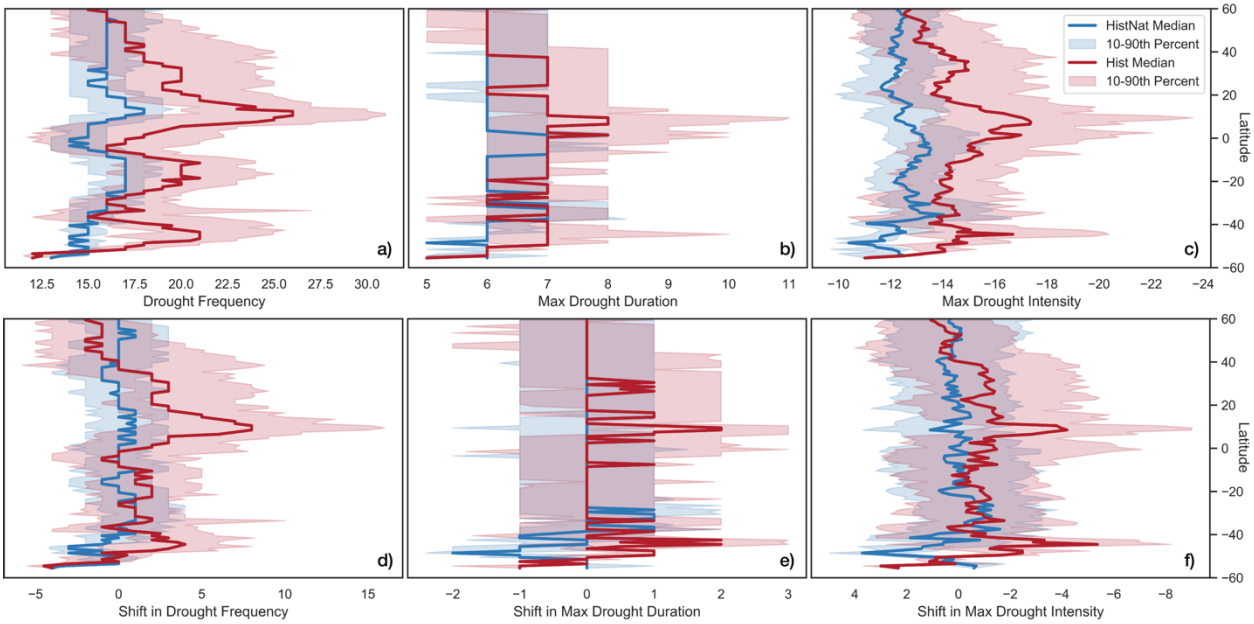

Figure 3.3. Zonal distribution of drought features. ***a)*** Latitudinal distribution of drought frequency in 1956-2005. ***b)*** Latitudinal distribution of maximum drought duration. ***c)*** Latitudinal distribution of maximum drought intensity. ***d)*** Latitudinal distribution of drought frequency change between the late 20th and late 19th century. Positive values represent increases in the number of droughts in 1956-2005 relative to 1851-1900. ***e)*** Latitudinal distribution of maximum drought duration change. Positive values represent increases in the maximum drought duration in 1956-2005 relative to 1851-1900. ***f)*** Latitudinal distribution of maximum drought intensity change. Negative values depict increases in the maximum drought intensity in 1956-2005 relative to 1851-1900.

To better understand in which regions drought features are more sensitive to the presence of anthropogenic forcing, we divided global land area into three terciles (Figure 3.4). In Figure 3.5, we present how drought features have shifted in the driest (left) and wettest (right) regions based on the median of annual precipitation. The subplots depict shifts for each drought characteristic, with a shift to the right indicating increases in drought frequency, duration, and intensity in the late 20th century relative to the late 19th century. We observe that wetter regions experienced larger shifts in drought features in historical simulations relative to natural-only

simulations. For example, 26.6% of the land area in the driest tercile exceeds the corresponding 90th percentile of the historical natural-only change in drought frequency. In contrast, 44.7% of the land area in the wettest tercile exceeds the 90th percentile of the historical natural-only change in drought frequency. However, all drought feature distributions from historical and historical natural-only conditions were significantly different under two-tailed, two-sample t-testing (Table 3.2). Areas with relatively low annual precipitation may have a lower capacity to experience change in drought characteristics. However, it is interesting to note the consistency in differences between historical and historical natural-only land area distributions in drought frequency (largest), intensity (average), and duration (smallest). This pattern may be due to the general sensitivity of the three drought features.

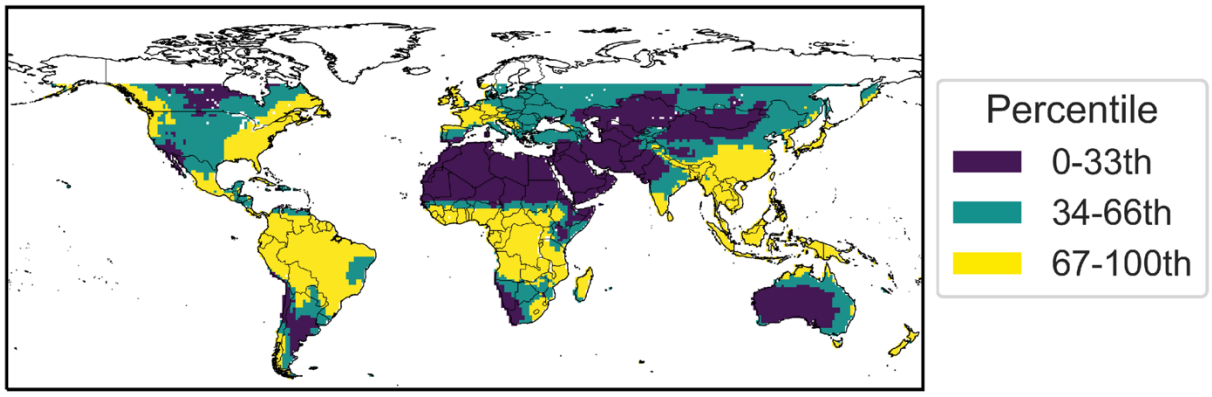

Figure 3.4: Land regions categorized by median annual precipitation percentiles. The tercile thresholds were defined using historical natural-only data. Each tercile represents a third of the land area covering 60^{o}S to 60^{o}N.

Table 3.2: Results from two-tailed two-sample t-test on historical and historical natural-only spatial distributions from dry, moderate, and wet land regions.

	0-33th percentile*		34-66th percentile		67-100th percentile	
	p-value	t-value, degrees of freedom (DOF)	p-value	t-value, DOF	p-value	t-value, DOF
Drought frequency	2.97E-11	6.658, 5744	1.42E-41	13.590, 5663	5.98E-214	32.222, 5367
Maximum drought duration	1.29E-05	4.365, 7438	9.87E-22	9.608, 7261	2.53E-109	22.571, 7076
Maximum drought intensity	6.22E-05	-4.007, 7243	1.25E-36	-12.709, 6977	3.19E-151	-26.782, 6769

*based on median annual precipitation from the historical natural-only dataset

To highlight the impact of regional changes on the agricultural sector, we show the distributions of drought features in regions with more than 50% of the land area classified as cropland (left) and in land area from 60^{o}S to 60^{o}N (right) in Figure 3.5 (Table 3.3). As an example, 64% of the land area in cropland regions exceeds the corresponding 90th percentile of drought frequency from historical natural-only conditions, while only 51% of the global land area exceeds the corresponding 90th percentile from natural-only conditions. As croplands are generally located in regions with ample precipitation, these results correspond well with our previous figure. However, they emphasize that regions across the world have experienced disparate sensitivities to anthropogenic forcing. In the context of meteorological drought conditions, agricultural regions (Figure 3.6; left panels) are relatively more sensitive to anthropogenic forcing in comparison to global land area (Figure 3.6; right panels). With rising populations and increased use of agricultural resources (for food and fuel), more intense droughts will have greater societal and environmental impacts.

Table 3.3: Results from two-tailed two-sample t-test on historical and historical natural-only spatial distributions from cropland and global land area.

	Cropland		Global land	
	p-value	t-value, DOF	p-value	t-value, DOF
Drought frequency	1.72E-182	31.508, 1531	0	69.882, 15005
Maximum drought duration	1.27E-60	16.902, 1945	0	38.591, 18857
Maximum drought intensity	5.36E-150	-28.064, 1803	0	-73.290, 17080

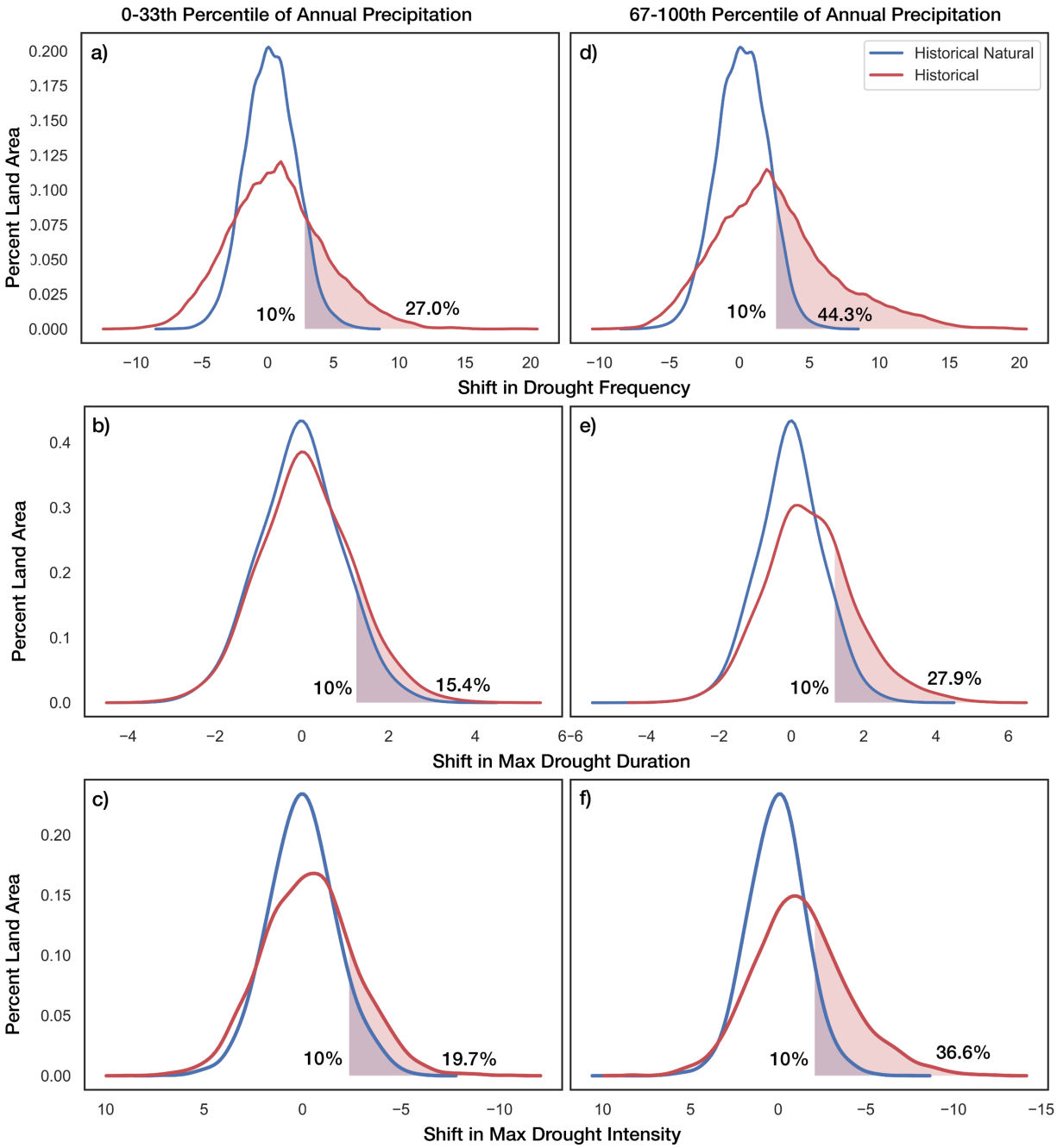

Figure 3.5. Shifts in drought features (1956-2005 relative to 1851-1900) for the driest (a, b, c) and wettest (d, e, f) land regions. Each PDF represents the distribution of shifts experienced by pixels within the specified land area. A shift to the right indicates relatively more frequent, longer, or more intense drought conditions in the more recent time period.

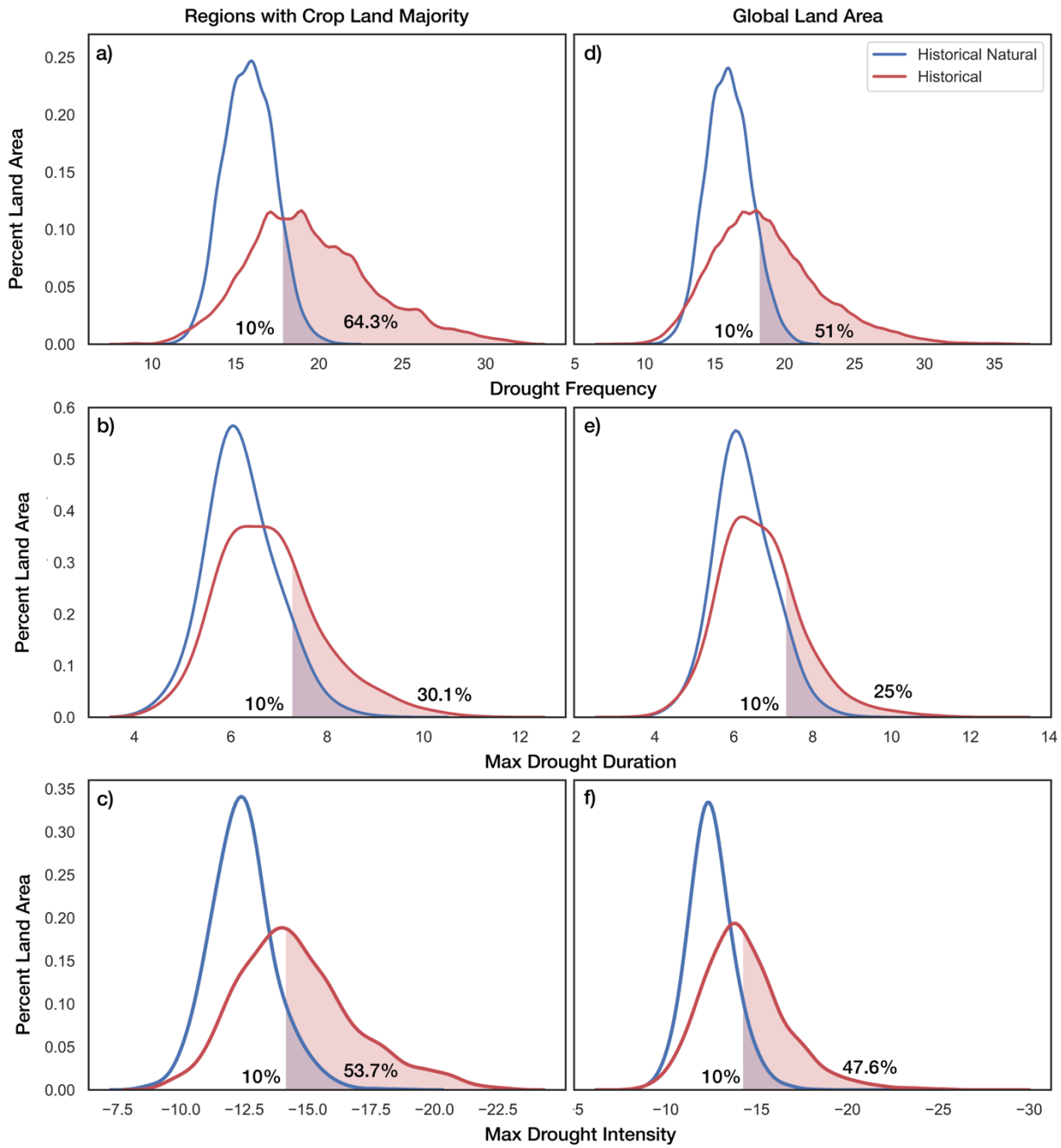

Figure 3.6. Cropland (a, b, c) versus global (d, e, f) land distributions of drought features (1956-2005). Each probability density function represents the distribution of drought features from pixels within the specified land area. Cropland pixels were pixels where more than 50% of the land area was classified for cropland use from Ramankutty et al. 2008.

From Figure 3.7, we can visualize the probability ratio (PR) of drought months occurring between 1956-2005. We calculated PR values for each land pixel using 6-month SPI values to understand climate change impacts on the frequency of drought events classified as SPI < -1.5. The resulting global PR pattern reflects the spatial shifts exhibited in Figures 3.1 and 3.2. Figure 3.7 also mirrors previous observations by Fischer and Knutti regarding the contribution of climate change to the global risk of extreme precipitation events (Fischer & Knutti, 2015). In their 2015 study, Fischer and Knutti observe smaller probabilities of extreme precipitation occurring in similar regions where we observe increases in the probability of drought events, such as Central America, Southern Europe and Northern Africa, and Eastern China (Fischer & Knutti, 2015). This indicates that these regions may be experiencing shifts at *both* tails of their distributions due to anthropogenic forcing.

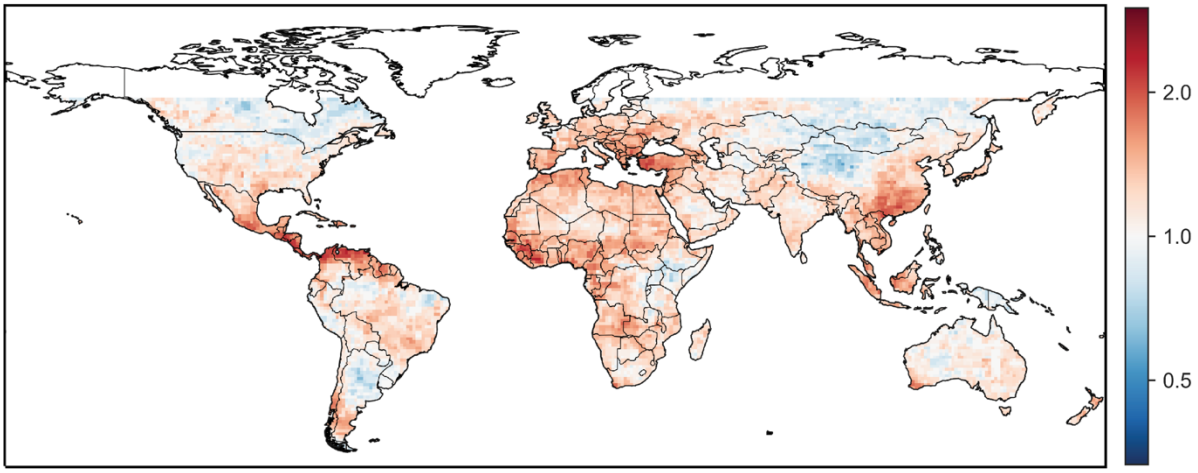

Figure 3.7. Probability Ratio (PR) of drought months during 1956-2005. The PR of each pixel is calculated from 6-month SPI values, where we defined historical natural-only SPI < -1.5 as the drought threshold. Values above 1 indicate a higher likelihood of drought events in historical conditions, while values below 1 indicate a lower likelihood in historical conditions.

3.4 Discussion and Conclusion

The main objective of this chapter was to examine the impact that anthropogenic forcing has had on the lower tail of the precipitation distribution with gridded data from climate model simulations. Overall, our results paint a global picture of how shifts in droughts would have been distributed under natural climate variability and how shifts in droughts have been impacted by the presence of anthropogenic forcing. Our results agree with Wehner et al.'s conclusion that the influence of anthropogenic forcing on regional North American meteorological droughts is not significant thus far (Wehner et al., 2017) In our earlier introduction of the literature, we also noted that Marvel et al. presented evidence of the influence of human activity on global soil moisture drought trends since the start of the 20th century (Marvel et al., 2019). Marvel et al. found evidence of increased drying in North America and Europe and wetting in South Asia and coastal East Asia (Marvel et al., 2019). Our spatial results for Europe and South and coastal East Asia generally agree with Marvel et al.'s conclusions. However, we found no substantial difference between North America's meteorological drought characteristics in historical and historical natural-only conditions. This may be due to differences in how precipitation and soil moisture have responded to anthropogenic forcing, or more directly, due to the fact that the PDSI drought index incorporates temperature information, which has already been documented to have strong responses to anthropogenic emissions (Stott et al., 2001).

We acknowledge the inherent limitations associated with our model-based detection study. Drying trends from Nasrollahi et al. showed that the majority of CMIP5 models mirror trends of areas under drought observed from Climatic Research Unit (CRU) data (Nasrollahi et al., 2015). However, there are still regional disparities that exist between CRU observations and model simulations regarding drying and wetting trends (Nasrollahi et al., 2015). As we lack a

good understanding of aerosol feedbacks, CMIP5 models are not able to reproduce real-world changes in drought features that may be influenced by anthropogenic aerosol emissions (Marvel et al., 2019). CMIP5 models also tend to overestimate the spread of Southern Hemisphere droughts and most models have trouble replicating regional precipitation trends when compared to ground-based observations (Nasrollahi et al., 2015). Most CMIP5 models also simulate a false double intertropical convergence zone in the Southern Tropics (Hirota et al., 2011; Hwang & Frierson, 2013; Li & Xie, 2013; Lin, 2007), which can have strong impacts on global precipitation, and consequentially, drought estimation. Due to these model biases, we acknowledge that there is a degree of error with regards to our results. However, since we compared differences between model experiments, the impacts of these model biases are reduced. As we examined temporal shifts between large time periods, we also reduced the influence of short-term interdecadal internal variability on our results.

Under anthropogenic forcing, we conclude that many regions have experienced notable increases in drought frequency, maximum drought duration, and maximum drought intensity. More specifically, we found that regions with higher annual precipitation were more sensitive to the presence of anthropogenic impacts. This study also highlights that if future changes in drought characteristics will continue in a manner consistent with our modeled shifts, there will be strong implications on water availability for agriculture and other socioeconomically important sectors dependent on water resources. The attribution of changes in drought characteristics and drought occurrences to anthropogenic climate change are important to aid in understanding our historically observed trends and shifts, and can contribute to the prediction of changes to come.

Chapter 4

The Impact of Anthropogenic Forcing on Concurrent Warm and Dry Extremes

This Chapter is currently in prep for submission.

Chiang, F., Greve, P., Mazdiyasni, O., Veldkamp, T., Wada, Y. and AghaKouchak A. “Impacts of Anthropogenic Forcing on Concurrent Temperature and Precipitation Extremes.”

4.1 Introduction

Recent climate research has shifted towards characterizing and understanding the changing risks of compound events, which can be defined as the concurrence of two or more natural hazards (Zscheischler et al., 2018). During the 2014 California drought, AghaKouchak et al. (2014) highlighted that the risk of concurrent extreme events has been increasing due to rising global temperatures (AghaKouchak et al., 2014). For example, in many regions of the United States, concurrent droughts and heatwaves have increased dramatically since the late 20th century (Mazdiyasni & AghaKouchak, 2015). In addition, Hao et al. (2013) conducted a global study on compound precipitation and temperature anomalies, and found that observations both show increases in joint dry and warm events from the mid to the late 20th century (Hao et al., 2013). Hao et al. (2013) also noted that the Coupled Model Intercomparison Project Phase 5 (CMIP5) climate model output broadly agrees with these observations.

In recent decades, there have been many detection and attribution studies attributing changes in mean or extreme temperature or precipitation events to climate change (Balan Sarojini et al., 2012; Bindoff et al., 2013; Christidis et al., 2005; Fischer & Knutti, 2015; Hegerl et al., 2006; P. A. Stott et al., 2001). Bindoff et al. (2013) summarized that the majority of the 1951-2010 increase in global mean temperatures can be attributed to the anthropogenic contribution to the atmosphere's greenhouse gases (Bindoff et al., 2013). In addition, Fischer and Knutti (2015) attributed changes in hot extremes and heavy precipitation to anthropogenic forcing (Fischer & Knutti, 2015). Although attribution studies have thoroughly examined the impact of climate change from a univariate perspective, current detection and attribution indices ignore dependencies between climate variables. Due to this, we still lack a strong understanding of the impacts of climate change on these interrelated variables.

To address this research gap, this study examined the influence of climate change on the concurrence of hydroclimatic extremes. For this study, we chose to examine low precipitation (dry) and high temperatures (warm) as a proxy for meteorological drought and warm spell conditions, as these extremes are especially impactful and relevant across many sectors (e.g. agriculture, energy, public and ecosystem health) (Ciais et al., 2005; De Bono et al., 2004).

Many previous studies have established that soil moisture plays an important role in connecting precipitation and temperature (Alexander, 2011; Hirschi et al., 2011; Koster et al., 2009; B. Mueller & Seneviratne, 2012; Seneviratne et al., 2010). Existing precipitation deficits can translate to low soil moisture conditions, which can increase the ratio of sensible to latent heat flux, thereby increasing the temperature of the local area (Seneviratne et al., 2010). Multiple studies using observations and model simulations have supported this physical coupling between precipitation and temperature. Mueller and Seneviratne (2012) conducted a global study investigating the impact of precipitation conditions on the subsequent occurrence of hot extremes, and identified several areas with strong couplings between precipitation deficits and hot extremes, especially in North and South America and Europe (B. Mueller & Seneviratne, 2012). Mueller and Seneviratne established that hot day occurrences were more likely to occur after higher precipitation deficits in comparison to lower precipitation deficits (B. Mueller & Seneviratne, 2012). Zscheischler and Seneviratne also quantified changes in the dependence between temperature and precipitation on a global scale (Zscheischler & Seneviratne, 2017). Zscheischler and Seneviratne showed that regions with more correlated temperature and precipitation experience more frequent concurrent hot and dry summers (Zscheischler & Seneviratne, 2017). Based on CMIP5 projections, Zscheischler and Seneviratne also found that changes in the negative relationship between temperature and precipitation are predicted to

translate to significant increases in dry and hot summers (Zscheischler & Seneviratne, 2017). Therefore, we assert it is important to examine the impact of historical climate change on the concurrence of extremes as our climate continues to warm.

In addition to observed and modeled changes in joint events, the second chapter of this dissertation also highlighted that changes in one variable may be dependent on the conditions of another. This conditional amplification of temperature increases over time is extremely relevant in the concurrence of extremes such as droughts and heatwaves, and thus, conditional analyses of this nature are important to better fully understand the changes associated with a warming climate.

In this chapter, we present the first formal concurrent precipitation and temperature detection and attribution study, examining climate model output representing 19th and 20th century historical climate with and without the influence of anthropogenic forcing. We asked two main research questions:

1. What is the anthropogenic impact on joint high temperature (warm) and low precipitation (dry) events?
2. What is the anthropogenic impact on exceedance probabilities of extreme temperatures (e.g. values above 90 percent), given specific drought conditions?

With these research questions, we evaluated how climate change has influenced the likelihood of joint warm and dry events as well as the likelihood of temperature exceedances conditioned on specified drought conditions. With this study, we also introduce the use of conditional exceedance probabilities in detection and attribution literature. In addressing these research questions, we can gain a better understanding of the changing risks of joint and conditional extremes, which can serve to strengthen future vulnerability and exposure studies.

4.2 Methodology

4.2.1 Data

For this study, we used an ensemble of the CMIP5 historical and historical natural-only model output of monthly precipitation and temperature from a total of 15 climate models (see Table 4.1 for the list of models used) (Taylor et al., 2011). The CMIP5 historical experiment imposes anthropogenic and natural conditions that reflect what have been documented in observations (Taylor et al., 2011). The historical natural-only experiment attempts to represent natural trends and variability with fixed pre-industrial concentrations of greenhouse gases and aerosols to represent our historical climate without any anthropogenic forcing (Taylor et al., 2011). Both the historical and historical natural-only experiments were initialized with the same preindustrial-Control data (Taylor et al., 2011). For a uniform multi-model analysis, we regridded all models to 1 degree resolution using nearest-neighbor interpolation.

Since the original time series is subject to seasonal effects, we standardized the historical and historical natural-only data from each pixel by using the pixel's historical natural-only data from 1850-2005. We followed the non-parametric standardization methodology introduced in Farahmand and AghaKouchak (2015) to generate each pixel's 3-month standardized precipitation index (SPI) and standardized temperature conditions on the last month of the SPI time window (Farahmand & AghaKouchak, 2015). With our non-parametric standardization approach, we can easily and consistently compare dry and warm conditions across regions. For standardizing both historical and historical natural-only data, we included a zero (representing the minimum possible precipitation over the course of the 3-month period) in the historical natural-only reference data to ensure that values present in the historical data and not present in the historical natural-only data would still be ranked accordingly.

Table 4.1. CMIP5 climate models used in chapter 4

Modeling Center	Institute ID	Model Name
Commonwealth Scientific and Industrial Research Organization (CSIRO) and Bureau of Meteorology (BOM), Australia	CSIRO-BOM	ACCESS1.3
Beijing Normal University (BNU)	BNU	BNU-ESM
Canadian Centre for Climate Modeling and Analysis	CCCMA	CanESM2
National Center for Atmospheric Research	NCAR	CCSM4
Centre National de Recherches Météorologiques / Centre Européen de Recherche et Formation Avancée en Calcul Scientifique	CNRM-CERFACS	CNRM-CM5
Commonwealth Scientific and Industrial Research Organization in collaboration with Queensland Climate Change Centre of Excellence	CSIRO-QCCCE	CSIRO-Mk3-6-0
LASG, Institute of Atmospheric Physics, Chinese Academy of Sciences and CESS, Tsinghua University	LASG-CESS	FGOALS-g2
NASA Goddard Institute for Space Studies	NASA GISS	GISS-E2-H GISS-E2-R
Institut Pierre-Simon Laplace	IPSL	IPSL-CM5A-LR IPSL-CM5A-MR
Japan Agency for Marine-Earth Science and Technology, Atmosphere and Ocean Research Institute (The University of Tokyo), and National Institute for Environmental Studies	MIROC	MIROC-ESM MIROC-ESM-CHEM
Meteorological Research Institute	MRI	MRI-CGCM3
Norwegian Climate Centre	NCC	NorESM1-M

4.2.2 Empirical Analysis

To examine the anthropogenic impact on joint warm and dry events, we used our standardized indices to empirically evaluate the number of individual warm and dry occurrences of 'critical events' across the globe. For each pixel, we defined critical events to be months below the 10^{th} percentile of the 3-month SPI and months above the 90^{th} percentile of the temperature index. We based the thresholds on percentiles calculated from each pixel's 1850-2005 historical natural-only time series. We then evaluated how individual occurrences of these critical events have been changing over time. For each pixel, we examined the median of the multi-model shift (or difference) in the number of dry months in 1931-2005 relative to 1850-1924 and the number of warm months for both historical and natural-only simulations.

Following this, we conducted a pixel by pixel evaluation of the empirical concurrence of low precipitation and high temperature events, finding the median multi-model shift in the number of concurrent dry and warm months in 1931-2005 relative to 1850-1924. To examine how concurrent events have been changing over time, we also generated a 30-year moving window time series of concurrences for all global land area from 60^{o}S to 60^{o}N. Starting at 1850 and shifting the window one year over at a time, we calculated the number of historical and historical natural-only concurrent months occurring in each 30-year window. We also examined the likelihood of events in the historical over the likelihood of events in the historical natural with the probability ratio concept (Fischer & Knutti, 2015). In essence, we generated the ratio of historical over historical natural-only concurrences during the 1931-2005 time period for all pixels. By using probability ratios, we could quantify the influence of anthropogenic forcing on joint occurrences of warm and dry events.

In addition, we studied the temporal evolution of warm and dry events on a regional basis by separating the global land area into regions established by the fifth Intergovernmental Panel on Climate Change (IPCC) report (AR5), which we will refer to as IPCC AR5 regions (IPCC, 2013). We used each regional median time series to generate 30-year moving window time series for dry occurrences, warm occurrences, and dry and warm concurrences.

4.2.3 Copula-based conditional analysis

Recently, copulas have become a popular tool to represent multivariate relationships in climate science. Copulas are multivariate distribution functions, which can model the dependence structure of two or more variables and aid in evaluating compound extremes, that by definition, occur infrequently (Nelsen, 2006; Zscheischler & Seneviratne, 2017). Copula theory allows us to examine features such as the joint and conditional behavior of extreme values, which otherwise may be difficult to study (Nelsen, 2006). Using copula theory, we can express the joint probability distribution of precipitation *(X)* and temperature *(Y)*,

$$F_{XY}(x, y) = \mathbf{C}[F_X(x), F_Y(y)] \tag{4.1}$$

where *F(x,y)* represents the cumulative joint probability, **C** is the copula cumulative distribution function, and $F_X(x)$ and $F_Y(y)$ represent the marginal probability distribution functions (PDF) of precipitation and temperature, respectively (SKLAR, 1959). For each pixel, we transformed the negative standardized precipitation and standardized temperature data into their uniform marginals, and then isolated the copula family that best represents the bivariate data. To transform the bivariate data into their uniform marginals, we employed this transformation for each pair of datapoints (x_i, y_i):

$$\left(\frac{n-R(x_i)+\frac{1}{2}}{n}, \frac{n-R(y_i)+\frac{1}{2}}{n}\right) \quad (4.2)$$

where i represents the pair number, n, the total number of pairs, and $R(x_i)$, the rank of x_i. We determined the best-fit copula family by using the BiCopSelect function in the R package, VineCopula, employing the Bayesian Information Criteria to select the family (Nagler et al., 2019). We then confirmed the goodness of fit of the best-fit copula family with VineCopula's BiCopGofTest function using White's information matrix equality (Nagler et al., 2019).

Since the copula fit and goodness of fit evaluation process is more mathematically and computationally involved than the empirical analysis, we simplified our analysis by using regional median raw precipitation and temperature time series from IPCC AR5 regions to create the standardized indices. To minimize strong autocorrelation, we used 3-month SPI and corresponding temperature index data from specific months to create seasonal (February, May, August, November) time series. Since seasonality can influence the nature of the relationship between temperature and precipitation, we also created boreal winter (February) and boreal summer (August) time series for each region. With the best-fit copula family for each region of interest, we calculated the probability of joint exceedance, *p*, at a given joint threshold (e.g. exceeding the 90th percentile (u) of temperature (U) AND the 90th percentile (v) of negative precipitation (V) under historical natural-only conditions) for each subsampled time series, represented by this equation (Serinaldi, 2015):

$$p = P[U > u \cap V > v] = 1 - u - v + \boldsymbol{C}(u, v) \quad (4.3)$$

To represent the difference between the historical and historical natural-only conditions, we calculated the ratio of the joint probability of exceeding the 90th percentile threshold in historical

conditions over the joint exceedance probability in historical natural-only conditions. We refer to this ratio as the 'joint probability ratio,' which we abbreviate as JPR.

We also selected the 10th percentile of precipitation from the historical natural-only scenario and generated conditional probability density functions (PDFs) of monthly temperature. From the conditional temperature PDFs, we extracted the probability of temperature exceedances conditioned on the 10th percentile of precipitation. In other words, we determined the conditional probability of temperature, *Y,* exceeding a threshold, *y,* at a given precipitation condition (*x)*, from the conditional marginal PDF:

$$f(X = x) = c[F_X(x), F_Y(y)]f_Y(y) \quad (4.4)$$

where *c* is the copula PDF and $f_Y(y)$ is the density function of the temperature marginal distribution (Madadgar & Moradkhani, 2013; Mazdiyasni et al., 2017). To examine the impact of anthropogenic forcing from a conditional perspective, we examined the probability of exceeding a set temperature threshold (e.g. the 90th percentile of temperature from the historical natural-only scenario) for the defined precipitation condition. We compared conditional exceedance probabilities generated from historical and historical natural-only model outputs in a 'conditional probability ratio,' which we abbreviate as CPR, to represent the difference between the two scenarios.

4.3 Results

4.3.1 Univariate dry and warm hotspots and shifts

To understand concurrent changes in dry and warm months, we first examined univariate dry occurrences and warm occurrences on a global scale. Figure 4.1a shows relatively uniform occurrences across the global land area of study in the historical natural-only scenario. Since our definition of dry events is based on the 10^{th} percentile of historical natural-only data from 1850-2005, this subplot shows that the second half of the time series is generally reflective of the entire time period. In addition, Figure 4.1b shows that very little change can be attributed to natural variability between the two time periods. On the other hand, Figure 4.1c depicts that under historical conditions, strong hotspots of dry months occur in tropical regions and parts of Europe and Asia. In addition, when examining shifts between 1931-2005 and 1850-1924, we see that dry months have increased in the corresponding regions (Figure 4.1d). Other parts of the globe have experienced decreases in dry occurrences, such as parts of North and South America, as well as Central Asia. In general, our historical scenario results generally match 1950-2010 drought frequency trends observed from the Global Precipitation Climatology Center precipitation dataset (Spinoni et al., 2014).

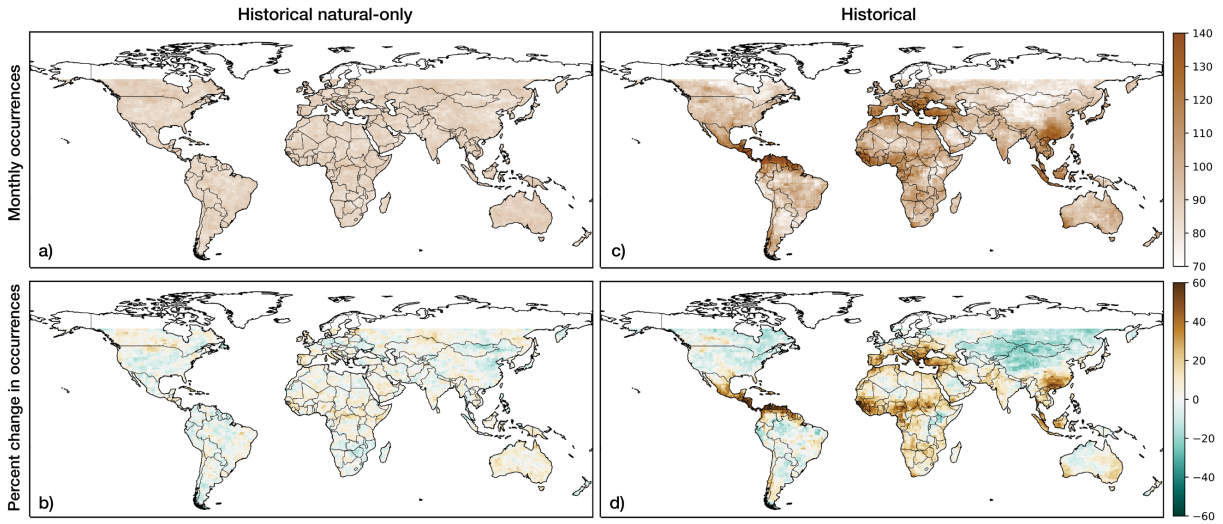

Figure 4.1. Dry month occurrences (1931-2005) and percent change in occurrences (1931-2005 relative to 1850-1924). A) Dry month occurrences from the CMIP5 historical natural-only multi-model ensemble median. The value expressed in each pixel represents the number of months with a 3-month SPI value lower than the 10th percentile of the pixel's historical natural-only climatology. B) Percent change in dry month occurrences from the historical natural-only data. C) Dry month occurrences from the historical ensemble median. D) Percent change in dry month occurrences from the historical data.

As our definition of high temperature occurrences is based on the 90th percentile of historical natural-only data from 1850-2005, Figure 4.2a shows that the historical natural-only warm occurrences from the 1931-2005 period is also reflective of the entire time period. Figure 4.2b also shows that very little naturally driven change occurs between the two time periods. In contrast, in the historical scenario, hotspots of warm occurrences are much more widespread across the globe, especially in the tropical regions (Figure 4.2c). In addition, we see a similar global pattern when examining the change in warm occurrences from 1931-2005 relative to 1850-1924 (Figure 4.2d). This mirrors results from previous studies that also examined CMIP5 simulations. For example, Fischer and Knutti (2015) found that tropical regions had much higher probability ratios of hot extremes (defined as the 99th percentile of pre-industrial model conditions) at present-day (0.85^{o}C) levels of warming (Fischer & Knutti, 2015). In addition, Perkins-Kirkpatrick and Gibson (2017) showed that related indicators such as number of

heatwave days are projected to experience similar spatial changes in the 21st century (Perkins-Kirkpatrick & Gibson, 2017). This indicates that the tropical regions may be experiencing a greater shift in the upper tail of the temperature distribution relative to higher latitudes.

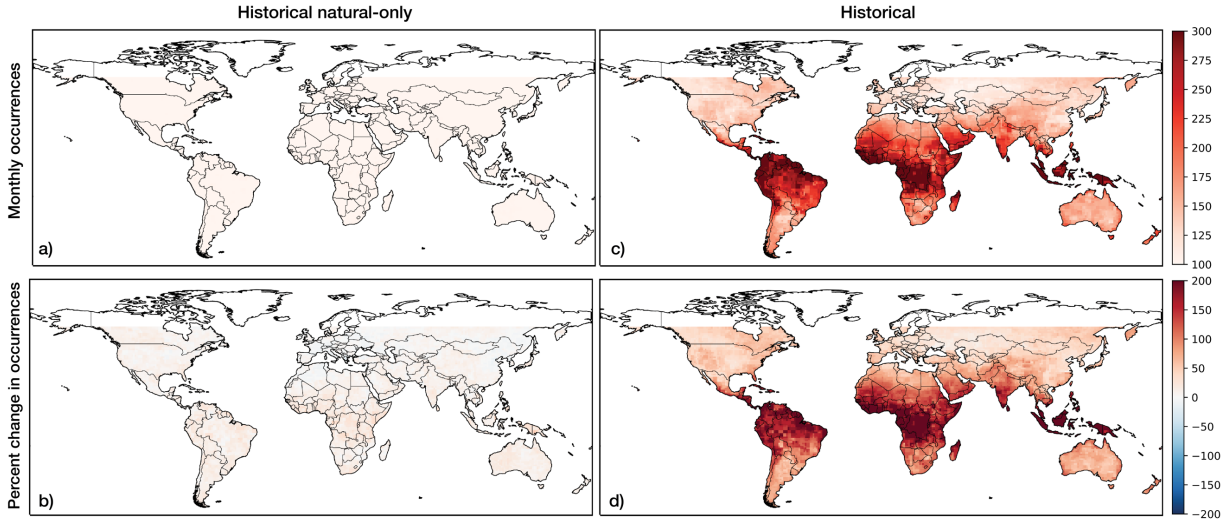

Figure 4.2. Warm month occurrences (1931-2005) and percent change in occurrences (1931-2005 relative to 1850-1924). A) Warm month occurrences from the CMIP5 historical natural-only multi-model median. Each pixel's value represents the number of months with a standardized temperature value higher than the 90th percentile of the pixel's historical natural-only climatology. B) CMIP5 historical natural-only percent change in warm month occurrences. C) CMIP5 historical median warm month occurrences. D) CMIP5 historical median percent change in warm month occurrences.

4.3.2 Joint dry and warm hotspots and shifts

In Figure 4.3, we can examine global hotspots of dry and warm months occurring simultaneously. In the historical natural-only subplots (Figures 4.3a-b), we do not see coherent hotspots or substantial increases in concurrent dry and warm months between the two time periods. This indicates that under naturally forced conditions, concurrences are not expected to increase or decrease significantly, which is consistent with what we observed for both dry and warm univariate occurrences from Figures 4.1a-b and 4.2a-b. Under historically forced conditions, we see substantial hotspots of dry and warm concurrences, primarily in the tropics, which reflect what we observed for warm occurrences under the historical scenario (Figure 4.3c).

Between 1931-2005 and 1850-1924, we found a similar global pattern of percent change in the occurrence of joint warm and dry months (Figure 4.3d). From a global perspective, it is evident that the general spatial pattern of warm occurrences plays a much larger role in determining the global pattern of joint dry and warm concurrences. This may be due to the sheer magnitude of change that temperature extremes have experienced relative to the change that pluvial and drought extremes have undergone as a result of anthropogenic forcing.

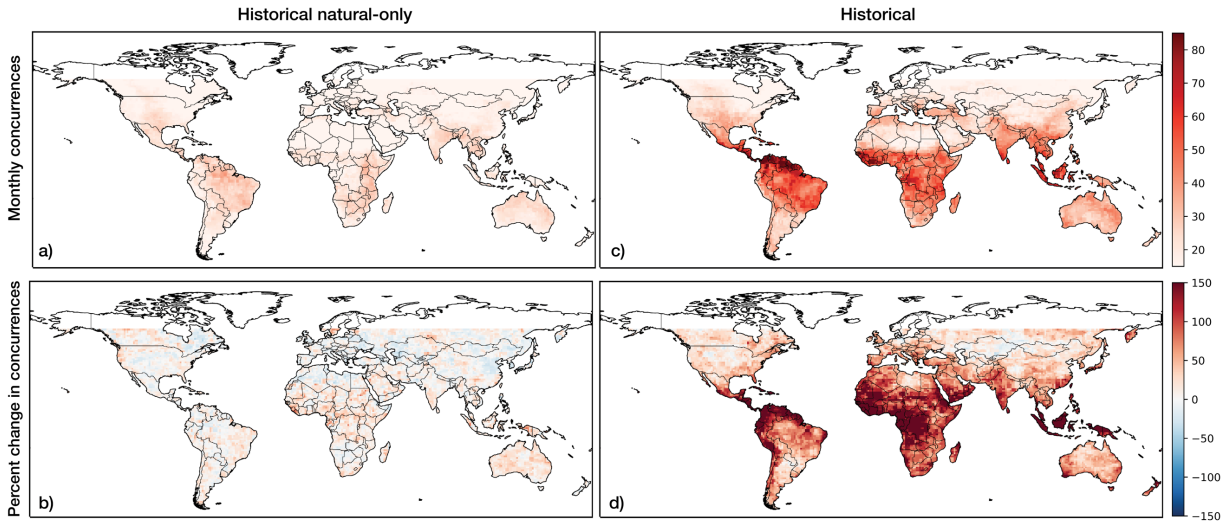

Figure 4.3. Dry and warm month joint occurrences (1931-2005) and percent change in concurrences (1931-2005 relative to 1850-1924). A) Dry and warm month concurrences from the CMIP5 historical natural-only multi-model median. Each pixel's value represents the number of months with a joint occurrence of standardized temperature above the pixel's historical natural 90th percentile and SPI value below the pixel's historical natural 10th percentile. B) CMIP5 historical natural-only percent change in concurrences. C) CMIP5 historical median concurrences. D) CMIP5 historical median percent change in concurrences.

We can also examine the global median time series of dry and warm concurrences from 1850-2005, which was created by counting the concurrences at the grid cell level first and then calculating the global land area median (Figure 4.4). On the global scale, we can see a clear divergence between historical and historical natural-only concurrences that begins in the early 20th century. At the end of the 20th century, the global median of warm and dry concurrences in

the historical scenario is 3 times higher than concurrences in the natural-only scenario, indicating that anthropogenic climate change contributed to making these events more probable on a global scale.

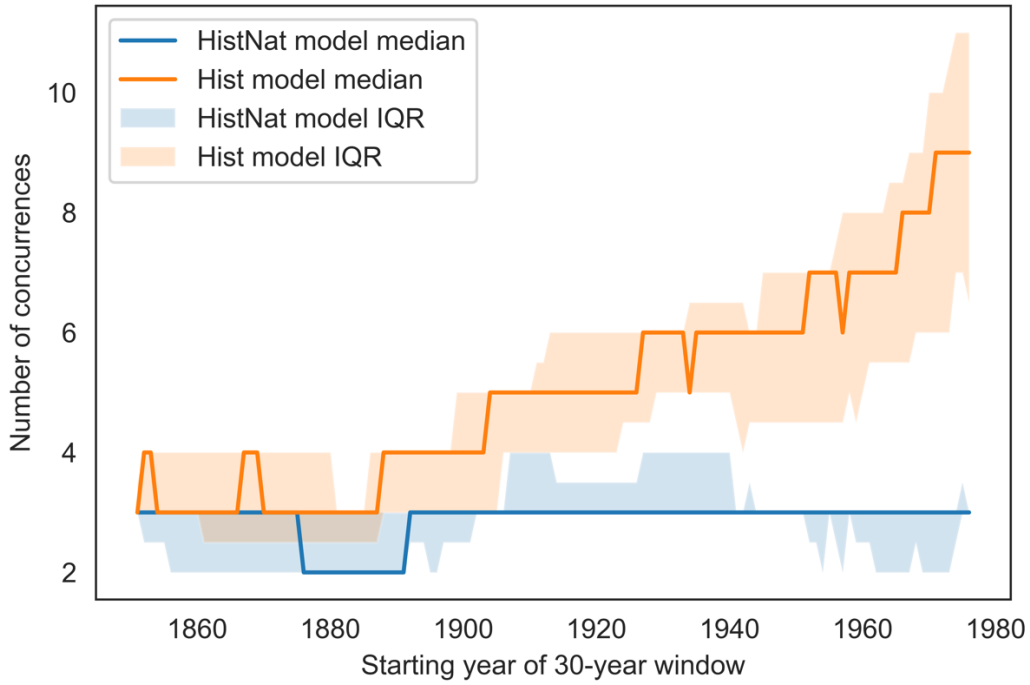

Figure 4.4. Global 30-year moving window time series of dry and warm concurrences. The historical (shown in orange) and historical natural-only (shown in blue) depicts the multi-model median and the interquartile range of values produced by the model ensemble. The number of concurrences represents the number of joint dry and warm months within the 30-year moving window.

Figure 4.5 shows the joint probability ratio or ratio of the likelihood of warm/dry events in the historical scenario relative to the historical natural-only scenario. We observe that the probability ratios for joint warm and dry months possess a more widespread spatial pattern in comparison to the global pattern of concurrences under the historical scenario. Joint occurrences of extreme temperature and precipitation deficits are more likely in the historical conditions relative to the historical natural-only conditions for most regions across the globe, especially in Central and South America, Western and Central Africa, and Southeast Asia. The probability

ratios in the Amazon, the Western Coast of South America, Mediterranean, Sahara, and West Asia indicate strong differences between historical and historical natural-only scenarios, which are not as readily seen when only examining results from the historical models. By examining probability ratios, we can highlight regions with a much greater likelihood of experiencing warm/dry events than we would have expected under conditions driven only by natural variability.

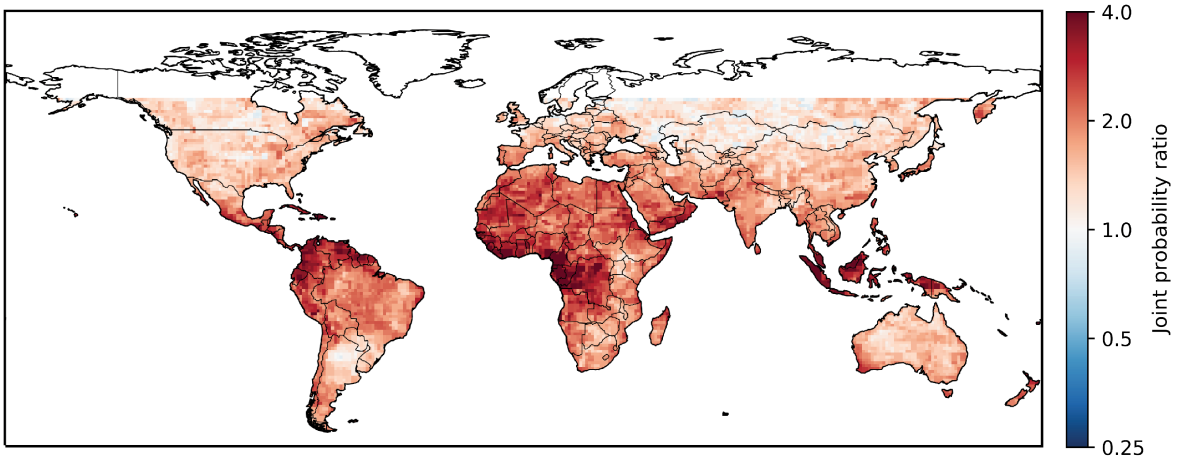

Figure 4.5. Global probability ratios of warm and dry concurrences in 1931-2005. Values above 1 indicate a higher probability of warm/dry events in the historical multi-model ensemble, while values below 1 indicate a higher probability of warm/dry events in the historical natural-only models.

4.3.3 Statistical significance and temporal evolution of warm and dry events by IPCC region

To examine the statistical significance of anthropogenic forcing on concurrent warm/dry events, we used spatial distributions from IPCC regions to conduct two-sided two-sample t-tests to compare the mean values of the number of concurrences under historical and historical natural-only conditions in 1931-2005. We found that all regions between 60°S and 60°N were significantly different (Table 4.2 lists the regional t-statistics, p-values, and degrees of freedom).

Table 4.2: Statistics from two-sided two-sample t-test comparing concurrences under historical and historical natural-only conditions for the last 75 years

	T-statistic	P-value	Degrees of Freedom
CNA	1.38E+01	7.20E-39	6.65E+02
AMZ	5.53E+01	0.00E+00	8.23E+02
CAM	2.19E+01	2.44E-74	2.59E+02
CAS	1.20E+01	1.10E-29	4.15E+02
CEU	1.59E+01	2.64E-50	6.32E+02
EAF	5.36E+01	1.02E-291	8.99E+02
EAS	2.51E+01	4.80E-117	1.11E+03
ENA	1.37E+01	1.88E-36	3.92E+02
MED	4.75E+01	2.31E-239	6.84E+02
NAS	3.49E+01	4.85E-237	4.60E+03
NAU	3.79E+01	1.99E-196	8.28E+02
NEB	4.45E+01	1.07E-166	3.52E+02
NEU	9.19E+00	4.87E-19	5.61E+02
SAF	4.43E+01	2.19E-242	8.23E+02
SAH	5.08E+01	0.00E+00	1.03E+03
SAS	3.50E+01	3.19E-166	6.87E+02
SAU	3.41E+01	2.12E-124	3.84E+02
SEA	4.39E+01	5.17E-200	4.53E+02
SSA	2.14E+01	4.95E-81	5.74E+02
TIB	1.66E+01	1.02E-54	6.73E+02
WAF	6.78E+01	0.00E+00	7.26E+02
WAS	3.07E+01	6.51E-152	1.01E+03
WNA	2.26E+01	4.24E-94	1.02E+03
WSA	2.75E+01	2.98E-90	2.38E+02

To gain a better understanding of how these univariate and bivariate events evolve temporally, we also examined individual and joint event time series on a regional basis. For each IPCC region, we examined how the likelihood of dry months, warm months, and dry and warm concurrences have changed in both historical and historical natural-only conditions. Figures 4.6a, b, and c display each of the regions which experienced increases in concurrences under historical conditions. First, we examine the four regions depicted in Fig 4.6a (the Amazon (AMZ), Central America/Mexico (CAM), East Africa (EAF), and South Asia (SAS)). Both AMZ and CAM regions show moderate increases in the likelihood of dry months as well as very substantial increases in the likelihood of warm months, which translate to strong increases in the likelihood of concurrences. In the EAF and SAS regions, we do not see notable changes in the likelihood of dry months, which translate to how the likelihood of concurrences evolves in the two regions as well. In these regions, the difference in the likelihood of concurrent warm/dry months does not diverge as quickly or dramatically between historical and historical natural-only conditions. On a regional basis, we can see that combinations of changes in the likelihood of dry months and warm months ultimately reflect on the concurrence likelihood, and simple increases in the likelihood of warm months do not translate proportionally to increases in concurrence likelihood. We also see evidence of this in the other IPCC regions depicted in Figures 4.6b and c.

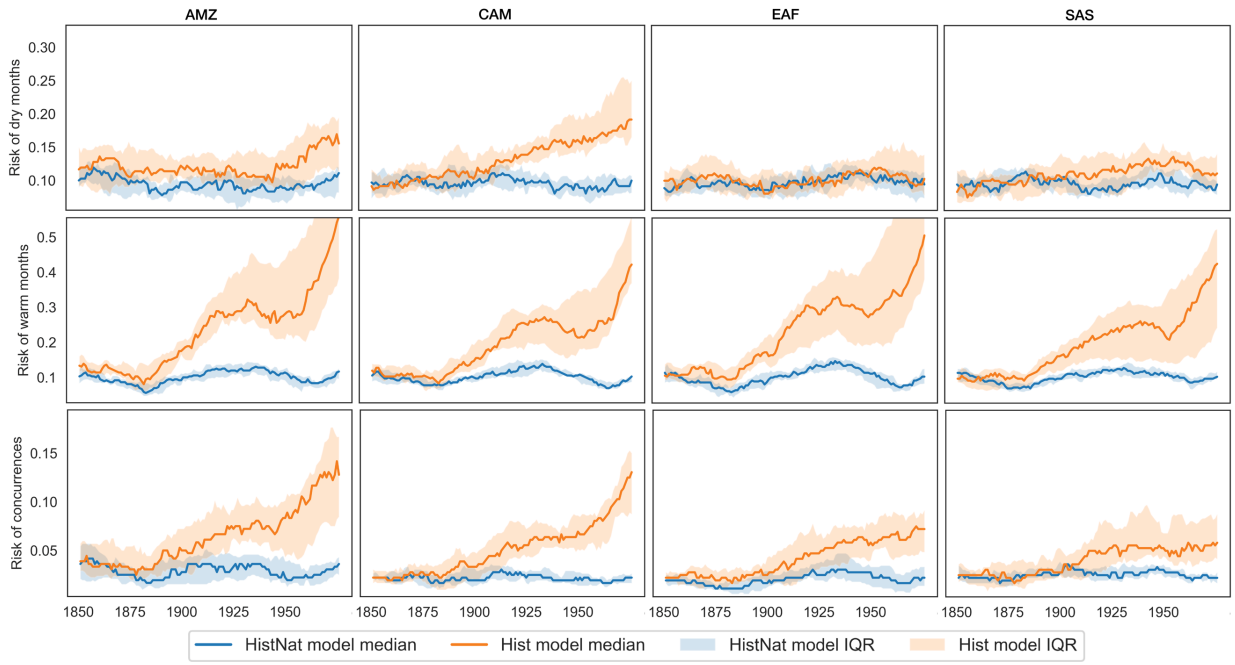

Figure 4.6a. IPCC regional time series of likelihood of dry occurrences, warm occurrences, concurrences. For the top three rows, the historical (shown in orange) and historical natural-only (shown in blue) depicts the multi-model median and the interquartile range of values within the 30-year moving window for each IPCC region. Regions shown in the figure are: Amazon (AMZ), Central America/Mexico (CAM), East Africa (EAF), and South Asia (SAS).

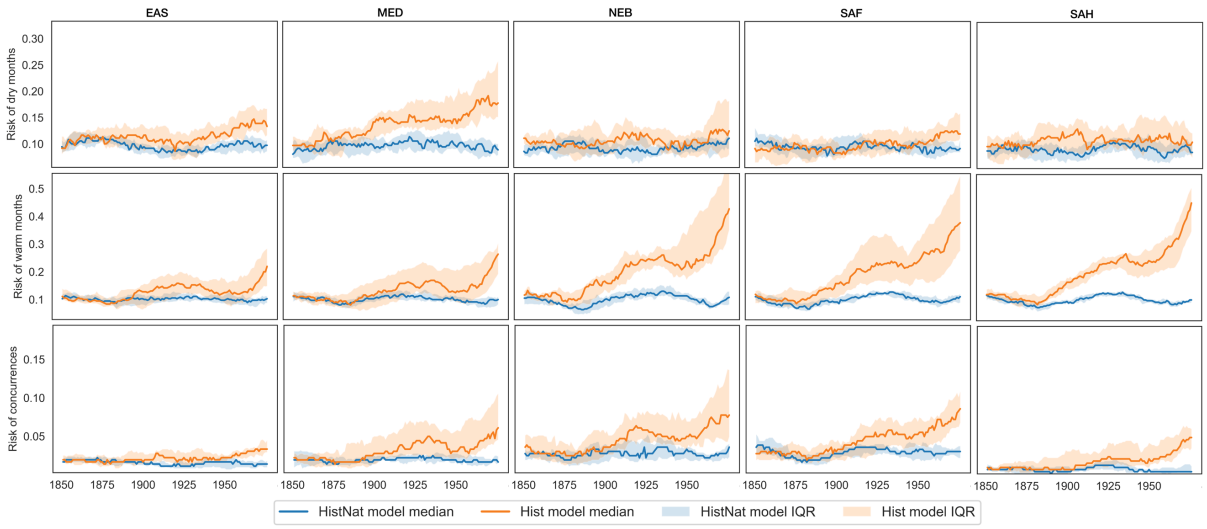

Figure 4.6b: IPCC regional time series (con't). East Asia (EAS), South Europe/Mediterranean (MED), North-East Brazil (NEB), Southern Africa(SAF), and Sahara (SAH).

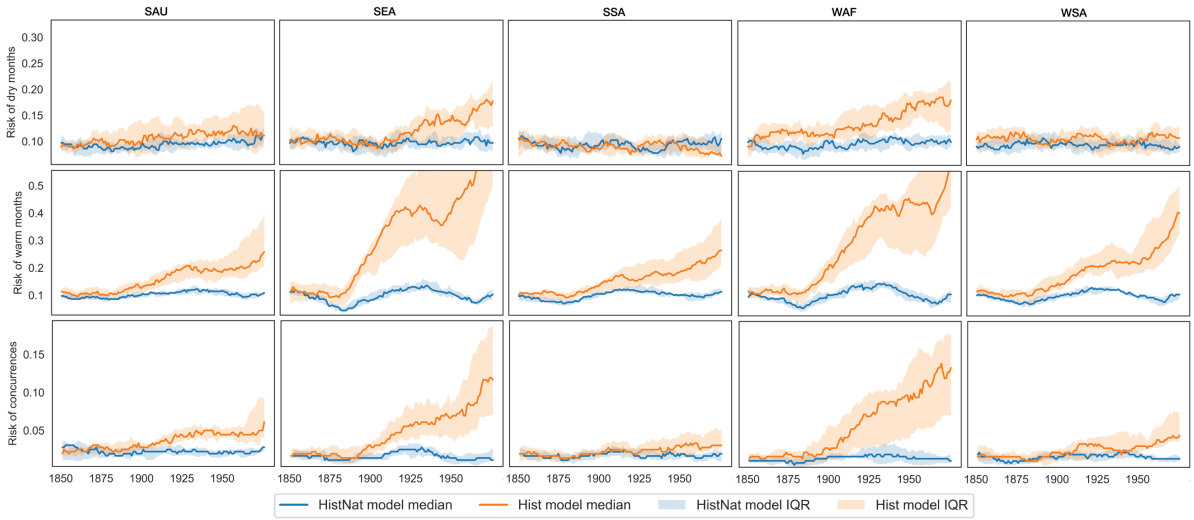

Figure 4.6c: IPCC regional time series (con't) South Australia/New Zealand (SAU), Southeast Asia (SEA), Southeastern South America (SSA), West Africa (WAF), and West Coast South America (WSA).

4.3.4 Conditional temperature exceedances by IPCC region

We also examined how conditional temperature exceedances differ in historical and historical natural-only scenarios from a regional perspective. To examine the effect of seasonality on conditional temperature exceedances, we subsampled 3-month SPI values from the end of each season (February, May, August, and November) to create a seasonal time series for each IPCC region. We also examined boreal winter and boreal summer seasons by subsampling 3-month SPI values from all February and August months, respectively. We fitted copula families to the historical and historical natural-only regional data and determined the best-fit copula families for each scenario and region (see Tables 4.3-5 for the best-fit copula families and goodness of fit p-values).

Figure 4.7a, b, and c display the seasonal, boreal winter, and boreal summer temperature historical and historical natural-only probability density functions (PDFs) for each IPCC region conditioned on the 10^{th} percentile of precipitation. For each of the figures, the top row, middle row, and bottom row of conditional PDFs relate to seasonal, boreal winter, and boreal summer subsamples. For each PDF, the area above the 90^{th} percentile of historical natural-only temperature is shaded in. All regions show substantially higher probabilities of exceeding the 90^{th} percentile historical natural-only temperature anomaly, however there are variations depending on the location and seasonality of the region. Across the regions, we can see that temperature exceedance probabilities differ based on seasonality, which may strengthen or weaken the temperature and precipitation relationship.

Table 4.3a: Best-fit copula families for seasonal data from IPCC regions

	Historical Natural-only	Historical
CNA	Gaussian	Gaussian
AMZ	Frank	Clayton
CAM	Frank	Survival Gumbel
CAS	Gaussian	Gumbel
CEU	Clayton	Survival Joe
EAF	Frank	Frank
EAS	Clayton	Survival Joe
ENA	Rotated Clayton 270 degrees	Rotated Joe 270 degrees
MED	Gaussian	Gaussian
NAS	Gaussian	Gaussian
NAU	Gaussian	Gaussian
NEB	Gaussian	Gaussian
NEU	Rotated Gumbel 90 degrees	Rotated Clayton 270 degrees
SAF	Gaussian	Gaussian
SAH	Gaussian	Survival Clayton
SAS	Frank	Gaussian
SAU	Gumbel	Frank
SEA	Rotated Clayton 90 degrees	Clayton
SSA	Gaussian	Frank
TIB	Gaussian	Rotated Clayton 270 degrees
WAF	Joe	Frank
WAS	Gaussian	Frank
WNA	Survival Clayton	Frank
WSA	Clayton	Gumbel

Table 4.3b: P-values from goodness of fit test for seasonal data from IPCC regions

	Historical Natural-only	Historical
CNA	0.57	0.38
AMZ	0.07	0.51
CAM	0.57	0.96969697
CAS	0.86	0.107526882
CEU	0.779069767	0.666666667
EAF	0.2	0.33
EAS	0.75308642	0.488095238
ENA	0.426966292	0.105263158
MED	0.71	0.58
NAS	0.96	1
NAU	0.11	0.81
NEB	0.84	0.91
NEU	0.18	0.35
SAF	0.86	0.92
SAH	0.73	0.57
SAS	0.4	0.31
SAU	0.13	0.78
SEA	0.448275862	0.55
SSA	0.68	0.32
TIB	0.83	0.9
WAF	0.333333333	0.62
WAS	0.46	0.48
WNA	0.65	0.97
WSA	0.757575758	0.6

Table 4.4a: Best-fit copula families for North Hemisphere winter data from IPCC regions

	Historical Natural-only	Historical
CNA	Survival Gumbel	Frank
AMZ	Gumbel	Survival Joe
CAM	Frank	Clayton
CAS	Rotated Clayton 90 degrees	Rotated Joe 270 degrees
CEU	Frank	Rotated Clayton 90 degrees
EAF	Gaussian	Frank
EAS	Clayton	Survival Joe
ENA	Rotated Joe 270 degrees	Rotated Joe 270 degrees
MED	Clayton	Survival Gumbel
NAS	Gaussian	Rotated Gumbel 90 degrees
NAU	Survival Gumbel	Gaussian
NEB	Clayton	Gaussian
NEU	Rotated Gumbel 270 degrees	Rotated Gumbel 90 degrees
SAF	Gaussian	Survival Gumbel
SAH	Rotated Gumbel 270 degrees	Gaussian
SAS	Frank	Gaussian
SAU	Joe	Gumbel
SEA	Frank	Gaussian
SSA	Joe	Frank
TIB	Rotated Clayton 270 degrees	Rotated Gumbel 90 degrees
WAF	Rotated Clayton 90 degrees	Rotated Joe 270 degrees
WAS	Frank	Gumbel
WNA	Survival Gumbel	Rotated Clayton 270 degrees
WSA	Gaussian	Gaussian

Table 4.4b: P-values from goodness of fit test for North Hemisphere winter data from IPCC regions

	Historical Natural-only	Historical
CNA	0.173469388	0.49
AMZ	0.446808511	0.84
CAM	0.25	0.65
CAS	0.235294118	0.7125
CEU	0.19	0.25
EAF	0.37	0.64
EAS	0.988636364	0.2375
ENA	0.666666667	0.520833333
MED	0.78125	0.177777778
NAS	0.34	0.43
NAU	0.4	0.55
NEB	0.96	0.33
NEU	0.43	0.91
SAF	0.87	0.294736842
SAH	0.464285714	0.8
SAS	0.73	0.64
SAU	0.343434343	0.434343434
SEA	0.41	0.97
SSA	0.727272727	0.33
TIB	0.885245902	0.11
WAF	0.87	0.073684211
WAS	0.52	0.166666667
WNA	0.847826087	0.166666667
WSA	0.36	0.46

Table 4.5a: Best-fit copula families for North Hemisphere summer data from IPCC regions

	Historical Natural-only	Historical
CNA	Gaussian	Frank
AMZ	Joe	Rotated Clayton 90 degrees
CAM	Clayton	Gaussian
CAS	Survival Gumbel	Survival Clayton
CEU	Gumbel	Clayton
EAF	Clayton	Frank
EAS	Clayton	Rotated Clayton 90 degrees
ENA	Survival Clayton	Gumbel
MED	Gaussian	Gaussian
NAS	Rotated Gumbel 270 degrees	Rotated Clayton 270 degrees
NAU	Clayton	Gaussian
NEB	Survival Joe	Gumbel
NEU	Survival Gumbel	Frank
SAF	Survival Gumbel	Gumbel
SAH	Frank	Survival Clayton
SAS	Frank	Clayton
SAU	Gaussian	Frank
SEA	Rotated Clayton 90 degrees	Clayton
SSA	Clayton	Frank
TIB	Gaussian	Rotated Clayton 270 degrees
WAF	Gaussian	Frank
WAS	Survival Gumbel	Frank
WNA	Survival Clayton	Survival Clayton
WSA	Clayton	Joe

Table 4.5b: P-values from goodness of fit test for North Hemisphere summer data from IPCC regions

	Historical Natural-only	Historical
CNA	0.73	0.26
AMZ	0.967213115	0.670588235
CAM	0.646464646	0.58
CAS	0.869565217	0.829268293
CEU	0.33	0.581632653
EAF	0.704081633	0.37
EAS	0.987341772	0.4375
ENA	0.25	0.139534884
MED	0.24	0.86
NAS	0.44	0.962025316
NAU	0.567010309	0.51
NEB	0.87654321	0.28125
NEU	0.242105263	1
SAF	0.406976744	0.949494949
SAH	0.55	0.920454545
SAS	0.28	0.94
SAU	0.88	0.95
SEA	0.474358974	0.63
SSA	0.873563218	0.59
TIB	0.56	0.282051282
WAF	0.93	0.71
WAS	0.333333333	0.23
WNA	0.91	0.69
WSA	0.642857143	1

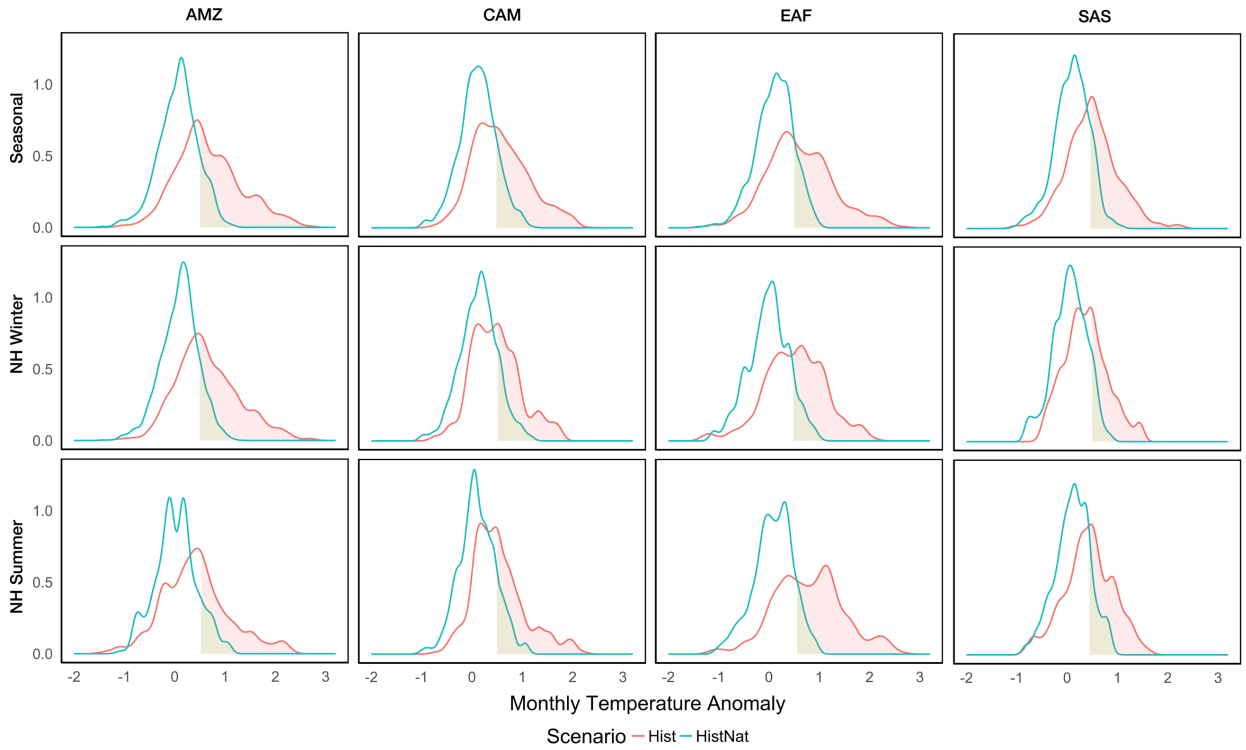

Figure 4.7a. IPCC regional conditional PDFs at the 10th percentile of precipitation. Seasonal conditional PDFs use quarterly data from each year, while Northern Hemisphere winter and summer conditional PDFs use February and August data from each year, respectively. Regions shown in the figure are: Amazon (AMZ), Central America/Mexico (CAM), East Africa (EAF), and South Asia (SAS).

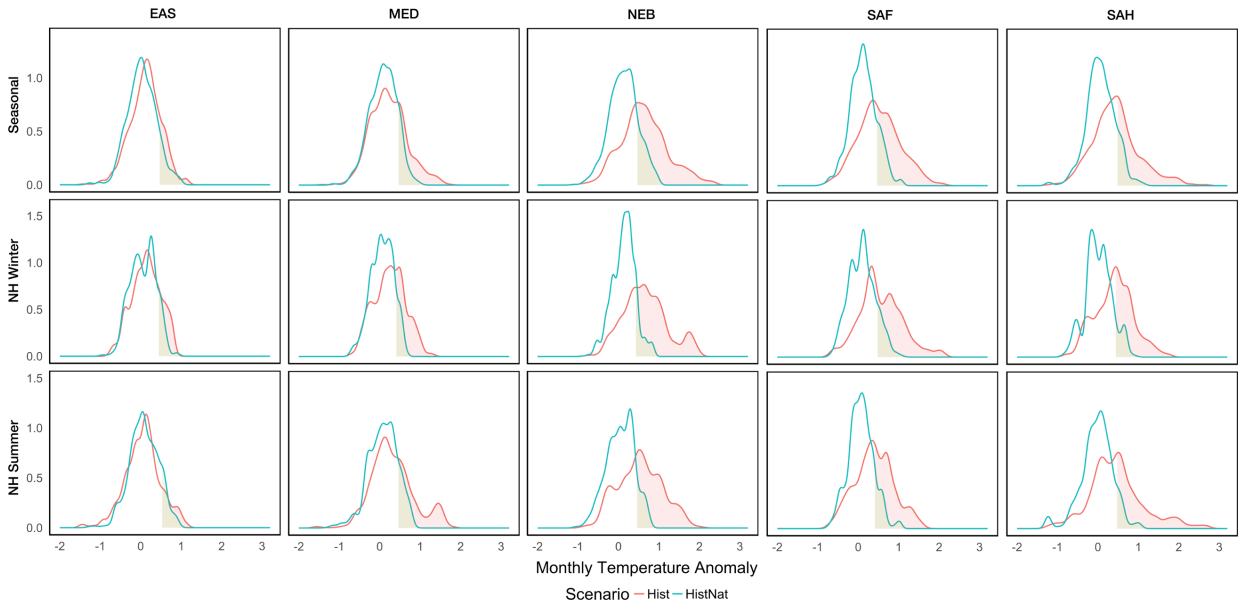

Figure 4.7b: IPCC regional conditional PDFs (con't). The regions shown in the figure are: East Asia (EAS), South Europe/Mediterranean (MED), North-East Brazil (NEB), Southern Africa(SAF), and Sahara (SAH).

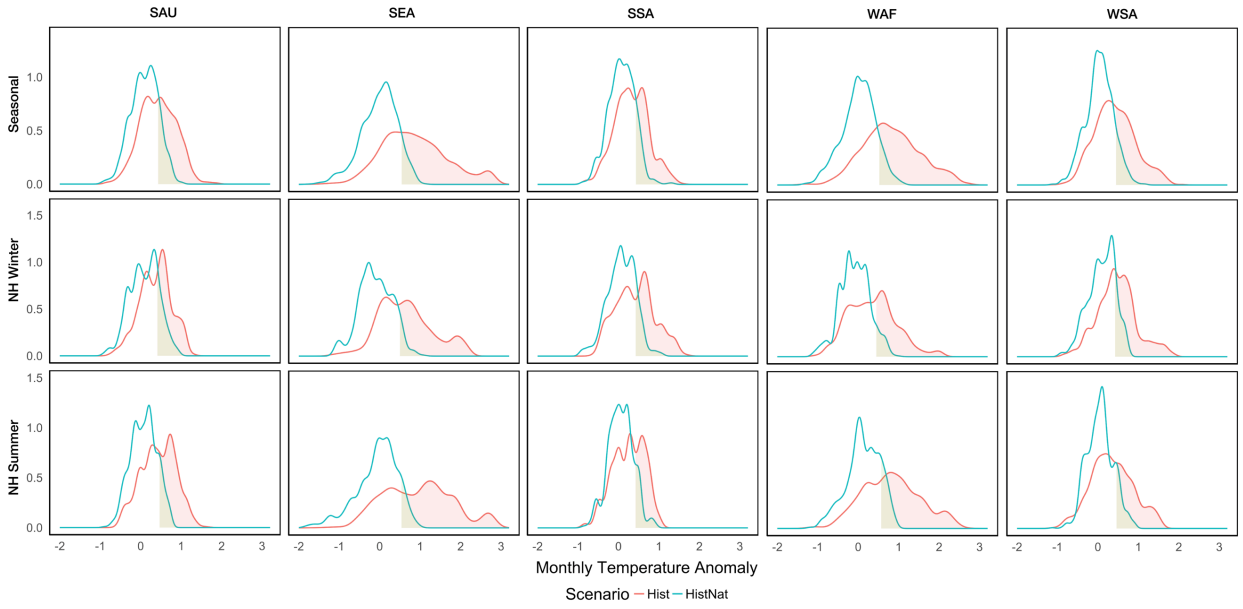

Figure 4.7c: IPCC regional conditional PDFs (con't). The regions shown in the figure are: South Australia/New Zealand (SAU), Southeast Asia (SEA), Southeastern South America (SSA), West Africa (WAF), and West Coast South America (WSA).

Figure 4.8 (a, b, c) presents global maps of copula-based joint probability ratios, which were created with a 90^{th} percentile threshold in mind. In general, the JPR maps correspond well with the empirically derived maps shown in Figures 4.3. As we outlined in the methodology of this chapter, we found the conditional exceedance probability ratios (CPRs) of each region based on the ratio of the probability of high temperature exceedances under historical conditions to the probability of exceedances under historical natural-only conditions (shaded regions in Figs. 4.7a, b, and c). Figure 4.8 (d, e, f) presents global maps of the CPR values associated with each IPCC region.

From these parametrically derived subplots, we can also see that most IPCC regions between 60^{o}N and 60^{o}S have 1) a higher likelihood of experiencing a joint exceedance in the historical case and 2) a higher likelihood of experiencing a high temperature exceedance under low precipitation conditions in the historical case. In addition, we see a greater divergence between the likelihood of historical and historical natural-only exceedances in North America during boreal summer conditions. This may be due to how anthropogenic emissions have influenced land-atmosphere interactions in North America, which can translate to tighter correlations between low precipitation conditions and high temperatures over land. We also see a greater divergence between the likelihood of historical and natural-only exceedances in Central Asia during boreal summer conditions. There are also regions (e.g. the Mediterranean region of Europe) known to be strongly influenced by land-atmosphere feedbacks, which experienced greater increases in joint probability ratios across seasonal, boreal winter, and boreal summer conditions. Further study may be needed to understand how seasonality influences the sensitivity of each region to anthropogenic forcing. Overall, this figure shows that JPR and CPR may reveal

differences in sensitivities to anthropogenic forcing, especially when seasonal conditions are accounted for.

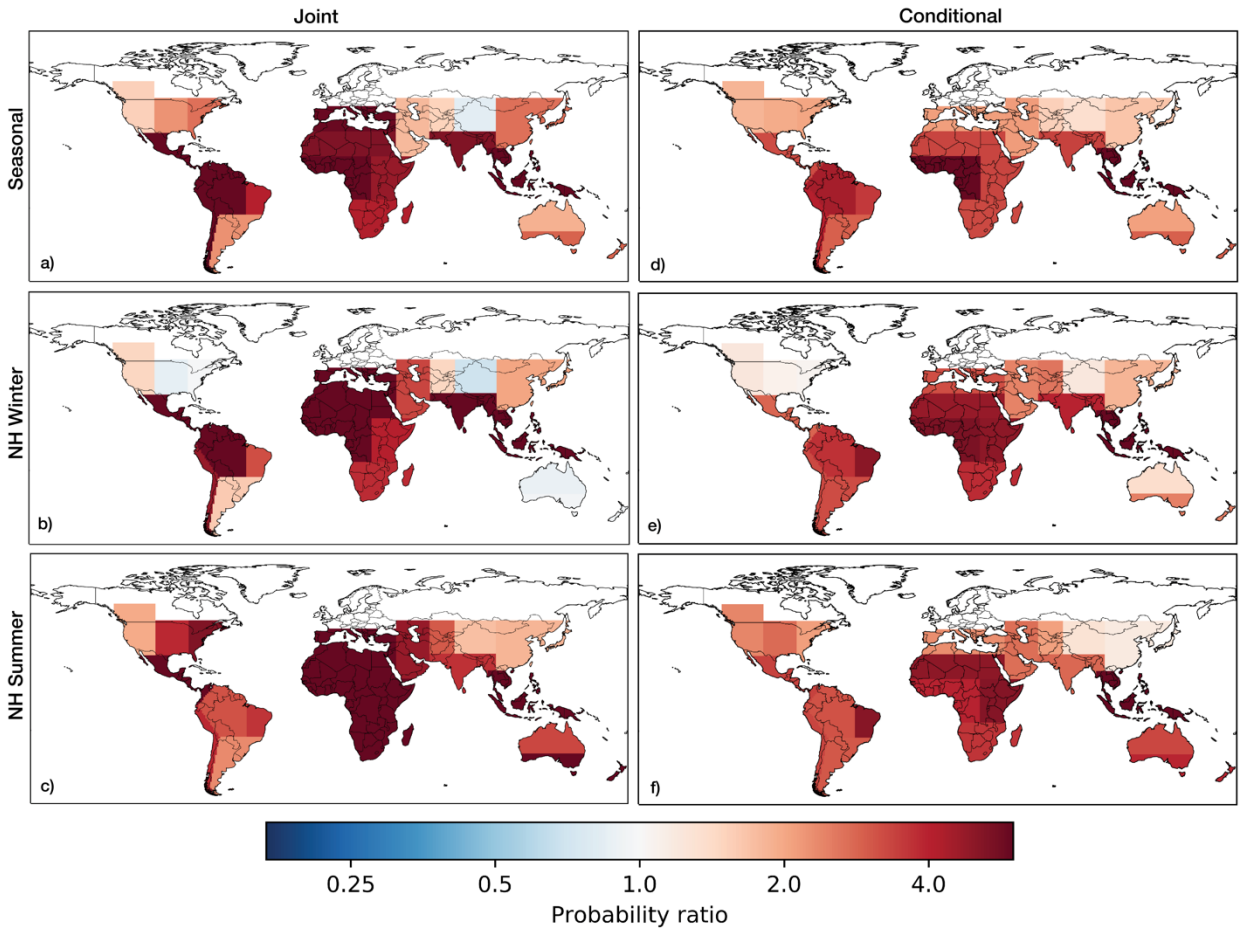

Figure 4.8. Copula-derived joint and conditional probability ratios (JPR and CPR). a) JPR mapped atop each IPCC region for seasonal months (derived from regional 3-month SPI time series of each February, May, August, November). b) JPR for boreal winter (derived from 3-month SPI of each February). c) JPR for boreal summer (derived from 3-month SPI of each August). d) CPR for seasonal months. e) CPR for boreal winter. f) CPR for boreal summer. For all subplots, PR > 1 represents a higher likelihood of exceeding the defined high temperature threshold in the historical scenario and PR < 1 represents a higher likelihood of exceeding the defined threshold in the historical natural-only scenario.

4.4 Discussion and Conclusion

4.4.1 Discussion

From our results, we established worldwide differences between historical and historical natural-only dry events, warm events, and dry and warm concurrences. The differences in joint occurrences are especially pronounced in the tropics and subtropics. From a global perspective, we found that joint dry and warm months are occurring 3 times more in the historical climate relative to the natural-only climate at the end of the 20th century relative to the mid-19th century. In addition, the global pattern of the probability ratio of joint warm and dry events showed that the globe has overwhelmingly been impacted by the presence of anthropogenic forcing. This highlights a clear impact of anthropogenic climate change on the joint behavior of these events. We also demonstrated that increases in conditional exceedance probabilities can also be attributed to anthropogenic emissions. These results show that anthropogenic climate change has impacted high temperature occurrences given a specified low precipitation anomaly. Overall, our findings highlight the clear impacts that anthropogenic climate change has on the joint and conditional behavior of warm and dry events.

Our findings have many implications in other fields of study. We expect that water-dependent sectors will experience strong physical ramifications from the concurrence of droughts and heatwaves, which may become more common under the shifts that we have documented. Sarhadi et al. (2018) highlighted that agricultural land areas have experienced substantial increases in the joint occurrence of warm/dry years (Sarhadi et al., 2018). This is crucial as the joint occurrence of warm/dry conditions have severe impacts on agriculture (Sarhadi et al., 2018; Zscheischler & Seneviratne, 2017). As we have mentioned previously,

droughts and high temperature events also negatively impact ecosystem conditions, in addition to energy production, public health, and many other sectors (Hatfield & Prueger, 2015; Mazdiyasni & AghaKouchak, 2015; Tarroja et al., 2018). Droughts and high temperatures can also increase the risk of wildfires, which can eventually trigger other hazards such as debris flows (AghaKouchak et al., 2018).

4.4.2 Study limitations

We acknowledge that there are biases associated with the exclusive use of model simulations, and here, we highlight the deficiencies of the model simulations that are specific to the study. Climate models do not consistently represent land-atmosphere feedbacks in a uniform fashion (Sippel et al., 2017). In addition, there has been evidence that some climate models may be too dry, and thus extremes are simulated to be hotter than observed (Vogel et al., 2018). Models also do not include recent findings, such as the impact of irrigation on hot extremes, which has been shown to significantly reduce the severity of local high temperatures (Lobell et al., 2008; N. D. Mueller et al., 2017; Thiery et al., 2017). Thus, regions that have experienced significant trends in irrigation, such as the upper Midwestern U.S., must be evaluated with the additional impact of irrigation in mind. Future studies that examine the impact of the presence (or absence) of irrigation on compound warm and dry events would contribute insight on how irrigation may influence the likelihood of these events. Overall, we acknowledge that model biases may contribute to a degree of error in the results presented. However, as we were comparing output from two model experiments for our analysis, the significance of these model biases was reduced.

4.4.3 Conclusion

From our results, we gained a better understanding of the widespread impact of climate change on concurrent dry and warm spells. The work directly considers the influence of anthropogenic climate change on joint occurrences of temperature and precipitation extremes, which had previously not been studied in detection and attribution literature. We also implemented conditional exceedance probabilities as an indicator to attribute changes in conditional risks to anthropogenic climate change. The conditional results provide a new indicator in detection and attribution literature, which allows us to consider how the risk of extreme events of one variable has changed under defined conditions of another variable. Through our conditional framework, we have provided a way of accounting for underlying moisture conditions while assessing the impact of climate change on temperature exceedances. This framework can be applied to other multivariate relationships and allow us to measure conditional risks and attribute those risks to anthropogenic climate change. Quantifying conditional risks is important to better prepare for extremes that are coupled to or dependent on other climate variables. On a broader level, the methods and results presented here can be utilized in future risk assessment studies to more accurately capture socio-economic, environmental, and infrastructural vulnerability and exposure to extremes. Gaining a better understanding of regional and global changes in concurrent events and conditional extremes, and the underlying drivers of these changes are important for improving local management practices and preparedness for future extremes. Given current climate change projections, we expect a further increase in the concurrency of such events, which makes this crucial.

Chapter 5

Summary and Conclusions

Through our introduction and literature review (Chapter 1), we outlined research gaps and opportunities in climate extremes and detection and attribution literature. We found that most existing studies of climate extremes focus on one variable or feature at a time. In this dissertation, we investigated the interactions between different climatic extremes as well as different features of an extreme to provide novel perspectives of how extremes are changing under warming temperatures. In Chapters 2-4, we presented evidence based on observational and model-based data that anthropogenic climate change has impacted 1) temperature shifts conditioned on drought conditions, 2) changes in the likelihood and magnitude of drought events, and 3) changes in the likelihood of concurrent warm and dry events. In this final chapter, we summarize the main conclusions for each study presented in this dissertation and the overall contributions of this dissertation.

5.1 Amplified Warming of Droughts in the United States in Observations and Model Simulations

Concurrent drought and heatwave events have been documented to cause severe environmental and socioeconomic impacts. These short-term events can be driven by land atmosphere interactions: for example, low soil moisture anomalies (characterized by antecedent low precipitation conditions) can increase air temperatures by impacting the local ratio of sensible to latent heat. Recent papers have documented that the concurrence of drought and heatwave events has been increasing in the United States. However, prior to this dissertation, existing literature had not explored historical and projected changes in temperature under specific climate conditions. In Chapter 2, we investigate how average U.S. temperatures following antecedent low precipitation anomalies have been changing in the 20th century and how temperatures are projected to change in model simulations. We concluded that, in many regions of the U.S., temperatures during dry meteorological conditions are warming faster than average climate conditions. Higher average temperatures under dry conditions can have strong implications for future risks of concurrent warm and dry extremes, especially in the context of climate change.

5.2 The Impact of Anthropogenic Forcing on Drought Characteristics

In recent years, detection and attribution studies have made substantial progress in understanding the impacts of anthropogenic forcing on mean and extreme climate variables.

However, prior to this dissertation, the long-term impacts of anthropogenic forcing on drought characteristics have not been explored. Chapter 3 presented an examination of the influence of anthropogenic forcing on drought characteristics. Using historical (with anthropogenic forcing) and historical natural-only climate models, we quantified the contribution of human activities to the likelihood, length, and magnitude of drought events. We found substantial regional shifts in drought frequency, maximum drought duration, and maximum drought intensity, especially in the wetter parts of the globe. We also found that, relative to all land pixels, agricultural land pixels (which are often located in relatively wet areas) exhibited increased sensitivity to anthropogenic climate change.

5.3 The Impact of Anthropogenic Forcing on Compound Warm and Dry Extremes

Recent climate research has recognized the importance of studying compound events to gain a more comprehensive perspective on the risks and impacts of extreme events. However, detection and attribution literature has generally ignored dependencies between climate variables. To improve our understanding of how anthropogenic climate change has affected historical occurrences of interrelated variables, Chapter 4 examined the impacts of climate change on concurrent warm and dry events. With historical and historical natural-only model simulations, we showed that significant increases in warm and dry months across the globe that can be attributed to the presence of anthropogenic forcing. We also introduced a new conditional indicator that quantifies the impact of anthropogenic forcing on the likelihood of high temperature exceedances under dry conditions.

5.4 Main Contributions

The research presented in this dissertation examines how climate change has impacted the nature of hydroclimatic extremes. In Chapter 2, we provided a new perspective on average temperature change conditioned on droughts, which have important implications for future concurrent event risks. We argued that drought conditions can reveal connections between atmospheric variables that are not immediately apparent when evaluating general climate conditions, showing the importance of conditional analysis in the study of anthropogenic climate change. In Chapters 3 and 4, we examined the impacts of anthropogenic forcing on drought characteristics and concurrent warm/dry events. We showed that the presence of anthropogenic climate conditions has resulted in substantial regional shifts in drought characteristics and highlight that water-dependent sectors (e.g. agriculture industry) are especially sensitive to these anthropogenically driven shifts. We also show that anthropogenic climate conditions have contributed to large increases in concurrent warm and dry months, which have significant implications for future impacts on environmental, socioeconomic, and public health. The studies put forward in this dissertation contribute to our understanding of the changing nature of hydroclimatic extremes, which can serve to aid in future efforts to prepare for extreme events.

References

AghaKouchak, A., Easterling, D., Hsu, K., Schubert, S., & Sorooshian, S. (Eds.). (2013). *Extremes in a Changing Climate: Detection, Analysis and Uncertainty*. Springer Netherlands. https://doi.org/10.1007/978-94-007-4479-0

AghaKouchak, A., Cheng, L., Mazdiyasni, O., & Farahmand, A. (2014). Global warming and changes in risk of concurrent climate extremes: Insights from the 2014 California drought. *Geophysical Research Letters*, *41*(24), 8847–8852. https://doi.org/10.1002/2014GL062308

AghaKouchak, A., Feldman, D., Hoerling, M., Huxman, T., & Lund, J. (2015). Water and climate: Recognize anthropogenic drought. *Nature News*, *524*(7566), 409. https://doi.org/10.1038/524409a

AghaKouchak, A., Huning, L. S., Chiang, F., Sadegh, M., Vahedifard, F., Mazdiyasni, O., et al. (2018). How do natural hazards cascade to cause disasters? *Nature*, *561*(7724), 458–460. https://doi.org/10.1038/d41586-018-06783-6

Alexander, L. (2011). Climate science: Extreme heat rooted in dry soils. *Nature Geoscience*, *4*(1), 12–13. https://doi.org/10.1038/ngeo1045

Allen, MR, Mutlow, C., Blumberg, G., Christy, J., McNider, R., & Llewellyn-Jones, D. (1994). Global change detection. *Nature*, *370*(6484), 24–24.

Allen, Myles. (2003). Liability for climate change. *Nature*, *421*(6926), 891–892. https://doi.org/10.1038/421891a

Asner, G. P., Brodrick, P. G., Anderson, C. B., Vaughn, N., Knapp, D. E., & Martin, R. E. (2015). Progressive forest canopy water loss during the 2012–2015 California drought. *Proceedings of the National Academy of Sciences*. https://doi.org/10.1073/pnas.1523397113

Balan Sarojini, B., Stott, P. A., Black, E., & Polson, D. (2012). Fingerprints of changes in annual and seasonal precipitation from CMIP5 models over land and ocean: PRECIPITATION CHANGES FROM CMIP5 MODELS. *Geophysical Research Letters*, *39*(21), n/a-n/a. https://doi.org/10.1029/2012GL053373

Barnett, T. P., Pierce, D. W., Hidalgo, H. G., Bonfils, C., Santer, B. D., Das, T., et al. (2008). Human-Induced Changes in the Hydrology of the Western United States. *Science*, *319*(5866), 1080–1083. https://doi.org/10.1126/science.1152538

Barnett, Tim P., & Schlesinger, M. E. (1987). Detecting changes in global climate induced by greenhouse gases. *Journal of Geophysical Research: Atmospheres*, *92*(D12), 14772–14780. https://doi.org/10.1029/JD092iD12p14772

Berg, A., Findell, K., Lintner, B., Giannini, A., Seneviratne, S. I., van den Hurk, B., et al. (2016). Land–atmosphere feedbacks amplify aridity increase over land under global warming. *Nature Climate Change*, *6*, 869874. https://doi.org/10.1038/nclimate3029

Bindoff, N. L., Stott, P. A., AchutaRao, K. M., Allen, M. R., Gillett, N., Gutzler, D., et al. (2013). Chapter 10 - Detection and attribution of climate change: From global to regional. In *Climate Change 2013: The Physical Science Basis. IPCC Working Group I Contribution to AR5*. Cambridge: Cambridge University Press. Retrieved from http://www.climatechange2013.org/images/report/WG1AR5_Chapter10_FINAL.pdf

Byrne, M. P., & O'Gorman, P. A. (2016). Understanding Decreases in Land Relative Humidity with Global Warming: Conceptual Model and GCM Simulations. *Journal of Climate*, *29*(24), 9045–9061. https://doi.org/10.1175/JCLI-D-16-0351.1

Chang, F.-C., & Wallace, J. M. (1987). Meteorological Conditions during Heat Waves and Droughts in the United States Great Plains. *Monthly Weather Review*, *115*(7), 1253–1269. https://doi.org/10.1175/1520-0493(1987)115<1253:MCDHWA>2.0.CO;2

Christidis, N., Stott, P. A., Brown, S., Hegerl, G. C., & Caesar, J. (2005). Detection of changes in temperature extremes during the second half of the 20th century. *Geophysical Research Letters*, *32*(20). https://doi.org/10.1029/2005GL023885

Ciais, P., Reichstein, M., Viovy, N., Granier, A., Ogée, J., Allard, V., et al. (2005). Europe-wide reduction in primary productivity caused by the heat and drought in 2003. *Nature*, *437*(7058), 529–533. https://doi.org/10.1038/nature03972

Dai, A. (2013). Increasing drought under global warming in observations and models. *Nature Climate Change*, *3*(1), 52–58. https://doi.org/10.1038/nclimate1633

De Bono, A., Peduzzi, P., Kluser, S., & Giuliani, G. (2004). Impacts of Summer 2003 Heat Wave in Europe. Retrieved from https://archive-ouverte.unige.ch/unige:32255

Diffenbaugh, N. S., Swain, D. L., & Touma, D. (2015). Anthropogenic warming has increased drought risk in California. *Proceedings of the National Academy of Sciences*, *112*(13), 3931–3936. https://doi.org/10.1073/pnas.1422385112

Dirmeyer, P. A., Jin, Y., Singh, B., & Yan, X. (2013). Trends in Land–Atmosphere Interactions from CMIP5 Simulations. *Journal of Hydrometeorology*, *14*(3), 829–849. https://doi.org/10.1175/JHM-D-12-0107.1

Dore, M. H. I. (2005). Climate change and changes in global precipitation patterns: what do we know? *Environment International*, *31*(8), 1167–1181. https://doi.org/10.1016/j.envint.2005.03.004

Dracup, J. A., Lee, K. S., & Paulson, E. G. (1980). On the definition of droughts. *Water Resources Research*, *16*(2), 297–302. https://doi.org/10.1029/WR016i002p00297

Easterling, D. R., Meehl, G. A., Parmesan, C., Changnon, S. A., Karl, T. R., & Mearns, L. O. (2000). Climate Extremes: Observations, Modeling, and Impacts. *Science*, *289*(5487), 2068–2074. https://doi.org/10.1126/science.289.5487.2068

Easterling, D. R., Kunkel, K. E., Wehner, M. F., & Sun, L. (2016). Detection and attribution of climate extremes in the observed record. *Weather and Climate Extremes*, *11*, 17–27. https://doi.org/10.1016/j.wace.2016.01.001

Farahmand, A., & AghaKouchak, A. (2015). A generalized framework for deriving nonparametric standardized drought indicators. *Advances in Water Resources*, *76*, 140–145. https://doi.org/10.1016/j.advwatres.2014.11.012

Fasullo, J. T. (2010). Robust Land–Ocean Contrasts in Energy and Water Cycle Feedbacks. *Journal of Climate*, *23*(17), 4677–4693. https://doi.org/10.1175/2010JCLI3451.1

Feng, H., & Liu, Y. (2015). Combined effects of precipitation and air temperature on soil moisture in different land covers in a humid basin. *Journal of Hydrology*, *531*, 1129–1140. https://doi.org/10.1016/j.jhydrol.2015.11.016

Ficklin, D. L., & Novick, K. A. (2017). Historic and projected changes in vapor pressure deficit suggest a continental-scale drying of the United States atmosphere. *Journal of Geophysical Research: Atmospheres*, *122*(4), 2061–2079. https://doi.org/10.1002/2016JD025855

Field, C. B., Barros, V., Stocker, T. F., & Dahe, Q. (Eds.). (2012). *Managing the Risks of Extreme Events and Disasters to Advance Climate Change Adaptation: Special Report of the Intergovernmental Panel on Climate Change*. Cambridge: Cambridge University Press. https://doi.org/10.1017/CBO9781139177245

Fischer, E. M., & Knutti, R. (2014). Detection of spatially aggregated changes in temperature and precipitation extremes. *Geophysical Research Letters*, *41*(2), 547–554. https://doi.org/10.1002/2013GL058499

Fischer, E. M., & Knutti, R. (2015). Anthropogenic contribution to global occurrence of heavy-precipitation and high-temperature extremes. *Nature Climate Change*, *5*(6), 560–564. https://doi.org/10.1038/nclimate2617

Fischer, E. M., Seneviratne, S. I., Lüthi, D., & Schär, C. (2007). Contribution of land-atmosphere coupling to recent European summer heat waves. *Geophysical Research Letters*, *34*(6). https://doi.org/10.1029/2006GL029068

Forrest, K., Tarroja, B., Chiang, F., AghaKouchak, A., & Samuelsen, S. (2018). Assessing climate change impacts on California hydropower generation and ancillary services provision. *Climatic Change*, *151*(3), 395–412. https://doi.org/10.1007/s10584-018-2329-5

Fu, Q., & Feng, S. (2014). Responses of terrestrial aridity to global warming. *Journal of Geophysical Research: Atmospheres*, *119*(13), 7863–7875. https://doi.org/10.1002/2014JD021608

Gräler, B., Berg, M. J. van den, Vandenberghe, S., Petroselli, A., Grimaldi, S., Baets, B. D., & Verhoest, N. E. C. (2013). Multivariate return periods in hydrology: a critical and practical review focusing on synthetic design hydrograph estimation. *Hydrology and Earth System Sciences*, *17*(4), 1281–1296. https://doi.org/10.5194/hess-17-1281-2013

Gumbel, E. J. (1963). Statistical Forecast of Droughts. *International Association of Scientific Hydrology. Bulletin*, *8*(1), 5–23. https://doi.org/10.1080/02626666309493293

Hao, Z., AghaKouchak, A., & Phillips, T. J. (2013). Changes in concurrent monthly precipitation and temperature extremes. *Environmental Research Letters*, *8*(3), 034014. https://doi.org/10.1088/1748-9326/8/3/034014

Hasselmann, K. (1993). Optimal Fingerprints for the Detection of Time-dependent Climate Change. *Journal of Climate*, *6*(10), 1957–1971. https://doi.org/10.1175/1520-0442(1993)006<1957:OFFTDO>2.0.CO;2

Hatfield, J. L., & Prueger, J. H. (2015). Temperature extremes: Effect on plant growth and development. *Weather and Climate Extremes*, *10*, 4–10. https://doi.org/10.1016/j.wace.2015.08.001

Hegerl, G. C., von Storch, H., Hasselmann, K., Santer, B. D., Cubasch, U., & Jones, P. D. (1996). Detecting Greenhouse-Gas-Induced Climate Change with an Optimal Fingerprint Method. *Journal of Climate*, *9*(10), 2281–2306. https://doi.org/10.1175/1520-0442(1996)009<2281:DGGICC>2.0.CO;2

Hegerl, G. C., Karl, T. R., Allen, M., Bindoff, N. L., Gillett, N., Karoly, D., et al. (2006). Climate Change Detection and Attribution: Beyond Mean Temperature Signals. *Journal of Climate*, *19*(20), 5058–5077. https://doi.org/10.1175/JCLI3900.1

Hegerl, G. C., Hoegh-Guldberg, O., Casassa, G., Hoerling, M. P., Kovats, R., Parmesan, C., et al. (2010). Good practice guidance paper on detection and attribution related to anthropogenic climate change.

Heim, R. R. (2015). An overview of weather and climate extremes – Products and trends. *Weather and Climate Extremes*, *10*, 1–9. https://doi.org/10.1016/j.wace.2015.11.001

Herrera-Estrada, J. E., Sheffield, J., Herrera-Estrada, J. E., & Sheffield, J. (2017). Uncertainties in Future Projections of Summer Droughts and Heat Waves over the Contiguous United States. *Journal of Climate*. https://doi.org/10.1175/JCLI-D-16-0491.1

Hidalgo, H. G., Das, T., Dettinger, M. D., Cayan, D. R., Pierce, D. W., Barnett, T. P., et al. (2009). Detection and Attribution of Streamflow Timing Changes to Climate Change in

the Western United States. *Journal of Climate*, *22*(13), 3838–3855. https://doi.org/10.1175/2009JCLI2470.1

HIRABAYASHI, Y., KANAE, S., EMORI, S., OKI, T., & KIMOTO, M. (2008). Global projections of changing risks of floods and droughts in a changing climate. *Hydrological Sciences Journal*, *53*(4), 754–772. https://doi.org/10.1623/hysj.53.4.754

Hirota, N., Takayabu, Y. N., Watanabe, M., & Kimoto, M. (2011). Precipitation Reproducibility over Tropical Oceans and Its Relationship to the Double ITCZ Problem in CMIP3 and MIROC5 Climate Models. *Journal of Climate*, *24*(18), 4859–4873. https://doi.org/10.1175/2011JCLI4156.1

Hirschi, M., Seneviratne, S. I., Alexandrov, V., Boberg, F., Boroneant, C., Christensen, O. B., et al. (2011). Observational evidence for soil-moisture impact on hot extremes in southeastern Europe. *Nature Geoscience*, *4*(1), 17–21. https://doi.org/10.1038/ngeo1032

Hoerling, M., Kumar, A., Dole, R., Nielsen-Gammon, J. W., Eischeid, J., Perlwitz, J., et al. (2012). Anatomy of an Extreme Event. *Journal of Climate*, *26*(9), 2811–2832. https://doi.org/10.1175/JCLI-D-12-00270.1

Houghton, E. (1996). *Climate change 1995: The science of climate change: contribution of working group I to the second assessment report of the Intergovernmental Panel on Climate Change* (Vol. 2). Cambridge University Press.

Huang, Jianping, Yu, H., Guan, X., Wang, G., & Guo, R. (2016). Accelerated dryland expansion under climate change. *Nature Climate Change*, *6*(2), 166–171. https://doi.org/10.1038/nclimate2837

Huang, Jin, & van den Dool, H. M. (1993). Monthly Precipitation-Temperature Relations and Temperature Prediction over the United States. *Journal of Climate*, *6*(6), 1111–1132. https://doi.org/10.1175/1520-0442(1993)006<1111:MPTRAT>2.0.CO;2

Hwang, Y.-T., & Frierson, D. M. W. (2013). Link between the double-Intertropical Convergence Zone problem and cloud biases over the Southern Ocean. *Proceedings of the National Academy of Sciences*, *110*(13), 4935–4940. https://doi.org/10.1073/pnas.1213302110

IPCC. (2013). Climate Change 2013: The Physical Science Basis. Contribution of Working Group I to the Fifth Assessment Report of the Intergovernmental Panel on Climate Change. Cambridge, United Kingdom and New York, NY, USA: Cambridge University Press. https://doi.org/10.1017/CBO9781107415324

Kam, J., Sheffield, J., & Wood, E. F. (2014). Changes in drought risk over the contiguous United States (1901–2012): The influence of the Pacific and Atlantic Oceans. *Geophysical Research Letters*, *41*(16), 5897–5903. https://doi.org/10.1002/2014GL060973

Karl, T. R., Meehl, G. A., Miller, C. D., Hassol, S. J., Waple, A. M., & Murray, W. L. (2008). *Weather and climate extremes in a changing climate*. US Climate Change Science Program.

Koster, R. D., Schubert, S. D., & Suarez, M. J. (2009). Analyzing the Concurrence of Meteorological Droughts and Warm Periods, with Implications for the Determination of Evaporative Regime. *Journal of Climate*, *22*(12), 3331–3341. https://doi.org/10.1175/2008JCLI2718.1

Lambert, F. H., Stott, P. A., Allen, M. R., & Palmer, M. A. (2004). Detection and attribution of changes in 20th century land precipitation. *Geophysical Research Letters*, *31*(10). https://doi.org/10.1029/2004GL019545

Leonard, M., Westra, S., Phatak, A., Lambert, M., van den Hurk, B., McInnes, K., et al. (2014). A compound event framework for understanding extreme impacts. *Wiley Interdisciplinary Reviews: Climate Change*, *5*(1), 113–128. https://doi.org/10.1002/wcc.252

Li, G., & Xie, S.-P. (2013). Tropical Biases in CMIP5 Multimodel Ensemble: The Excessive Equatorial Pacific Cold Tongue and Double ITCZ Problems. *Journal of Climate*, *27*(4), 1765–1780. https://doi.org/10.1175/JCLI-D-13-00337.1

Lin, J.-L. (2007). The Double-ITCZ Problem in IPCC AR4 Coupled GCMs: Ocean–Atmosphere Feedback Analysis. *Journal of Climate*, *20*(18), 4497–4525. https://doi.org/10.1175/JCLI4272.1

Livneh, B., & Hoerling, M. P. (2016). The Physics of Drought in the U.S. Central Great Plains. *Journal of Climate*, *29*(18), 6783–6804. https://doi.org/10.1175/JCLI-D-15-0697.1

Lobell, D. B., Bonfils, C. J., Kueppers, L. M., & Snyder, M. A. (2008). Irrigation cooling effect on temperature and heat index extremes. *Geophysical Research Letters*, *35*(9). https://doi.org/10.1029/2008GL034145

Madadgar, S., & Moradkhani, H. (2013). A Bayesian Framework for Probabilistic Seasonal Drought Forecasting. *Journal of Hydrometeorology*, *14*(6), 1685–1705. https://doi.org/10.1175/JHM-D-13-010.1

Martin, E. R. (2018). Future Projections of Global Pluvial and Drought Event Characteristics. *Geophysical Research Letters*, *45*(21), 11,913-11,920. https://doi.org/10.1029/2018GL079807

Marvel, K., Cook, B. I., Bonfils, C. J. W., Durack, P. J., Smerdon, J. E., & Williams, A. P. (2019). Twentieth-century hydroclimate changes consistent with human influence. *Nature*, *569*(7754), 59–65. https://doi.org/10.1038/s41586-019-1149-8

Massey, F. J. (1951). The Kolmogorov-Smirnov Test for Goodness of Fit. *Journal of the American Statistical Association*, *46*(253), 68–78. https://doi.org/10.2307/2280095

Maurer, E. P., & Hidalgo, H. G. (2008). Utility of daily vs. monthly large-scale climate data: an intercomparison of two statistical downscaling methods. *Hydrology and Earth System Sciences*, *12*(2), 551–563. https://doi.org/10.5194/hess-12-551-2008

Maurer, Edwin P., Brekke, L., Pruitt, T., & Duffy, P. B. (2007). Fine-resolution climate projections enhance regional climate change impact studies. *Eos, Transactions American Geophysical Union*, *88*(47), 504–504. https://doi.org/10.1029/2007EO470006

Mazdiyasni, O., & AghaKouchak, A. (2015). Substantial increase in concurrent droughts and heatwaves in the United States. *Proceedings of the National Academy of Sciences*, *112*(37), 11484–11489. https://doi.org/10.1073/pnas.1422945112

Mazdiyasni, O., AghaKouchak, A., Davis, S. J., Madadgar, S., Mehran, A., Ragno, E., et al. (2017). Increasing probability of mortality during Indian heat waves. *Science Advances*, *3*(6), e1700066. https://doi.org/10.1126/sciadv.1700066

McDonald, J. H. (2009). *Handbook of biological statistics* (Vol. 2). Baltimore, MD: Sparky House Publishing.

McHugh, T. A., Morrissey, E. M., Reed, S. C., Hungate, B. A., & Schwartz, E. (2015). Water from air: an overlooked source of moisture in arid and semiarid regions. *Scientific Reports*, *5*, 13767. https://doi.org/10.1038/srep13767

Meehl, G. A., Arblaster, J. M., & Tebaldi, C. (2007). Contributions of natural and anthropogenic forcing to changes in temperature extremes over the United States. *Geophysical Research Letters*, *34*(19). https://doi.org/10.1029/2007GL030948

Mehran, A., Mazdiyasni, O., & AghaKouchak, A. (2015). A hybrid framework for assessing socioeconomic drought: Linking climate variability, local resilience, and demand: HYBRID FRAMEWORK ASSESSING WATER STRESS. *Journal of Geophysical Research: Atmospheres*, *120*(15), 7520–7533. https://doi.org/10.1002/2015JD023147

Michael Waskom, Olga Botvinnik, drewokane, Paul Hobson, Yaroslav Halchenko, Saulius Lukauskas, et al. (2016). *seaborn: v0.7.0 (January 2016)*. Zenodo. https://doi.org/10.5281/zenodo.45133

Min, S.-K., Zhang, X., Zwiers, F. W., & Hegerl, G. C. (2011). Human contribution to more-intense precipitation extremes. *Nature*, *470*(7334), 378–381. https://doi.org/10.1038/nature09763

Min, S.-K., Zhang, X., Zwiers, F., Shiogama, H., Tung, Y.-S., & Wehner, M. (2013). Multimodel Detection and Attribution of Extreme Temperature Changes. *Journal of Climate*, *26*(19), 7430–7451. https://doi.org/10.1175/JCLI-D-12-00551.1

Mueller, B., & Seneviratne, S. I. (2012). Hot days induced by precipitation deficits at the global scale. *Proceedings of the National Academy of Sciences*, *109*(31), 12398–12403. https://doi.org/10.1073/pnas.1204330109

Mueller, N. D., Butler, E. E., McKinnon, K. A., Rhines, A., Tingley, M., Holbrook, N. M., & Huybers, P. (2016). Cooling of US Midwest summer temperature extremes from cropland intensification. *Nature Climate Change*, *6*(3), 317–322. https://doi.org/10.1038/nclimate2825

Mueller, N. D., Rhines, A., Butler, E. E., Ray, D. K., Siebert, S., Holbrook, N. M., & Huybers, P. (2017). Global Relationships between Cropland Intensification and Summer Temperature Extremes over the Last 50 Years. *Journal of Climate*, *30*(18), 7505–7528. https://doi.org/10.1175/JCLI-D-17-0096.1

Nagler, T., Schepsmeier, U., Stoeber, J., Brechmann, E. C., Graeler, B., Erhardt, T., et al. (2019). VineCopula: Statistical Inference of Vine Copulas (Version 2.2.0). Retrieved from https://CRAN.R-project.org/package=VineCopula

Nasrollahi, N., AghaKouchak, A., Cheng, L., Damberg, L., Phillips, T. J., Miao, C., et al. (2015). How well do CMIP5 climate simulations replicate historical trends and patterns of meteorological droughts? *Water Resources Research*, *51*(4), 2847–2864. https://doi.org/10.1002/2014WR016318

Nelsen, R. B. (2006). *An Introduction to Copulas* (2nd ed.). New York: Springer-Verlag. Retrieved from https://www.springer.com/gp/book/9780387286594

Palmer W. (1965). Meteorological Drought, Research paper no. 45. *U.S. Weather Bureau*, *58*.

Perkins-Kirkpatrick, S. E., & Gibson, P. B. (2017). Changes in regional heatwave characteristics as a function of increasing global temperature. *Scientific Reports*, *7*(1), 1–12. https://doi.org/10.1038/s41598-017-12520-2

Prospero, J. M., & Lamb, P. J. (2003). African Droughts and Dust Transport to the Caribbean: Climate Change Implications. *Science*, *302*(5647), 1024–1027. https://doi.org/10.1126/science.1089915

Ramankutty, N., Evan, A. T., Monfreda, C., & Foley, J. A. (2008). Farming the planet: 1. Geographic distribution of global agricultural lands in the year 2000: GLOBAL AGRICULTURAL LANDS IN 2000. *Global Biogeochemical Cycles*, *22*(1), n/a-n/a. https://doi.org/10.1029/2007GB002952

Rosenzweig, C., & Urban Climate Change Research Network (Eds.). (2011). *Climate change and cities: first assessment report of the Urban Climate Change Research Network*. Cambridge : New York: Cambridge University Press.

Santer, B. D., Brüggemann, W., Cubasch, U., Hasselmann, K., Höck, H., Maier-Reimer, E., & Mikolajewica, U. (1994). Signal-to-noise analysis of time-dependent greenhouse warming experiments. *Climate Dynamics*, *9*(6), 267–285.

Santer, B. D., Taylor, K. E., Wigley, T. M. L., Penner, J. E., Jones, P. D., & Cubasch, U. (1995). Towards the detection and attribution of an anthropogenic effect on climate. *Climate Dynamics*, *12*(2), 77–100. https://doi.org/10.1007/BF00223722

Sarhadi, A., Ausín, M. C., Wiper, M. P., Touma, D., & Diffenbaugh, N. S. (2018). Multidimensional risk in a nonstationary climate: Joint probability of increasingly severe warm and dry conditions. *Science Advances*, *4*(11), eaau3487. https://doi.org/10.1126/sciadv.aau3487

Sarojini, B. B., Stott, P. A., Black, E., & Polson, D. (2012). Fingerprints of changes in annual and seasonal precipitation from CMIP5 models over land and ocean. *Geophysical Research Letters*, *39*(21). https://doi.org/10.1029/2012GL053373

Seneviratne, S. I., Lüthi, D., Litschi, M., & Schär, C. (2006). Land–atmosphere coupling and climate change in Europe. *Nature*, *443*(7108), 205–209. https://doi.org/10.1038/nature05095

Seneviratne, S. I., Corti, T., Davin, E. L., Hirschi, M., Jaeger, E. B., Lehner, I., et al. (2010). Investigating soil moisture–climate interactions in a changing climate: A review. *Earth-Science Reviews*, *99*(3), 125–161. https://doi.org/10.1016/j.earscirev.2010.02.004

Seneviratne, S. I., Nicholls, N., Easterling, D., Goodess, C. M., Kanae, S., Kossin, J., et al. (2012). Changes in Climate Extremes and their Impacts on the Natural Physical Environment. In C. B. Field, V. Barros, T. F. Stocker, & Q. Dahe (Eds.), *Managing the Risks of Extreme Events and Disasters to Advance Climate Change Adaptation* (pp. 109–230). Cambridge: Cambridge University Press. https://doi.org/10.1017/CBO9781139177245.006

Serinaldi, F. (2015). Dismissing return periods! *Stochastic Environmental Research and Risk Assessment*, *29*(4), 1179–1189. https://doi.org/10.1007/s00477-014-0916-1

Sheffield, J., & Wood, E. F. (2008). Projected changes in drought occurrence under future global warming from multi-model, multi-scenario, IPCC AR4 simulations. *Climate Dynamics*, *31*(1), 79–105. https://doi.org/10.1007/s00382-007-0340-z

Sheffield, J., Wood, E. F., & Roderick, M. L. (2012). Little change in global drought over the past 60 years. *Nature*, *491*(7424), 435–438. https://doi.org/10.1038/nature11575

Sheffield, J., Barrett, A., & Others, B., Daniel Bennett, [And 38. (2014). Regional climate processes and projections for North America: CMIP3/CMIP5 differences, attribution and outstanding issues. https://doi.org/10.7289/V5DB7ZRC

Sippel, S., Zscheischler, J., Mahecha, M. D., Orth, R., Reichstein, M., Vogel, M., & Seneviratne, S. I. (2017). Refining multi-model projections of temperature extremes by evaluation against land–atmosphere coupling diagnostics. *Earth System Dynamics*, *8*(2), 387–403. https://doi.org/10.5194/esd-8-387-2017

SKLAR, M. (1959). Fonctions de repartition a n dimensions et leurs marges. *Publ. Inst. Statist. Univ. Paris*, *8*, 229–231.

Smith, A. B., & NOAA National Centers For Environmental Information. (2020). U.S. Billion-dollar Weather and Climate Disasters, 1980 - present (NCEI Accession 0209268) [Data set]. NOAA National Centers for Environmental Information. https://doi.org/10.25921/STKW-7W73

Smolka, A. (2006). Natural disasters and the challenge of extreme events: risk management from an insurance perspective. *Philosophical Transactions of the Royal Society A: Mathematical, Physical and Engineering Sciences*, *364*(1845), 2147–2165. https://doi.org/10.1098/rsta.2006.1818

Spinoni, J., Naumann, G., Carrao, H., Barbosa, P., & Vogt, J. (2014). World drought frequency, duration, and severity for 1951–2010. *International Journal of Climatology*, *34*(8), 2792–2804. https://doi.org/10.1002/joc.3875

Spinoni, J., Vogt, J. V., Naumann, G., Barbosa, P., & Dosio, A. (2018). Will drought events become more frequent and severe in Europe? *International Journal of Climatology*, *38*(4), 1718–1736. https://doi.org/10.1002/joc.5291

Spracklen, D. V., Arnold, S. R., & Taylor, C. M. (2012). Observations of increased tropical rainfall preceded by air passage over forests. *Nature*, *489*(7415), 282–285. https://doi.org/10.1038/nature11390

Stéfanon, M., Drobinski, P., D'Andrea, F., Lebeaupin-Brossier, C., & Bastin, S. (2014). Soil moisture-temperature feedbacks at meso-scale during summer heat waves over Western Europe. *Climate Dynamics*, *42*(5), 1309–1324. https://doi.org/10.1007/s00382-013-1794-9

Stone, D. A., Allen, M. R., Stott, P. A., Pall, P., Min, S.-K., Nozawa, T., & Yukimoto, S. (2009). The detection and attribution of human influence on climate. *Annual Review of Environment and Resources*, *34*.

Stott, P. A., Tett, S. F. B., Jones, G. S., Allen, M. R., Ingram, W. J., & Mitchell, J. F. B. (2001). Attribution of twentieth century temperature change to natural and anthropogenic causes. *Climate Dynamics*, *17*(1), 1–21. https://doi.org/10.1007/PL00007924

Stott, Peter A. (2003). Attribution of regional-scale temperature changes to anthropogenic and natural causes. *Geophysical Research Letters*, *30*(14).

Stott, Peter A., Stone, D. A., & Allen, M. R. (2004). Human contribution to the European heatwave of 2003. *Nature*, *432*(7017), 610–614. https://doi.org/10.1038/nature03089

Stott, Peter A., Gillett, N. P., Hegerl, G. C., Karoly, D. J., Stone, D. A., Zhang, X., & Zwiers, F. (2010). Detection and attribution of climate change: a regional perspective. *WIREs Climate Change*, *1*(2), 192–211. https://doi.org/10.1002/wcc.34

Su, H., Yang, Z.-L., Dickinson, R. E., & Wei, J. (2014). Spring soil moisture-precipitation feedback in the Southern Great Plains: How is it related to large-scale atmospheric conditions? *Geophysical Research Letters*, *41*(4), 1283–1289. https://doi.org/10.1002/2013GL058931

Tarroja, B., Chiang, F., AghaKouchak, A., & Samuelsen, S. (2018). Assessing future water resource constraints on thermally based renewable energy resources in California. *Applied Energy*, *226*, 49–60. https://doi.org/10.1016/j.apenergy.2018.05.105

Taylor, K. E., Stouffer, R. J., & Meehl, G. A. (2011). An Overview of CMIP5 and the Experiment Design. *Bulletin of the American Meteorological Society*, *93*(4), 485–498. https://doi.org/10.1175/BAMS-D-11-00094.1

Tett, S. F., Stott, P. A., Allen, M. R., Ingram, W. J., & Mitchell, J. F. (1999). Causes of twentieth-century temperature change near the Earth's surface. *Nature*, *399*(6736), 569–572.

Thiery, W., Davin, E. L., Lawrence, D. M., Hirsch, A. L., Hauser, M., & Seneviratne, S. I. (2017). Present-day irrigation mitigates heat extremes. *Journal of Geophysical Research: Atmospheres*, *122*(3), 1403–1422. https://doi.org/10.1002/2016JD025740

Trenberth, K. (2011). Changes in precipitation with climate change. *Climate Research*, *47*(1), 123–138. https://doi.org/10.3354/cr00953

Trenberth, K. E., Dai, A., van der Schrier, G., Jones, P. D., Barichivich, J., Briffa, K. R., & Sheffield, J. (2014). Global warming and changes in drought. *Nature Climate Change*, *4*(1), 17–22. https://doi.org/10.1038/nclimate2067

Van Loon, A. F., Gleeson, T., Clark, J., Van Dijk, A. I. J. M., Stahl, K., Hannaford, J., et al. (2016). Drought in the Anthropocene. *Nature Geoscience*, *9*, 89–91. https://doi.org/10.1038/ngeo2646

Vautard, R., Yiou, P., D'Andrea, F., Noblet, N. de, Viovy, N., Cassou, C., et al. (2007). Summertime European heat and drought waves induced by wintertime Mediterranean rainfall deficit. *Geophysical Research Letters*, *34*(7). https://doi.org/10.1029/2006GL028001

Vicente-Serrano, S. M., Gouveia, C., Camarero, J. J., Beguería, S., Trigo, R., López-Moreno, J. I., et al. (2013). Response of vegetation to drought time-scales across global land biomes.

Proceedings of the National Academy of Sciences, *110*(1), 52–57. https://doi.org/10.1073/pnas.1207068110

Vogel, M. M., Zscheischler, J., & Seneviratne, S. I. (2018). Varying soil moisture-atmosphere feedbacks explain divergent temperature extremes and precipitation projections in central Europe. *Earth System Dynamics*, *9*(3), 1107–1125. https://doi.org/10.5194/esd-9-1107-2018

Walsh, J. E., Jasperson, W. H., & Ross, B. (1985). Influences of Snow Cover and Soil Moisture on Monthly Air Temperature. *Monthly Weather Review*, *113*(5), 756–768. https://doi.org/10.1175/1520-0493(1985)113<0756:IOSCAS>2.0.CO;2

Wehner, M. F., Arnold, J. R., Knutson, T., Kunkel, K. E., & LeGrande, A. N. (2017). *Ch. 8: Droughts, Floods, and Wildfires. Climate Science Special Report: Fourth National Climate Assessment, Volume I*. U.S. Global Change Research Program. https://doi.org/10.7930/J0CJ8BNN

Wilhite, D. A. (2000). Drought as a natural hazard: concepts and definitions.

Wilhite, D. A., Svoboda, M. D., & Hayes, M. J. (2007). Understanding the complex impacts of drought: A key to enhancing drought mitigation and preparedness. *Water Resources Management*, *21*(5), 763–774. https://doi.org/10.1007/s11269-006-9076-5

Williams, A. P., Seager, R., Abatzoglou, J. T., Cook, B. I., Smerdon, J. E., & Cook, E. R. (2015). Contribution of anthropogenic warming to California drought during 2012–2014. *Geophysical Research Letters*, *42*(16), 6819–6828. https://doi.org/10.1002/2015GL064924

Wuebbles, D. J., Fahey, D. W., & Hibbard, K. A. (2017). Climate science special report: fourth national climate assessment, volume I.

Zhang, T. (2005). Influence of the seasonal snow cover on the ground thermal regime: An overview. *Reviews of Geophysics*, *43*(4). https://doi.org/10.1029/2004RG000157

Zhang, X., Zwiers, F. W., & Stott, P. A. (2006). Multimodel multisignal climate change detection at regional scale. *Journal of Climate*, *19*(17), 4294–4307.

Zhang, X., Zwiers, F. W., Hegerl, G. C., Lambert, F. H., Gillett, N. P., Solomon, S., et al. (2007a). Detection of human influence on twentieth-century precipitation trends. *Nature*, *448*(7152), 461–465. https://doi.org/10.1038/nature06025

Zhang, X., Zwiers, F. W., Hegerl, G. C., Lambert, F. H., Gillett, N. P., Solomon, S., et al. (2007b). Detection of human influence on twentieth-century precipitation trends. *Nature*, *448*(7152), 461–465. https://doi.org/10.1038/nature06025

Zhou, Z.-Q., Xie, S.-P., Zheng, X.-T., Liu, Q., & Wang, H. (2014). Global Warming–Induced Changes in El Niño Teleconnections over the North Pacific and North America. *Journal of Climate*, *27*(24), 9050–9064. https://doi.org/10.1175/JCLI-D-14-00254.1

Zscheischler, J., & Seneviratne, S. I. (2017). Dependence of drivers affects risks associated with compound events. *Science Advances*, *3*(6), e1700263. https://doi.org/10.1126/sciadv.1700263

Zscheischler, J., Westra, S., Hurk, B. J. J. M. van den, Seneviratne, S. I., Ward, P. J., Pitman, A., et al. (2018). Future climate risk from compound events. *Nature Climate Change*, *8*(6), 469. https://doi.org/10.1038/s41558-018-0156-3